Alma Mater Studiorum – Università di Bologna

DOTTORATO DI RICERCA IN

BIOINGEGNERIA

Ciclo XXIII

Settore scientifico-disciplinare di afferenza:

ING-INF/06 BIOINGEGNERIA ELETTRONICA E INFORMATICA

TITOLO TESI

Foetal heart rate recording: analysis and comparison of different methodologies

Presentata da: Ing. Mariano Ruffo

Coordinatore Dottorato	**Relatori**
Prof. Angelo Cappello	Prof. Mario Cesarelli
	Prof. Paolo Bifulco
	Ing. Maria Romano

Esame finale anno 2011

INDEX

Abstract

Monitoring foetal health is a very important task in clinical practice to appropriately plan pregnancy management and delivery. In the third trimester of pregnancy, ultrasound cardiotocography is the most employed diagnostic technique: foetal heart rate and uterine contractions signals are simultaneously recorded and analysed in order to ascertain foetal health.

Because ultrasound cardiotocography interpretation still lacks of complete reliability, new parameters and methods of interpretation, or alternative methodologies, are necessary to further support physicians' decisions.

To this aim, in this thesis, foetal phonocardiography and electrocardiography are considered as different techniques.

Further, variability of foetal heart rate is thoroughly studied. Frequency components and their modifications can be analysed by applying a time-frequency approach, for a distinct understanding of the spectral components and their change over time related to foetal reactions to internal and external stimuli (such as uterine contractions). Such modifications of the power spectrum can be a sign of autonomic nervous system reactions and therefore represent additional, objective information about foetal reactivity and health.

However, some limits of ultrasonic cardiotocography still remain, such as in long-term foetal surveillance, which is often recommendable mainly in risky pregnancies. In these cases, the fully non-invasive acoustic recording, foetal phonocardiography, through maternal abdomen, represents a valuable alternative to the ultrasonic cardiotocography. Unfortunately, the so recorded foetal heart sound signal is heavily loaded by noise, thus the determination of the foetal heart rate raises serious signal processing issues. A new algorithm for foetal heart rate estimation from foetal phonocardiographic recordings is presented in this thesis.

Different filtering and enhancement techniques, to enhance the first foetal heart sounds, were applied, so that different signal processing techniques were implemented, evaluated and compared, by identifying the strategy characterized on average by the best results.

In particular, phonocardiographic signals were recorded simultaneously to ultrasonic cardiotocographic signals in order to compare the two foetal heart rate series (the one estimated by the developed algorithm and the other provided by cardiotocographic device). The algorithm performances were tested on phonocardiographic signals recorded on pregnant women, showing reliable foetal heart rate signals, very close to the ultrasound cardiotocographic recordings, considered as reference.

The algorithm was also tested by using a foetal phonocardiographic recording simulator developed and presented in this research thesis. The target was to provide a software for simulating recordings relative to different foetal conditions and recordings situations and to use it as a test tool for comparing and assessing different foetal heart rate extraction algorithms.

Since there are few studies about foetal heart sounds time characteristics and frequency content and the available literature is poor and not rigorous in this area, a data collection pilot study was also conducted with the purpose of specifically characterising both foetal and maternal heart sounds.

Finally, in this thesis, the use of foetal phonocardiographic and electrocardiographic methodology and their combination, are presented in order to detect foetal heart rate and other functioning anomalies. The developed methodologies, suitable for longer-term assessment, were able to detect heart beat events correctly, such as first and second heart sounds and QRS waves. The detection of such events provides reliable measures of foetal heart rate, potentially information about measurement of the systolic time intervals and foetus circulatory impedance.

1. INTRODUZIONE

1.1 Historical Highlights

It is of great interest to obtain clinical information about foetal health during pregnancy and labour. Auscultation of the foetal heart by applying the ear to the pregnant woman's abdomen it is an old practice that was reinforced after the invention of the stethoscope in the early 19th century, increasing its diagnostic capability. Stethoscopic auscultation of the foetal heart developed throughout the century, as its potential to recognise foetal well-being was realised. Interest grew in how to recognise changes in Foetal Heart Rate (FHR) that might predict and prevent foetal distress and/or intrapartum foetal death through obstetric intervention. Pinard's version of the foetal stethoscope appeared in 1876. Criteria for the normal FHR set in the latter part of the 19th century remained virtually unchanged until the 1950's. During the same period, interest and research increased into the significance of meconium staining of the amniotic fluid as a means of predicting foetal well-being. By the beginning of the 20th century, auscultation of the foetal heart was an established practice.

Advances in the techniques of auscultation were limited, mainly by inability to detect subtle changes or provide continuous surveillance, until the advent of audiovisual technologies in the early 20th century. These promised the possibility of a continuous form

of monitoring. Early electrocardiographic techniques were limited by their inability to sufficiently eliminate maternal ECG signal. This problem was addressed by the use of the foetal scalp electrode in 1960.

A considerable advance in technology with which to detect the foetal heartbeat came in 1964 when the Doppler principle was applied. In 1968, the first commercially available Electronic Foetal Monitor (EFM) applied Doppler's principle of a distinct change in frequency when a Ultra Sonique (US) waveform is reflected from a moving surface. Subsequently, the use of EFM increased rapidly.

The monitoring of foetal scalp blood acid-base was developed in Germany in the 1960s and was introduced clinically as an adjunct to continuous electronic foetal heart-rate monitoring to increase its specificity.

Medical and socio-economic advances transformed maternal birth outcomes in the 19th and 20th centuries. While the original aim of intrapartum EFM was to prevent harm, it was introduced on to the labour wards in the 1950s with the emphasis on improving foetal birth outcomes by detecting foetal hypoxia, before it led to death or disability. Like intermittent auscultation in the 19th century, continuous EFM was introduced clinically before its effectiveness had been fully evaluated scientifically.

A number of retrospective observational studies published in 1972-76 reported a decrease in perinatal mortality in those women who had continuous EFM as opposed to those who had selective EFM or no EFM at all [1]. While these studies were encouraging, the methodological biases of observational studies (they may overestimate the true effects of a given intervention) prompted a need for randomised controlled trial evidence to more rigorously evaluate the use of intrapartum EFM on perinatal mortality and morbidity.

1.2   Work task

Foetal diagnostics is very important in clinical practice to appropriately plan pregnancy management and delivery. Unlikely, non-invasive monitoring of the foetus well-being is not an easy task to achieve and some limits in the most diffused pre-natal diagnostic techniques, still remain.

In this thesis, new parameters or methods of interpretation and alternative methodologies for non-invasive foetal monitoring are presented in order to further support physicians' decisions. In particular, different methodologies of foetal heart rate monitoring were analysed and compared: ultrasonographic Doppler cardiotocography (US-CTG), phonocardiography (PCG) and electrocardiography (ECG).

Concerning Doppler cardiotocography, US-CTG data provide physicians relevant information about foetal development and permit to assess conditions such as foetal distress. Hence, an incorrect evaluation of the foetal status can be of course very dangerous. However, although US-CTG is the most spread diagnostic technique in clinical environments, mainly in the third trimester of pregnancy, its interpretation still lacks of complete reliability so that new methods for a complete and certain assessment of foetal well-being could be very helpful.

To this aim, indexes related to variability of foetal heart rate (FHRV) are particularly advocated in bibliography as useful, since, already in adult subjects, FHRV is acknowledged as an important parameter for the evaluation of healthy conditions. Thus, time dependent spectrum analysis, from US-CTG recordings, of the FHRV frequency components and their modifications were carried on by applying a time-frequency

approach, in order to better identify the spectral components related to foetal reactions to internal and external stimuli and their change over time. Being UC strong stimuli for the foetus and his autonomic nervous system (ANS), the FHRV response to UC was analyzed and characterized. Such modifications of the FHRV power spectrum can be a sign of ANS reaction and therefore represent additional, objective information about foetal reactivity and health during labour.

However, it is important to underline that since foetal heart rate is intrinsically an uneven series, in order to produce an evenly sampled series a zero-order, linear or cubic spline interpolation are usually employed in some cardiotocographic devices on the market. This is not suitable for frequency analyses because interpolation process can produce alterations of the power spectral density that, for example, affects the estimation of the sympatho-vagal balance (computed as low-frequency/high-frequency ratio), which represents an important clinical parameter. In order to estimate the frequency spectrum alterations of the foetal heart rate variability signal due to interpolation and cardiotocographic storage rates, the Lomb method, as suggested by other authors to study the uneven heart rate series in adults, was used to prove an overestimation due to the interpolation process and to the storage rate.

This thesis aim was also to analyse a valuable alternative to traditional US-CTG: the phonocardiography (FPCG), a passive and low cost recording of foetal heart sounds.

Firstly an analysis of FPCG mean characteristics in the time and frequency domains is presented. In particular, a data collection pilot study was conducted with the purpose of specifically identifying both foetal and maternal heart sounds characteristics, since the

available literature is not rigorous in this area. Those data were useful to understand better FPCG signals and to obtain precious information for software developing.

After, a simulating software of FPCG signals relative to different foetal states (physiological and pathological) and recording conditions (for example different kinds and levels of noise) and a new algorithm for FHR estimation from FPCG recordings are here presented. Both software were developed utilising information obtained by means of the data collection pilot study.

The described simulating software can be useful as a teaching tool for demonstration to medical students and others but also for testing and assessment of foetal heart rate extraction algorithms from foetal phonocardiographic recordings.

Concerning the developed algorithm for FHR estimation, owing to the extremely noisy nature of FPCG signals, different filtering, signal enhancement techniques and logic blocks for reliable detection of heartbeats were applied, so that different signal processing paths were implemented. The performances of the different paths were tested comparing the estimated FHR signals with those of simultaneously recorded US-CTG (currently considered reference technique), in order to identify the most reliable path. Beside, the FPCG simulator software was used to test the algorithm developed in order to estimate its performance in cases of different signal to noise recordings.

Inside the FPCG monitoring described in this thesis, an Italian experience of foetal home monitoring is presented to show the advantages of this methodology (such as the reduction of the need of travel for patients and consequently of their stress). It is based on a telemedicine system (consisting of phonocardiograph home monitors able to transfer data by GPRS to a remote server where gynaecologists can consult patient recordings) that

increases the possibility of foetal long-term home surveillance which in turn could raise the efficiency of the service offered to pregnant women.

Finally, the use of foetal phonocardiographic and electrocardiographic methodologies and their combination was described in this thesis, in order to detect the FHR and other functioning anomalies. Software processing methodologies, suitable for longer-term assessment, were presented to detect heart beat events, such as first and second heart sounds and QRS waves, which provide reliable measures of heart rate, potentially information about measurement of the systolic time intervals and foetus circulatory impedance.

The research activities, described in this thesis, have produced several scientific results published on scientific journal and book chapters or presented at national and international congresses. Below the list of all the publications is reported:

-Papers published on scientific journal:

- M. Ruffo, M. Cesarelli, M. Romano, P. Bifulco, A. Fratini. An algorithm for FHR estimation from foetal phonocardiographic signals. Biomedical Signal Processing and Control, Vol. 5, Issue 2, April 2010, pp. 131-141

- M. Romano, M. Cesarelli, P. Bifulco, M. Ruffo, A. Fratini, G. Pasquariello: Time-frequency analysis of CTG signals. Current Development in Theory and Application of Wavelets, Vol. 3, Issue 2, August 2009, pp. 169 - 192

- G. Gargiulo, P. Bifulco, M. Cesarelli, M. Ruffo, M. Romano, R A. Calvo, C. Jin, A. van Schaik; An Ultra-high Input Impedance ECG Amplifier for Long Term

Monitoring of Athletes. Medical Devices: Evidence and Research, Vol. 2010:3, July 2010, pp. 1 – 9

- M. Cesarelli, M. Romano, M. Ruffo, P. Bifulco, G. Pasquariello; Foetal heart rate variability frequency characteristics with respect to uterine contractions. Journal of Biomedical Science and Engineering, Vol. 3, Issue 10, Oct. 2010, pp. 1014 – 1021

- M. Cesarelli, M. Romano, M. Ruffo, P. Bifulco, G. Pasquariello, A. Fratini; PSD modifications of FHRV due to interpolation and CTG storage rate. In press by Biomedical Signal Processing and Control (Available online 18 November 2010)

- Abstract of papers presented at National and International congresses:

- M. Ruffo, M. Romano, M. Cesarelli, P. Bifulco: Extraction of heart rate from fetal phonocardiographic signals. Primo Congresso Nazionale di Bioingegneria – GNB-2008

- M. Cesarelli, M. Ruffo, M. Romano, P. Bifulco, F. Kovacs, S. Iaccarino: An Algorithm for fetal heart rate extraction from maternal abdomen sounds. 4th European Congress For Medical and Biomedical Engineering 2008, November 23-27, Antwerp – MBEC 2008

- M. Ruffo, M. Cesarelli, M. Romano, P. Bifulco, A. Fratini, G. Pasquariello, S. Iaccarino: Comparison of software developed for FHR extraction from PCG signals. Medical Physics and Biomedical Engineering World Congress 2009, September 7-12, Munich

- M. Cesarelli, M. Romano, M. Ruffo, P. Bifulco, G. Pasquariello, A. Fratini: PSD modifications of FHRV due to CTG storage rate. 9th International Conference on

Information Technology and Applications in Biomedicine- ITAB 2009, November 5-7, Larnaca, Cyprus

- M. Cesarelli, M. Romano, M. Ruffo, P. Bifulco, M. Iaccarino, S. Iaccarino: Home care phonocardiography: an Italian experience. 9th International Conference on Information Technology and Applications in Biomedicine- ITAB 2009, November 5-7, Larnaca, Cyprus

- M. Ruffo, M. Cesarelli, M. Romano, P. Bifulco: Testing a FHR extraction algorithm by means of a simulating software of foetal phonocardiographic recordings. Secondo Congresso Nazionale di Bioingegneria – GNB-2010

- G. Donadono , M. Ruffo, M. Romano, P. Bifulco, M. Cesarelli, D. Gargiulo, A. Fratini: Recording of fetal heart sound using a PVDF piezoelectric film sensor. Secondo Congresso Nazionale di Bioingegneria – GNB-2010

- M. Ruffo, M. Cesarelli, M. Romano, P. Bifulco, A. Fratini; A simulating software of fetal phonocardiographic signals. The 10th IEEE International Conference on Information Technology and Applications in Biomedicine, ITAB 2010, Corfu, Greece, November 2-5, 2010

- Book chapters

- M. Ruffo, M. Cesarelli, C. Jin, G. Gargiulo, A. McEwan, C. Sullivan, P. Bifulco, M. Romano, R. W. Shephard, A. van Schaik: Non invasive foetal monitoring with a combined ECG - PCG system. "Biomedical Engineering, Trends, Researches and Technologies", To be published by INTECH, Jan. 2011

16

2. FOETAL AND UTERINE PHYSIOLOGY

2.1 Embryo development overview

2.1.1 Foetal heart development

Cardiovascular system very early reaches an adequate functional state in order to support a complex organism like embryo. The primordium of the heart forms in the cardiogenic plate located at the cranial end of the embryo. The most critical period of foetal heart development is between three and seven weeks after fertilization, when a simple heart tube assumes the shape of a four-chambered heart. In fact, the heart actually begins beating by the 22nd day of life (or the fifth week of gestation). In more detail, in the human embryo, the mesodermal germ layer gives rise to the entire cardiovascular system (heart, blood vessels and blood cells). The heart develops from two simple epithelial tubes which fuse to form a single chambered heart that is efficiently pumping blood by the fourth week of embryonic development.

Twenty-three days following conception, the single, simple epithelial heart tube lies within the embryo's pericardial cavity. At this time there are three cell layers present within the

heart tube. The inner layer, known as cardiac jelly, is a structureless mass of cells which contain very few nuclei. The second and third layers are known as the cardiac mantle and will eventually give rise to the epicardium and myocardium.

The heart tube contains three specific areas: the cranial portion, the caudal portion and the bulbus cordis. As development progresses, the cranial dilates to form the aortic sac which will give rise to the aortic arches. The caudal also dilates to form the early embryonic ventricle. The remaining mid-portion forms the bulbus cordis which has three distinct areas of development. Two of these areas give rise to the body of the right ventricle, the aortic root and the parts of the ascending aorta. The remaining portion connects the primitive right ventricle to the truncus arteriosus. In this phase, the two atria are partly separate but there is just one big ventricle. As the heart tube grows and becomes longer it usually bends to the right, because of its need space. Rightward bending is responsible for the initial positioning of the primitive ventricle.

The cardiac jelly now acts as a valve for movement of blood from the atrial end of the heart tube to the distal end. By the 24th day of gestation, the primitive ventricles have expanded and the cardiac jelly contains trabecula or supporting structures. As growth quickly continues, the conotruncal region (area distal to the primitive right ventricle) moves centrally with torsion and twisting, giving rise to the anatomical curve of the aorta and the pulmonary artery.

Between 4th and 5th week, external form of the heart is established and interatrial and interventricular septi form. By the end of the 8th week partitioning is completed and the foetal heart has formed. New changes there will be only after birth, when foetal circulation gets itself reorganised.

It is nice to observe that during the foetal heart's developmental stages, the heart actually takes on several distinct appearances. These heart structures resemble other animal hearts. During the first phase, the tube-like heart is much like a fish heart. The second phase, with two chambers, resembles a frog heart. The three-chambered phase is similar to a snake or turtle heart. The final four-chambered heart structure distinguishes the human heart.

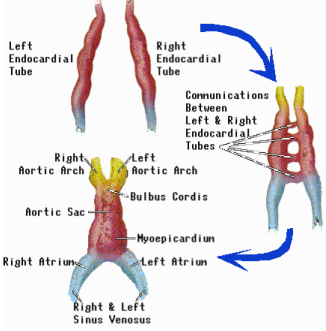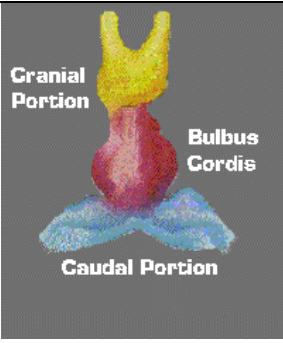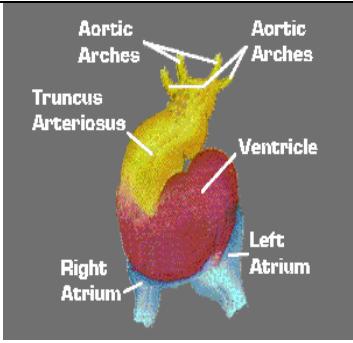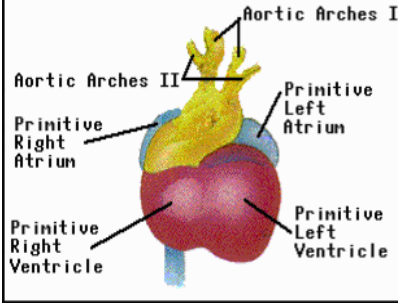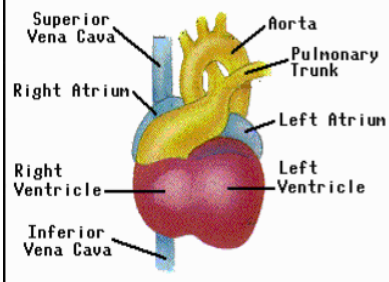|		
		Atria are separate but there is one ventricle
Epithelial tubes	Specific areas of the heart tube	
All parts of the heart are recognisable	Aorta has its anatomical curve	

Figure 1: different phases of foetal heart development

2.1.2   Foetal blood circulation

The foetal circulation is one of the first organ systems to need to be able to function properly in order to sustain the foetus. Before a circulatory system has developed, nutrients and oxygen diffuse through the extraembryonic coelem and yolk sac from the placenta. As the embryo increases in size, its nutrient needs increase and the amount of tissue easily reached by diffusion decreases. Hence the circulation must develop quickly and accurately.

However, throughout the foetal stage of development, the maternal blood supplies the foetus with O2 and nutrients and carries away its wastes. These substances diffuse between the maternal and foetal blood through the placental membrane.

In the foetal circulatory system, the umbilical vein transports blood rich in O2 and nutrients from the placenta to the foetal body. The umbilical vein enters the body through the umbilical ring and travels along the anterior abdominal wall to the liver. About 1/2 the blood it carries passes into the liver. The other 1/2 of the blood enters a vessel called the ductus venosus of Aranzio which bypasses the liver. The ductus venosus travels a short distance and joins the inferior vena cava. There, the oxygenated blood from the placenta is mixed with the deoxygenated blood from the lower parts of the body. This mixture continues through the vena cava to the right atrium. In the adult heart, blood flows from the right atrium to the right ventricle then through the pulmonary arteries to the lungs. In the fetus the lungs are non-functional and the blood largely bypasses them. As the blood from the inferior vena cava enters the right atrium, a large proportion of it is shunted directly into the left atrium through an opening called the foramen ovale. A small valve, septum primum is located on the left side of the atrial septum overlies the foramen ovale and helps prevent blood from moving in the reverse direction. The rest of the foetal blood entering

the right atrium, including a large proportion of the deoxygenated blood entering from the superior vena cava, passes into the right ventricle and out through the pulmonary trunk. Only a small volume of blood enters the pulmonary circuit, because the lungs are collapsed, and their blood vessels have a high resistance to flow. Enough blood reaches the lung tissue to sustain them. Most of the blood in the pulmonary trunk bypasses the lungs by entering a foetal vessel called the ductus arteriosus of Botallo which connects the pulmonary trunk to the descending portion of the aortic arch. The more highly oxygenated blood that enters the left atrium through the foramen ovale is mixed with a small amount of deoxygenated blood returning from the pulmonary veins. This mixture moves into the left ventricle and is pumped into the aorta. Some of it reaches the myocardium through the coronary arteries and some reaches the brain through the carotid arteries. The blood carried by the descending aorta is partially oxygenated and partially deoxygenated. Some of it is carries into the branches of the aorta that lead to various parts of the lower regions of the body. The rest passes into the umbilical arteries, which branch from the internal iliac arteries and lead to the placenta. There the blood is reoxygenated.

Both ductus venosus of Aranzio and ductus arteriosus of Botallo are completely closed after birth.

It is worth mentioning that the concentration of haemoglobin in foetal blood is about 50 % greater than in maternal blood. Foetal haemoglobin is slightly different chemically and has a greater affinity for O_2 than maternal haemoglobin. This is a sort of safety mechanism; in fact because of this characteristic, foetus can overcome relatively short lacks of oxygen.
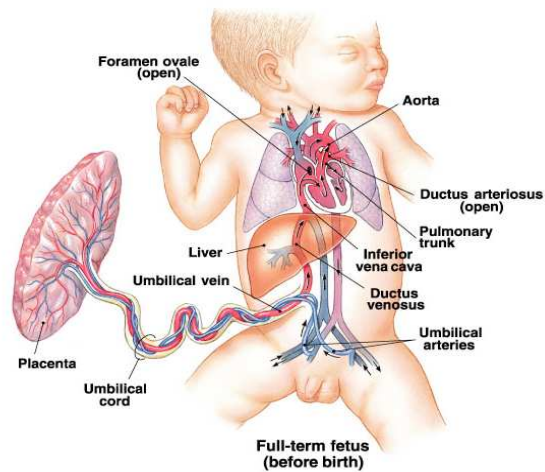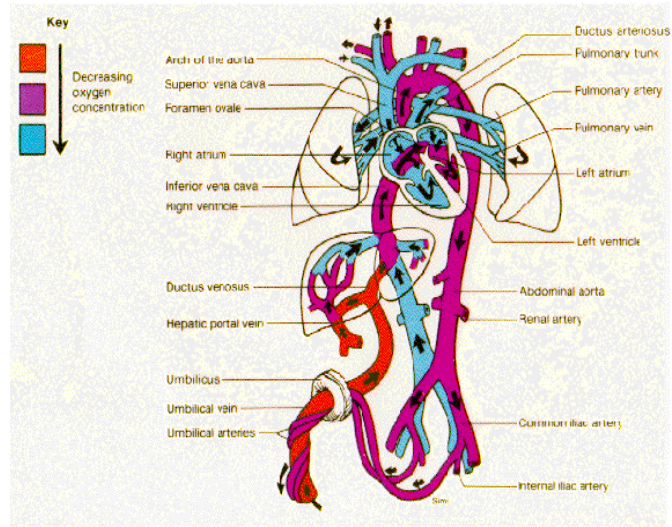
Figure 2: on the top and on the bottom, pictures of foetal blood circulation

2.1.3   Heart electrical activity

Throughout the heart are clumps of specialized cardiac muscle tissue whose fibres contain only a few myofibrils. Electrical impulse originates in the Sinoatrial (S-A) Node (in the foetus, it is completely developed at 6th week of gestation), which consists of a small

elongated mass of specialized muscle tissue just beneath the epicardium. Fibres are continuous with those of the atrial muscle fibres. Membranes of the nodal cells are in contact with each other and have the ability to excite themselves. Without being stimulated by nerve fibres or any other outside agents, the nodal cells initiate impulses that spread into the surrounding myocardium and stimulate the cardiac muscle fibres to contract; this activity is rhythmic. As a cardiac impulse travels from the S-A node into the atrial myocardium, the right and left atria contract almost simultaneously. Cardiac impulses pass along fibres to the atrioventricular node (A-V node), which is located in the floor of the right atrium just beneath the endocardium. Fibres that conduct the cardiac impulse into the A-V node have very small diameters and conduct impulses slowly and cause the impulse to be delayed. Impulse is delayed still more as it travels through the A-V node. This delay allows time for the atria to empty and the ventricles to fill with blood. Impulse now passes into a group of large fibres that make up the A-V bundle (Bundle of His) and the impulse moves rapidly through them. A-V bundle divides into the right and left bundle branches. About 1/2 way down, the branches give rise to enlarged Purkinje fibres. Purkinje fibres spread from the interventricular septum into the papillary muscles and then continue downward to the apex of the heart (see Figure 3: electrical conduction system of the heart). Stimulated by the impulses on the Purkinje fibres, the ventricular walls contract with a twisting motion which squeezes blood out of the ventricular chambers and forces it into arteries.

The heart can be viewed as two separate pumps represented by the right and left halves of the heart. Each pump consists of a primer pump (the atrium) and a power pump (the ventricle). Both atrial primer pumps complete the filling of the ventricles with blood and both ventricular power pumps produce the major force that causes blood to flow through

the pulmonary and systemic arteries. The cardiac cycle refers to the repetitive pumping process that begins with the onset of cardiac muscle contraction and ends with the beginning of the next contraction. The duration of the cardiac cycle varies among people and also varies during an individual's lifetime. In an adult subject, the normal cardiac cycle (0.7-0.8 sec.) depends on two factors: capability of cardiac muscle to contract and functional integrity of the conducting system. Abnormalities of cardiac muscle, the valves, or the conducting system of the heart may alter the cardiac cycle and compromise the pumping effectiveness of the heart.

The described impulse transmission through the conduction system generates electrical currents that can be detected on the body's surface. In a typical ECG record, three clearly recognisable waves accompany each cardiac cycle.

P-Wave (small upward wave) which indicates atrial depolarization, which is the spread of the impulse from the S-A node through the two atria. A fraction of a second after the P-wave begins, the atria contract.

QRS-Wave or Complex. It begins as a downward deflection, continues as a large, upright, triangular wave and ends as a downward wave at its base. Represents ventricular depolarization, the spread of the electrical impulse through the ventricles. Shortly after the QRS wave begins, the ventricles undergo contraction. T-Wave (dome-shaped upward wave) indicates ventricular repolarization.
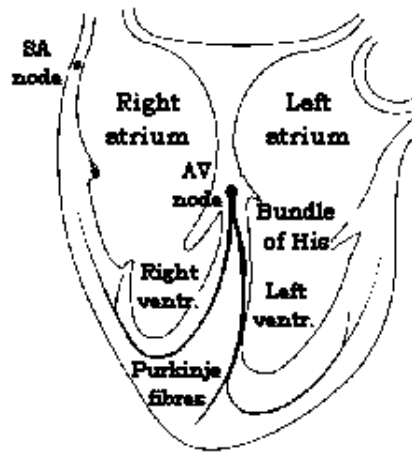
Figure 3: electrical conduction system of the heart

Through labour and delivery, we can invasively record foetal heart electrical activity by means of direct scalp foetal ECG, attaching electrodes to the presenting part of the foetus after membrane rupture. Otherwise, after 16th week's gestation, we can adopt the external abdominal ECG, putting electrodes on the maternal abdomen. With this technique, there is an overlap between foetal (typical amplitude ranges 100-600 μV [2]) and maternal (whose amplitude is greater of 1 or 2 orders) ECG, so a subtraction algorithm is necessary.

2.1.4   Heart beat regulation

Venous return is the amount of blood that returns to the heart during each cardiac cycle. It determines an intrinsic regulation of the heart beat. An increase in venous return causes an increase in cardiac output and stretches the S-A node, so the heart rate increases. However, foetal heart rate variability is also intimately related to foetal central nervous system;

particularly, the most important mechanism immediately involved in producing heart rate variability is the autonomic innervations of the heart **Errore. L'origine riferimento non è stata trovata.**. The cardioregulatory centre in the medulla oblongata regulates the parasympathetic and sympathetic nervous control of the heart.

Parasympathetic stimulation is supplied by the cardiac branches of the vagus nerve. It is of primary importance in producing beat-to-beat variability **Errore. L'origine riferimento non è stata trovata.**. It decreases heart rate and can cause a small decrease in the force of contraction (stroke volume). This component of cardiac innervations is well suited to a role of fine tuning the heart rate on a beat-to-beat basis because of the very rapid decrease in heart rate which occurs whit vagal nerve stimulation, and the nearly equally rapid recovery after the end of a series of impulses. Moreover, postganglionic neurones secrete acetylcholine which increases membrane permeability to K^+, producing hyperpolarization of the membrane.

Sympathetic stimulation is supplied by the cardiac nerves which are projections of the cervical sympathetic chain ganglia (spinal nerve). Sympathetic stimulation increases heart rate and force of contraction (stroke volume). Changes in heart rate with stimulation of cardiac sympathetic innervation are slower compared to stimulation of cardiac vagal innervations. Moreover, it dilates vessels in skeletal and cardiac muscle.

Other specific control mechanisms play an important role in heart beat regulation, such as the effect of blood pressure, pH, CO2, O2, extracellular ion concentration and body temperature.

About the effect of the blood pressure, baroreceptors (stretch sensory receptors are in the walls of certain large arteries i.e. internal carotids and aorta) function is to measure

indirectly blood pressure. In response to an increase in blood pressure, the baroreceptor reflexes decrease sympathetic stimulation and increase parasympathetic stimulation (see Figure 4).
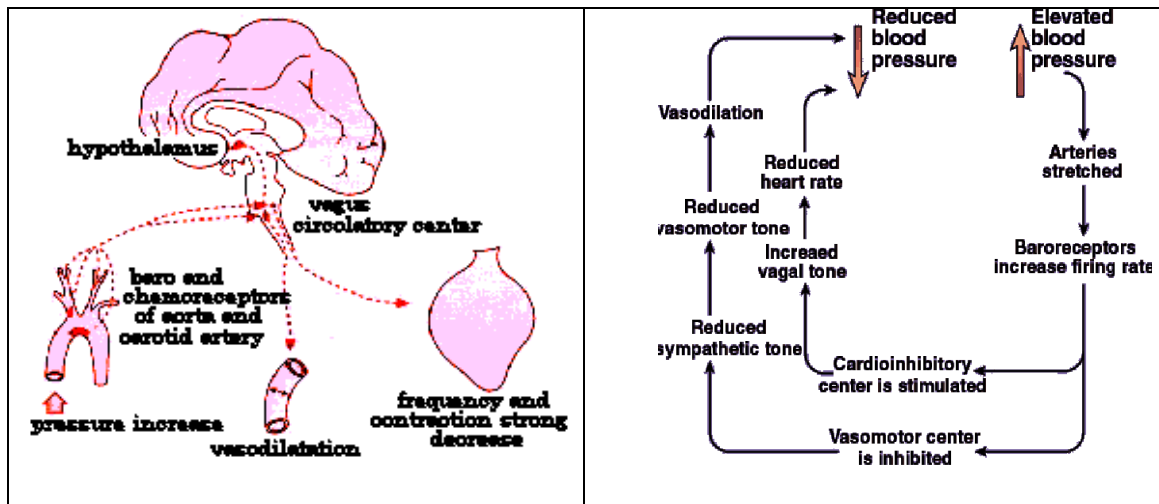
Figure 4: on the left cardiocirculatory regulation in case of pressure increase and on the right description of the feed-back related to blood pressure

Chemoreceptors in the brain, aortic arc and carotids monitor blood CO_2, O_2, and pH levels. In response to increased CO_2, decreased pH, or decreased O_2, autonomic nervous system reflexes increase sympathetic stimulation and decrease parasympathetic stimulation.

An increase or decrease in extracellular K^+ decreases heart rate. Increased extracellular Ca^{2+} increases the force of contraction of the heart and decreases the heart rate. Decreased Ca^{2+} levels produce the opposite effect.

Finally, heart rate increases when body temperature increases and decreases when body temperature decreases.

2.1.5   Uterus anatomy

The human uterus is a massive, hollow, pear-shaped organ with a thick wall, situated deeply in the pelvic cavity between bladder and rectum. It is composed of two distinct anatomic regions: the cervix and the corpus. The corpus is further divided into the lower uterine segment and the fundus. The cervix is a narrow cylindrical passage which connects at its lower end with the vagina. At its upper end, the cervix widens to form the lower uterine segment (isthmus); the lower uterine segment in turn widens into the uterine fundus. The corpus is the body of the uterus which changes in size and structure during pregnancy to accommodate itself to the needs of the growing embryo. Extending from the top of the uterus on either side are the fallopian tubes (oviducts); these tubes are continuous with the uterine cavity and allow the passage of an ova (egg) from the ovaries to the uterus where the egg may implant if fertilized.

Spatial organisation of the smooth muscle fibres in the uterine wall is complicated and still remains the matter of debate. The thick wall of the uterus is formed of three layers: endometrium, myometrium, and serosa or perimetrium. The endometrium (uterine mucosa) is the innermost layer that lines the cavity of the uterus. Throughout the menstrual cycle, the endometrium grows progressively thicker with a rich blood supply to prepare the uterus for potential implantation of an embryo. In the absence of implantation, a portion of this layer is shed during menstruation. The myometrium is the middle and thickest layer of the uterus and is composed of smooth (involuntary) muscle. The myometrium contracts during menstruation to help expel the sloughed endometrial lining and during childbirth to propel the foetus out of the uterus. The outermost layer, or serosa, is a thin fibrous layer

contiguous with extrauterine connective tissue structures such as ligaments that give mechanical support to the uterus within the pelvic cavity.

Non-pregnant uterine size and position varies with age and number of pregnancies.
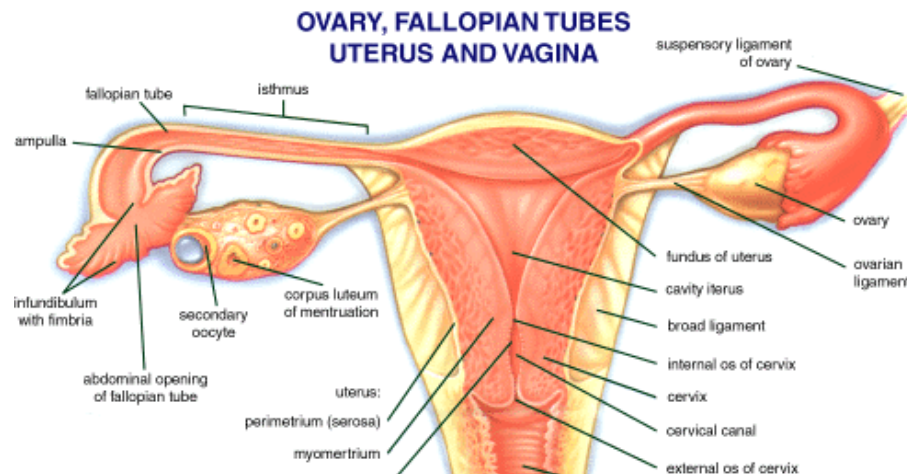
Figure 5: uterus or womb

2.1.6   Uterine contractions

Uterine wall structure is aimed to effective expulsion of foetus if pregnancy is about to terminate. Although biological mechanisms prevent massive contractions of uterus during pregnancy, the uterine wall never remains quiet. Every single muscle fibre possesses the possibility to change its membrane potential slowly, which results in depolarisation. Working potential it generates may be transmitted to other cells in a close neighbourhood,

but the area it can spread on strongly depends on local properties of signal propagation. In course of a physiological pregnancy the intercellular communication is poorly developed, which seems to be a mechanism of a foetus' safety. This leads to the lack of coordination between muscle fibres which produces a kind of fibrillation of uterine wall with almost no significance rise of pressure inside its cavity. In a full term pregnancy, or in some pathological circumstances even sooner, uterine wall becomes well coordinated and uterine contractions frequent, intense, persistent and painful. Low resistance intercellular connections – gap junctions appear in a smooth muscle tissue enhancing trigger wave propagation. Even though there is no specialised trigger wave conducting system in uterus, gap junctions enable it to contract as a whole, presenting a specific pattern of contraction. The certain degree of synchronisation of smooth muscle cells amplifies uterine working potentials, since their appearance results from spatial and temporal summation of electrical activity of single fibres [4].

In spite of the fact that the uterine contractility is predominantly commanded by hormonal and biochemical factors (estrogens, oxytocin, prostaglandins), there are indications that the sympathetic and parasympathetic innervation of the uterus may also have a considerable influence upon it. Independently of the majority of the uterine contractions being endocrinally and biochemically triggered, the myometrial contractile activity exhibits a very peculiar characteristic that seems to demonstrate the existence of a precise nervous coordination: it is the "triple descending gradient." This gradient gives the uterine contractility its typical expulsive pattern.

According to Caldeyro-Barcia [5] the uterine contractile waves originate in "pacemakers" situated around the uterine insertion of the Fallopian tubes, one on the right and the other

on the left. This author describes the "triple descending gradient" with the following characteristics (seeFigure 1 figure 6):

1) the propagation of the contractile wave along the uterus has a descending direction;

2) the systolic phase of the contraction lasts more at the uterine fundus and less at the inferior parts of the organ;

3) the contractions are stronger in the upper parts of the uterus than in the lower ones.

It seems somewhat difficult to explain this so precise and symmetric coordination of the myometrium contractile waves exclusively by means of the hormonal mechanisms that trigger them. Even the double spiral arrangement of most myometrial fibres throughout the uterus does not seem to be, only by itself, capable of entirely explaining the "triple descending gradient" - regardless of being an essential condition for its occurrence. Several facts suggest that the neurovegetative system may have some coordinating activity upon the uterine contractions.
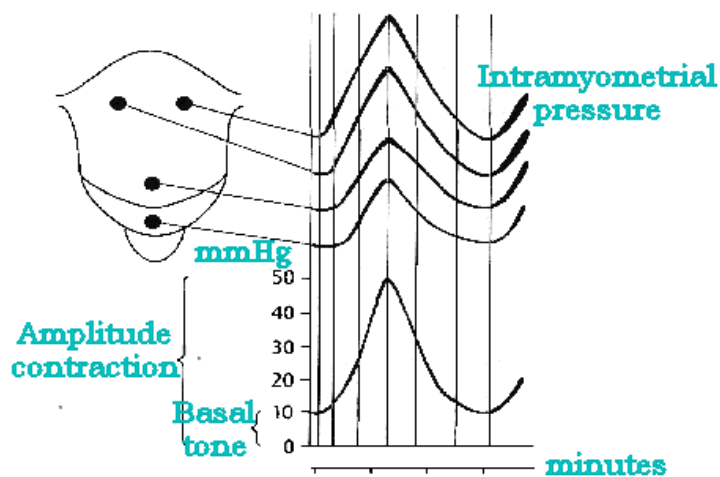
Figure 6: effect of triple descending gradient and resulting uterine contraction

Concerning their characteristics, uterine contractions become very rhythmic and regular in shape during labour, when the hypophysis releases a large dose of oxytocin. The contraction length ranges between 15 and 20 seconds at the begin of the labour and between 60 and 70 seconds at the end (expulsive period).

Approximately at 20th week of gestation irregular contractions with very small amplitude, called Alvarez's waves, are present. They represent a located muscular contraction. In physiological conditions, their frequency decreases and their amplitude increases with gestation progress. In the second period of gestation, a large part of the uterus contracts itself giving rise to Braxton-Hicks' contractions, also slang called "preparations contractions". After 30th week, these contractions gradually become more frequent and strong [6].

3. FOETAL SURVEILLANCE

3.1 Cardiotocography Measurement

The cardiotocography (CTG) techniques adopted to record the FHR and Uterine Contractions (UC) signals can be either direct (e.g. using the ECG signal recorded by means of foetal scalp electrodes and direct intrauterine pressure measurement by means of appropriate catheter or sensor insertion) or indirect (trough the maternal abdomen).

Direct measurements provide more accurate values: direct access to amniotic fluid permits to evaluate absolute intrauterine pressure; foetal scalp ECG availability allows a good evaluation of inter-heartbeats rate. However, direct methods can only be used during labour, after membranes rupture; moreover, this implies ethical problems and infection risk.

Therefore, the most employed methods in clinical practice are those indirect, such as US-Doppler cardiography, abdominal ECG, phonocardiography to measure the HRV and extra-abdominal pressure detection or abdominal EMG to detect changes relates to UC.

Using the latter techniques, it is possible to record FHR and UC by means of probes (or electrodes) placed onto the maternal abdomen. For example, a US-Doppler probe can be utilised to record FHR signal by detecting heart motion and blood flow. While, another

probe, incorporating a pressure transducer, can record the increased pressure exerted by uterus on abdominal wall, which is an indirect effect of uterine contraction.

3.2   Clinical relevance of cardiotocography

Among many techniques to provide information about foetal health, external Cardiotocography (CTG) is the most diffused indirect, diagnostic method in clinical practice, during last pregnancy stage and labour [2].Often CTG or EFM terms are used as synonymous. CTG is based on the simultaneous recording of FHR and UC (also referred as toco signal). Cardiotocographic recordings (CTGs) provide physicians some information about foetal development and well-being; particularly, FHR signal permits also to assess maturation of Autonomous Nervous System (ANS) of the foetus; in fact, FHR modifications mean ANS reactions to stimuli [7]. Toco signal evaluation allows mainly to check labour progress and to avoid, for example, premature births, although it is also an additional source of information for estimating foetal well-being.

CTG usefulness is widely demonstrated in literature [2], especially in antepartum period; since its introduction in the '60s, EFM led to a considerable reduction of perinatal morbidity and mortality. Moreover, cardiotocography recording is the only medical report having legal value in Italy and in some other countries. Nevertheless, physicians generally analyse CTGs by a visual inspection. The efficiency of this method depends on observer's expertise and training, but obviously it lacks of objectivity and reproducibility and it is subject to human error. Moreover, many factors can influence FHR and its variability.

Much important factors are, for example, physiological mechanisms, like thermoregulatory oscillations; maturational changes with advancing gestational age; maternal medication; foetal behavioural states (foetus alternates sleep and awake states and, in each state, periods of more or less activity, giving rise to four different behavioural states) [8].

Still nowadays, there is a very high intra- and interobserver variation in the assessment of FHR patterns, which could lead to an incorrect evaluation of foetal status [8][9][10] and a lack of standardised definitions [7].

The concept of routine FHR monitoring has been subject to much criticism and debate. Nevertheless, there is general agreement concerning the urgency for the detection of foetal distress. Electronic monitoring of the FHR is the most commonly employed method to detect foetal distress and continuous EFM should be recommended particularly for high-risk pregnancy. CTG can be utilised from the 24th week of gestation to delivery; however, in clinical routine, it is generally employed from the 35th week's gestation, once or twice in a week. Cardiotocography recording can be simply carried out also by midwives, it supplies data in real-time and allows also off-line revisions [2].

To assess foetal health and reactivity, gynaecologists and obstetrics evaluate specific clinical signs, generally by an eye inspection of recorded signals. Parameters of great interest are: FHR mean value (related to week's gestation), FHR variability, FHR accelerations, FHR decelerations, and foetal movements. During labour, physicians pay also attention to shape, intensity and frequency of UCs, correlating them to changes induced in the FHR. It is worth reminding that if a distress situation is falsely diagnosed for a foetus, an unnecessary intervention may occur; on the other side, if the foetus is erroneously diagnosed to be in a healthy situation, the care that it needs may be denied

[10]. Thus, a reliable, objective and reproducible method for CTGs interpretation is of crucial importance [10].

Numerical analysis of CTGs was found essential as a more accurate tool in the assessment of foetal conditions, consequently, some authors developed computerized systems to analyse CTGs [11][12][13][14], in order to provide more objective means of CTGs reporting and quantitative evaluation of specific parameters [15]. Generally, automatic classifiers presented in literature base their analysis on the same parameters adopted by clinicians (accelerations, decelerations, contractions detection, etc.). This kind of approach, in the time domain, led to a partial reduction of intra- and interobserver variation but did not show significant clinical improvements with respect to the traditional analysis achieved by visual inspection. Indeed, the selected set of parameters is not always able to highlight important risky conditions as foetal hypoxia or academia [16][17].

It is well known, from literature, that, in adults, the HR Variability (HRV) frequency analysis is a useful, non-invasive and powerful means to investigate ANS activity [18]. The powers of the different components characterizing HRV spectrum seem reflect, in their reciprocal relationship, changes in the sympathovagal balance both in physiological and pathological conditions [19]. Perinatal foetal monitoring was the first area of clinical medicine in which heart rate variability is used as an important clinical variable. Moreover, it has been demonstrated that also for the foetus, the Variability (often referred as fluctuations), of the HR around its baseline (FHRV) could be a valid support for a more objective analysis and for a better knowledge of ANS reactions and its functional state [20][21]. However, additional multiple information are needed about various aspects of the foetal status. For example, it can be very important to better define and detect foetal reactivity; to develop an automatic classifier of foetal behavioural states (some of them can

be sometimes confused with pathological conditions); to study and understand in depth physiological mechanisms underlying some FHR modifications.

3.3 FHR signal

Some of the FHR signal features and their variation are very important in FHR analysis and recording, in order to monitor the foetal well-being.

According to the FIGO (International Federation of Gynaecology and Obstetrics) guidelines, the baseline of a FHR recording is defined as the mean level of the FHR, when this is stable, accelerations and decelerations being absent, determined over a period of 5 to 10 min [22] [13]. The FHR is under constant variation from the baseline. This variability reflects a healthy nervous system, chemoreceptors, baroreceptors and cardiac responsiveness.

Foetal hypoxia, congenital heart anomalies and foetal tachycardia cause decreased variability. However, reduced baseline variability is common also during foetal sleep cycles.

The minor fluctuations in baseline FHR occurring at 3 to 5 cycles per minute. It is measured by estimating the difference in beats per minute between the highest peak and lowest trough of fluctuation in a one-minute segment of the trace [13].

Beat-to-beat or short term variability is the oscillation of the FHR around the baseline in amplitude of 5 to 10 bpm [23][23].

Long term variability is a somewhat slower oscillation in heart rate and has a frequency of 3 to 10 cycles per minute and amplitude of 10 to 25 bpm [23][23]. Clinically, loss of beat-to-beat variability is more significant than loss of long-term variability [23]. Statistically, variability is commonly expressed by the width of the distribution of either RR intervals or heart rates [8].

Other authors proposed a modification to FIGO's ambiguous interdependence of definitions: baseline should be defined as the line that corresponds to the mean FHR level in the absence of foetal movements and uterine contractions rather than in the absence of accelerations and decelerations, as it is necessary to define a baseline rate before identification of an acceleration or deceleration is possible [22]. Also this definition is ambiguous and difficult to apply, mainly in automated analysis software. Some authors adopted another definition and consider the baseline as the running average of HR in the absence of accelerations and decelerations [11][13], without specifying a time interval (for the average).

However, regardless of the way of calculating it, normal range of baseline is 120-160 bpm [23][23]. Prematurity, maternal anxiety and maternal fever may increase the baseline rate, while foetal maturity decreases the baseline rate, since progressive vagal dominance occurs as the foetus approaches term [23] (see Figure 7). A baseline of between 110 and 100 is considered to be suspicious and one below 100 as pathological [8].
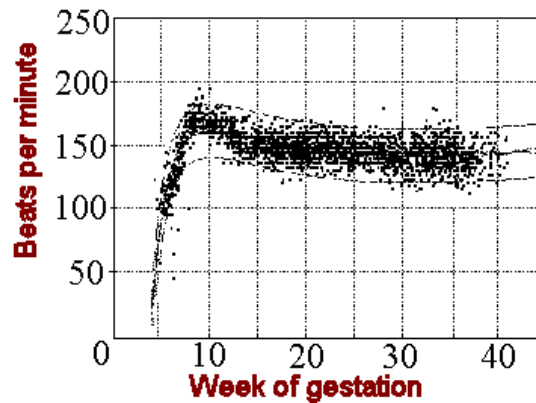
Figure 7: mean FHR versus week of gestation

Foetal tachycardia is defined as a baseline HR greater than 160 bpm [23][23] for more than 10 min [6]. Tachycardia is considered mild when the HR is 160 to 180 bpm and severe when greater than 180 bpm [6] [23]. Some of the possible causes of foetal tachycardia are foetal hypoxia, maternal fever, parasympatholytic drugs, sympathomimetic drugs and prematurity [23]. On the other hand, foetal bradycardia is defined as a baseline HR less than 120 bpm [23][23] for more than 3 min [6]. Bradycardia is severe if FHR is less than 100 bpm [6]. Some of the possible causes of foetal severe bradycardia are prolonged cord compression, cord prolapse, tetanic uterine contractions, epidural and spinal anaesthesia, maternal hypotension and post-maturity [8] [23]. However, it is possible to say that almost any stressful situation in the foetus evokes the baroreceptor reflex, which elicits selective peripheral vasoconstriction and hypertension with a resultant bradycardia [23]. Both these patterns (tachycardia and bradycardia) often are not associated with severe foetal distress unless decreased variability or another abnormality is present [23][23].

FHR patterns present also periodic changes as accelerations and decelerations. Both are defined as deviations from baseline with a certain amplitude and duration and can be present also in conditions of tachycardia or bradycardia.

Accelerations are transient increases of the FHR from the baseline of at least 10 bpm for at least 15 bpm [6]. They are usually associated with foetal movements, vaginal examinations, uterine contractions, umbilical vein compression, foetal scalp stimulation, external acoustic stimulation or transient hypoxia, which actives sympathetic system by means of chemoreceptors. The presence of accelerations is considered a reassuring sign of foetal well-being [23] and a good indicator of good perinatal outcome [13]. Vice versa, the significance of no accelerations on an otherwise normal CTG is unclear [13]. However, a series of accelerations may create confusion. If one acceleration immediately follows another during a series of gross body movements, there is insufficient time for the FHR to return to the baseline level and the accelerations may fuse into tachycardia, as can regularly be observed during the 4F state (see following paragraphs). The number of accelerations in associations with foetal movements increases with advancing gestational age and has been related to advancing maturity of the foetal nervous system [8].

Recapitulating, it is possible to say that some studies evaluated changes in FHR pattern with advancing gestation and found a gradual fall in baseline with advancing gestational age up to 30 weeks corresponding to the progressive vagal dominance [23]. Similarly, an increase in variability was seen and an increase in the number of accelerations [13], which become larger in amplitude and duration [8]. Transient decrease of the FHR below the baseline level of at least 10 bpm for at least 15 bpm [6].

Decelerations can be classified into early, variable and late decelerations and each type can be connected to a specific pathophysiological phenomenon [8].

<u>Early decelerations:</u> they are caused by foetal head compression during uterine contractions, resulting in vagal stimulation and slowing of the HR. They represent uniform, repetitive, periodic slowing of FHR corresponding to the contractions. This type of deceleration has a uniform shape, with a slow onset that coincides with the start of the contraction and a slow return to the baseline that coincides with the end of the contraction. Thus, it has a characteristic mirror image of the contraction. Although these decelerations are not associated with foetal distress and thus are reassuring, especially during the second stage of labour, they must be carefully differentiated from the other, non-reassuring decelerations [23].

<u>Late decelerations:</u> they are associated with uteroplacental insufficiency and are provoked by uterine contractions. Any decrease in uterine blood flow or placental dysfunction can cause late decelerations. A late deceleration is a symmetric fall in the foetal heart rate, beginning at or after the peak of the uterine contraction and returning to baseline only after the contraction has ended. The descent and return are gradual and smooth. Regardless of the depth of the deceleration, all late decelerations are considered potentially ominous [23]. They are particularly found in association with severe intrauterine growth retardation, a reduction in the amount of amniotic fluid and abnormal flow-velocity waveforms in foetal or umbilical vessels [8]. Moreover, in some studies, a marked increase in the number of cerebral palsy was found in association with multiple late decelerations. This risk was further increased if both late decelerations and reduced baseline variability were present [13].
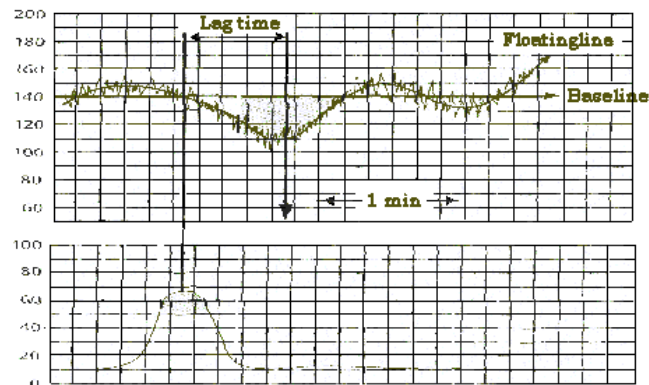
Figure 8: on the top example of late deceleration, on the bottom relative UC

Variable decelerations: they are shown by an acute fall in the FHR with a rapid downslope and a variable recovery phase. They are characteristically variable in duration and intensity. Time relationships with contraction cycle are variable and may occur in isolation. Variable decelerations are baroreceptor mediated and reflect changes in the blood pressure of the foetus due to compression of the umbilical cord [8]. Pressure on the cord initially occludes the umbilical vein, which results in an acceleration and indicates a healthy response. This is followed by occlusion of the umbilical artery, which results in the sharp downslope. Finally, the recovery phase is due to the relief of the compression and the sharp return to the baseline, which may be followed by another healthy brief acceleration or shoulder. Variable decelerations may be classified according to their depth and duration as mild, moderate and severe (depth below 70 bpm and duration longer than 60 s) [23]. Uncomplicated variable decelerations were not consistently shown to be associated with

poor neonatal outcome (reduced five-minute Apgar scores – see chap. 6- or metabolic acidosis) [13].

Prolonged decelerations: they are abrupt decreases in FHR values to levels below the baseline that lasts at least 60-90 seconds [13]. These decelerations become pathological if they cross two contractions.

3.3.1   FHR patterns

Silent trace: it corresponds to an oscillation amplitude of 5 bpm or less; sometimes, oscillations in the range of 3 to 5 bpm with normal oscillation frequency are observed during rest periods in normal foetuses [6][3].

Reduced undulating trace: it has an oscillation amplitude of 5-10 bpm [6].

Undulating trace: it presents an oscillation amplitude in the range 11-25 bpm. This kind of trace represents the physiological reactions to internal and/or external stimuli of a healthy foetus [6].

Saltatory trace: it corresponds to oscillations greater than 25 bpm [3]. It is common in presence of frequent and large foetal movements.
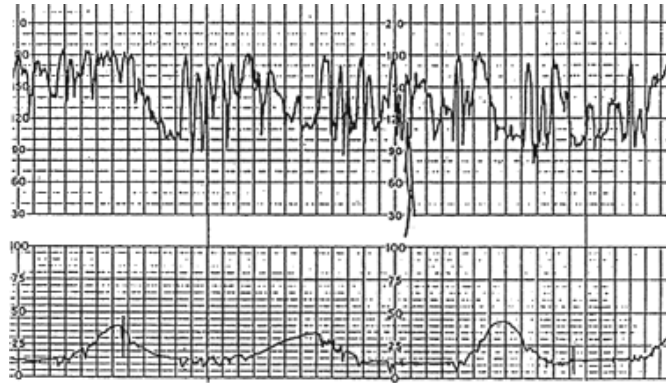
Figure 9: example of saltatury FHR trace (on the top) andUC signal (on the bottom)

Sinusoidal trace: the definition of sinusoidal FHR patterns varies in the literature. However, it is generally considered as a regular, smooth, oscillation of the baseline long-term variability resembling a sine wave [13]. It occurs with a frequency of 2 to 5 cycles per minute and an amplitude range of 5 to 15 bpm. It is also characterized by a stable baseline FHR of 120 to 160 bpm and absent beat-to-beat variability [23]. It is rare but ominous and associated with high rates of foetal morbidity and mortality.

3.3.2   Foetal behavioural states

Foetal intrauterine behaviour is not stable but it consists of continuous alternation of states characterized by significant changes in foetal motility, heart rate, hemodynamics,

metabolism and response to stimulation [25]. Characteristic behavioural states do exist for the human foetus. These states have been called 1F to 4F and resemble states in the neonate. States 1F and 2F are similar to non-REM sleep or quiet sleep and REM sleep or active sleep respectively. The foetus spends most of the time in these two states.

Behavioural states are defined as combinations of physiological and behavioural variables, repeatedly recurring, not only in the same subject [25]. In particular, each state can be characterized by a particular combination of 3 variables: presence or absence of foetal eye movements and body movements, and FHR patterns. From about 36 weeks these combinations can be recognized during longer periods without interruptions, and with clear state transitions [26].

The four foetal behavioural states were defined as follows [26]:

State 1F: quiescence, which may be regularly interrupted by brief gross body movements. Eye movements absent. Stable FHR pattern, with a narrow oscillation bandwidth. Isolated accelerations occur, strictly related to movements.

State 2F: frequent and periodic gross body movements, mostly stretches and retroflexions, and movements of the extremities. Eye movements continually present. The FHR shows a wider oscillation bandwidth with frequent accelerations in association with movements.

State 3F: gross body movements absent, and eye movements continually present. The FHR is stable, but has a wider oscillation bandwidth than in state 1F and a more regular oscillation frequency than in state 2F. No accelerations.

State 4F*:* vigorous, continual activity with many trunk rotations. Eye movements present. The FHR pattern is unstable, showing large and long-lasting accelerations, often fused into sustained tachycardia.

It is important to emphasize that these states are clearly established only near term, by about 36 week of gestation [3] [25].
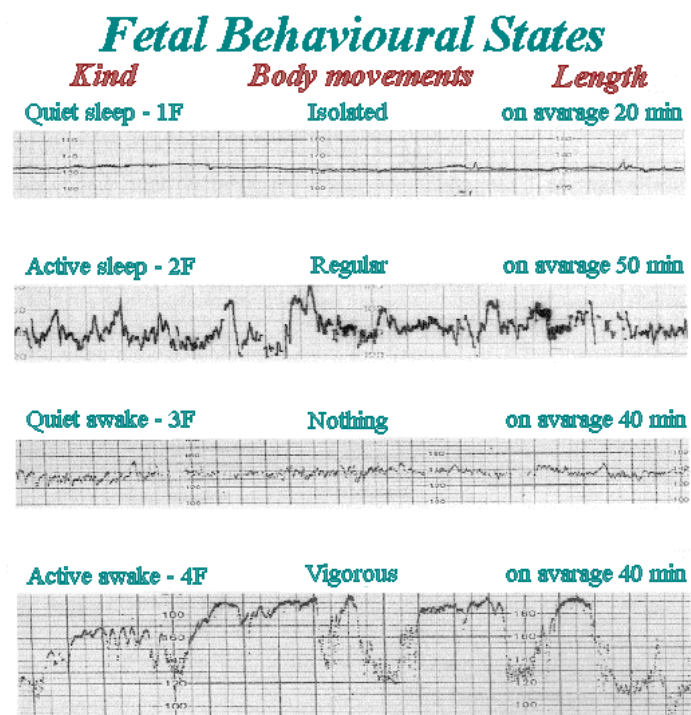
Figure 10: characteristic FHR patterns in foetal behavioural states

Knowledge of foetal behavioural states is necessary for an adequate interpretation of the foetal heart rate patterns [26].

3.3.3   Interpretation of EFM

First of all, interpretation of EFM requires a definition of what is normal. The definition of normal should be derived by the identification of cases where values outside a given normal range increase the likelihood of the adverse outcomes. Clearly, the impact of individual FHR features on perinatal outcome is varied. In clinical practise, CTGs are not analysed on individual features. Instead, an overall assessment of a number of features is made and these are used to make clinical decisions in the light of clinical factors and the stage of labour [13].

It is possible to refer to the following categorisation of FHR features.

Feature	Baseline (bpm)	Variability (bpm)	Decelerations (dec)	Accelerations
Reassuring	110-160	≥5	None	Present
Non-reassuring	100-109 161-180	<5 for ≥40 but less than 90 min.	Early dec. Variable dec. Single prolonged dec up to 3 minutes.	The absence of accelerations with an otherwise normal CTG is of uncertain significance
Abnormal	<100 >180 Sinusoidal pattern ≥ 10 min.	<5 for ≥90 min.	Atypical variable dec. Late dec. Single prolonged dec >3 minutes.	

Table 1: categorisation of Foetal Heart Rate features

Based on this categorisation of FHR features, it is possible to make the following categorisation of FHR traces

Category	Definition
Normal	A CTG where all four features fall into the reassuring category
Suspicious	A CTG whose features fall into one of the non-reassuring categories and the remaining features are reassuring
Pathological	A CTH whose features fall into two or more non-reassuring categories or one or more abnormal categories

Table 2: categorisation of Foetal Heart Rate traces

However, the CTG trace should be interpreted only in the context of the clinical scenario, and any therapeutic intervention should consider the maternal condition as well as that of the foetus [23]. Generally, the agreement between experts on normal FHR traces is significantly better than that seen with suspicious or pathological traces.

3.4 UC signal

About uterine contractions signal, the main features are: frequency, intensity and resting tone [6]: the frequency is the number of uterine contractions in time unit or number of contractions in 10 min; the resting tone or Basal tone is the lowest pressure recorded in absence of uterine contractions, its value is about 10 mmHg (this definition and value refer to direct measurements of intrauterine pressure); the intensity is the difference between recorded maximum pressure and resting tone.

3.4.1 Physiological conditions

In physiological conditions, the uterine activity is characterised by a resting tone $<= 15$ mmHg and UC with intensity of 30-50 mmHg and frequency of 2-5 contractions in 10 min. [6]. During delivery, three kinds of contractions can be observed.

Kind I, 80% of contractions at the labour onset, is characterized by a slow upslope and a fast downslope after contraction's apex.

Kind II, less than 30%, is bell shaped, symmetrically respect to the contraction's apex.

Kind III, from 20% at the onset of labour to 90% or more in expulsive period, is symmetric respect to kind I, fast upslope and slow downslope.
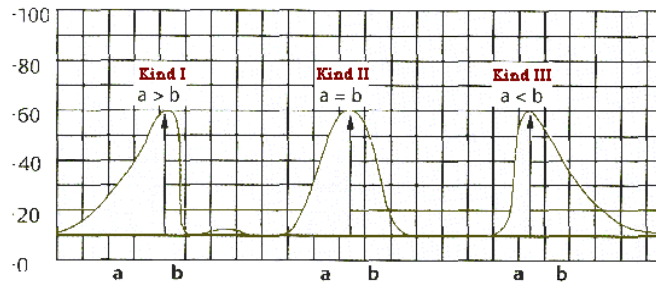
Figure 11: different kinds of uterine contractions

3.4.2   Pathological conditions

Only some of the most common kinds of pathologies will be reported in this study. Some of them are uterine hypokinesia or hyperkinesia. In the first case the contractions have low intensity and frequency, for example due to sedatives. In the second case, the contractions have high intensity and frequency; in this situation, for example due to excessive dosage of oxytocin, between two subsequent contractions there is not sufficient time for an adequate recovery of oxygen, so a respiratory acidosis can rise.

3.5   FHR recording

The most important aim of foetal surveillance is to avoid intrauterine death or permanent damages to the foetus. So, in industrialised countries, all pregnant women periodically take pregnancy and foetal well-being controls. It is very important to collect right information about foetus' health also in order to correctly plan successive diagnostic tests. The widespread diagnostic tool, ultrasonographic Doppler cardiotocography (US-CTG), has some limitations: some pathologies and some anomalies of cardiac functioning are not detectable. Moreover, although frequent and/or long-term FHR monitoring is recommendable, mainly in risky pregnancies, there is no strong evidence how long application of ultrasound irradiation can be taken as absolutely harmless for the foetus. Finally, the high quality ultrasound devices are so expensive that they are not available for home care use. Therefore, in the last years, many efforts are been paid by the scientific community to find a suitable alternative.

The development of new electronic systems and sensors now offer the potential of effective monitoring of foetal phonocardiography (FPCG) and foetal electrocardiography (FECG) with passive, fully non-invasive low cost digital recording systems that could be suitable also for home monitoring. These advances provide the opportunity of extending the recordings of the current commonly used US-CTG from relative short to long term, and provide new previously unavailable measures of cardiac function.

The objective of foetal monitoring is to assess foetal well-being and status including the pattern of foetal growth and maturation, oxygen availability, neurogical function and

cardiac function. There are two situations for which FHR provides important information about the condition of the foetus: a normal reactive foetal monitor tracing identifies a foetus that has no trouble with the events of labour and a non-reactive, non-reassuring tracing with complete loss of reactivity and variability identifies a foetus that is unable to respond [27]. It is expected that as the foetus moves the heart rate will temporarily accelerate in response to stimulation by the nervous system. If after foetal movement the physician observes two to three accelerations of greater than 15 beats per minute for 15 seconds the result of the non stress test is indicated as Reactive. Alternatively the test is deemed to be Non-reactive if no accelerations were observed or the observed accelerations did not meet the criteria for a reactive test. It is interesting to compare the clinical significance of both the reactive and non-reactive results; the reactive result is considered a reasonably reliable indicator of reassuring foetal development and well-being whereas the non-reactive result can have more than one explanation and consequently isn't as useful. If the non stress test was deemed to be non-reactive it could be concluded that: the foetus is compromised, the patient is incorrectly positioned, the test is being effected by drugs in the maternal system or the result is false [28].

FHR can be monitored by means of different techniques: CTG, magnetocardiography, electrocardiography (ECG), phonocardiography (PCG), described in the following paragraphs.

3.5.1 *Ultrasonographic Doppler cardiotocography*

CTG is one of the most diffused, non-invasive pre-natal diagnostic techniques, in clinical practice, to monitor foetal health, both in ante partum and intra partum period. In some countries, it is a medical report with legal value. CTG monitoring has been proved to be useful, especially in ante partum period; since its introduction in the 1960s, electronic foetal monitoring led to a considerable reduction of perinatal morbidity and mortality. It can be used from the 24th week of gestation to delivery. However, in clinical routine, it is generally used from the 35th week. In CTG monitoring, FHR and uterine contractions (UC) are simultaneously recorded by means of two probes placed on the maternal abdomen: an ultra sounds Doppler probe for FHR signal and a pressure transducer for UC signal [29].

FHR monitoring using the Doppler shift resulting from the movements of the heart is a standard examination in most obstetrical wards. It consists in aiming an ultrasonic beam at the foetal heart. The ultrasound reflected from the heart walls and/or valves is slightly Doppler shifted as a result of the movements of the heart. After demodulation this Doppler shift is used to extract the FHR and the results plotted continuously as a function of time. Most foetal monitors use continuous wave ultrasound but some of the latest models use pulsed ultrasound. The ultrasonic frequencies used range from 1-2 MHz [30].

The advantage of the Doppler ultrasound technique is that it can be virtually assured that a recording of FHR will be obtained. The disadvantages of such systems are that they require intermittent repositioning of the transducer and are only suitable for use with highly trained midwifes. Because the procedure involves launching a 2 MHz signal towards the foetus, the use of Doppler ultrasound is not suitable for long periods of FHR monitoring.

Moreover, although frequent and/or long-term FHR monitoring is recommendable, mainly in risky pregnancies, there is no strong evidence if long applications of ultrasound irradiations can be taken as absolutely harmless for the foetus [31]. Therefore, in the last years, many efforts have been paid by the scientific community to find a suitable alternative.

The major limitation of the Doppler ultrasound technique is its sensitivity to movement. The movement of the mother can result in Doppler-shifted reflected waves, which are stronger than the cardiac signal. Thus the Doppler ultrasound technique is inappropriate for long-term monitoring of the FHR, as it requires the patients to be bed-rested. Moreover, the detection of the heartbeat using Doppler ultrasound relies upon a secondary effect (the mechanical movement of the heart) and is therefore not as accurate for beat-to-beat analysis as detection of the QRS complex. Allied to this drawback is the fact that most Doppler systems rely upon some form of averaging to produce their In addition, FHR is the only parameter obtained by Doppler ultrasound; some pathologies and anomalies of cardiac functionality are not detectable, while research has shown that a global assessment of morphological and temporal parameters of the foetal electrocardiogram (FECG) of the foetus during gestation or acoustic recording of foetal heart sounds can provide additional information about the foetal well-being [32][33][34].

3.5.2 Foetal magnetocardiography

The foetal magentography (FMCG) is based on the measurement of the magnetic fields produced in association with cardiac electrical activity [27]. The recording uses the SQUID (Superconducting Quantum Interference Device) biomagnetometry technique. The FMCG contains morphological and temporal similarity to the FECG even though they are based on very different types of measurements, i.e., the electrical field and the magnetic field.

The disadvantages of the FMCG are size, cost and complexity of the required instrumentation. It can be recorded reliably from the 20th week and onward. Moreover, it is mainly unaffected by the insulating effects of the vernix caseosa and the existence of preferred conduction pathways. The FMCG remains reliable for measuring the foetal electrocardiological activity throughout the second and third trimesters of pregnancy.

Thus far reported, the FMCG is generally of a higher quality than the FECG as it has the advantage of exhibiting virtually no interference from the maternal ECG. The FMCG can be used to classify arrhythmias such as heart blocks and atrial flutter, and to diagnose a prolonged QT-syndrome. Using FMCG, there are studies of detecting foetuses with congenital heart diseases.

Finally, it does still remain a research tool and is currently little used in clinical routine because of its size, cost, complexity of the required instrumentation and cumbersome sensors [35][36][37].

3.5.3   Foetal phonocardiography

The preliminary evaluation done by Baskaran and Sivalingam [38] has shown that there are three significant differences in the characteristics of foetal heart sounds between intrauterine growth retarded and normal foetuses in the antenatal period. Although it was just a preliminary study, but it has, in fact, further inspired the possibility to employ FPCG to identify foetuses at risk. This could be a significant contribution to the pressing clinical problem faced by some unborn and newly born babies. FPCG performs a recording of UC by means of a usual pressure transducer and a passive (no energy beam is transmitted to the foetus), fully non-invasive and low cost acoustic recording of foetal heart sounds [32][33] [34]. This signal can be captured by placing a small acoustic sensor on mother's abdomen without the use of gel and, if appropriately recorded, it is a sensitive signal very useful in providing clinical indication.

The foetal heart is basically divided into two pairs of chambers and has four valves: the mitral and tricuspid valves. In the foetal cardiac cycle, when the ventricles begin to contract, the blood attempt to flow back into the lower pressure atrial chambers: this reverse flow of blood is arrested by the shutting of the mitral and tricuspid valves , which produces the first heart sound (S1). Whenever the pressure in the ventricular chambers becomes too high for the pulmonary valves to withstand, they open, and the pressurized blood is rapidly ejected into the arteries. While the ventricles are being evacuated, the pressure of the remaining blood decreases with respect to that in the arteries. This pressure gradient causes the arterial blood to flow back into the ventricles. The pulmonary valves, arrest this reverse flow by shutting, which gives rise to the second heart sound (S2) [39].

The intensity of S1 is generally increased by greater pressure within the left ventricle as the resistance within the pulmonary artery increases and as the blood passes from the left atrium. This greater pressure results in the closure of the mitral valve with greater force, thus producing a more intense sound [40]. On the other hand, S2 is considered to be particularly more useful when diagnosing cardiac disease [40] and is produced by the ejection of blood from the ventricles out through the aorta and pulmonary artery [41].

In conclusion FPCG provides valuable information concerning the physical state of unborn in the womb and has the potential for detection of cardiac functionality anomalies, such as murmur, split effect, extra systole, bigeminal/trigeminal atrial. Such phenomena are not obtainable with the traditional CTG technique or other methods [38][42][43].

3.5.4   Foetal electrocardiography

FECG [44][45] has been also deeply studied, but its recording through multiple electrodes placed on the maternal abdomen makes difficult to obtain high quality signals; moreover, the automated evaluation of FECG is less accurate than CTG [33].

ECG is a graphical recording of the electrical potentials generated in association with heart activity. Aristotle first noted electrical phenomena associated with living tissues and Einthoven was able to measure the electrical activity of the heart in 1901 that resulted in the birth of electrocardiography [27]. As the heart is not directly accessible, cardiac electrical activity is usually inferred from measurements recorded at the surface of the body, e.g., at the arms, legs, and chest.

Electronic foetal monitoring can be external (outside), internal (inside), or both.

Internal methods for acquiring the FECG are invasive because internal monitoring involves placement of a small plastic device about the size of a pencil eraser through the cervix. A spiral wire called the foetal scalp electrode is placed just beneath the skin of the foetal scalp. The foetal scalp electrode then transmits direct information about the FHR through a wire to the foetal monitor that prints out this information. Because the internal foetal monitor is attached directly to the baby, the FECG signal is sometimes much clearer and more consistent than with an external monitoring device. However, there may be a slight risk of infection with internal monitoring.

Obviously, a foetal scalp electrode cannot be used ante partum period as there is a significant risk of causing a mark or small cut on the foetal head [46].

In contrast, methods utilizing the abdominal FECG have a greater prospect for long-term monitoring of FHR (e.g., 24 h) and foetal well-being using signal-processing techniques.

In fact, the FECG is an electrical signal that can be obtained non-invasively by applying multi-channel electrodes placed on the abdomen of a pregnant woman; therefore the three main characteristics that need to be obtained from the FECG extraction for useful diagnosis include [47]: FHR, waveform amplitudes and waveform duration.

The detection of FECG signals with powerful and advanced methodologies is becoming a very important requirement in biomedical engineering with the increasing in FECG signal analysis in clinical diagnosis and biomedical applications. The FECG contains potentially valuable information that could assist clinicians in making more appropriate and timely decisions during labour, but the FECG signal is vulnerable to noise, and difficulty of processing it accurately without significant distortion has impeded its use.

4. ULTRASONOGRAPHIC DOPPLER CARDIOTOCOGRAPHY

US-CTG is one of the most diffused, non-invasive pre-natal diagnostic techniques, in clinical practice, to monitor foetal health, both in ante partum and intra partum period. In some countries, it is a medical report with legal value. US-CTG monitoring has been proved to be useful, especially in ante partum period; since its introduction in the 1960s, electronic foetal monitoring led to a considerable reduction of perinatal morbidity and mortality. It can be used from the 24th week of gestation to delivery. However, in clinical routine, it is generally used from the 35th week.

Cardiotocographic data provides physicians information about healthy foetal development. To assess foetal health and reactivity, gynaecologists and obstetrics evaluate specific clinical signs (average value of FHR, number and kind of accelerations and decelerations in FHR signal, number and intensity of UC and their correlation with FHR modifications, etc). Interpretation of CTG is generally based on eye inspection of the clinicians. The validity of this diagnostic procedure is still limited by the lack of objectivity and reproducibility. Moreover, important physiological mechanisms, like thermoregulatory oscillations, maturational changes with advancing gestational age, foetal behavioural states and maternal drugs can influence FHR. An incorrect evaluation of foetal status is of course very dangerous. On one hand a falsely diagnosed foetal distress may lead to an unnecessary intervention; on the other hand, an incorrect diagnosis of foetal well-being may deny the necessary care [8].

Therefore, more detailed information about the foetal status are necessary and can be particularly useful during the last period of gestation. To achieve this aim, several analysis methodologies have been proposed in recent years (FHR variability analysis, non-linear methodologies, automatic software, etc. [3][48][13][49].

Great interest has been dedicated to the variability of the FHR around its baseline, named FHR variability (FHRV), which, like so for adults, could be a base for a more powerful, detailed and objective analysis, both in ante partum and in intra partum period [20][50][51][52][53].

FHRV can be analysed both in time domain and in frequency domain. However, the power spectral density (PSD) seems to be the index that best recovers all the information present in the HR series [54]. In particular, due to non-stationary nature of FHR, the time-frequency analysis of the FHRV is generally employed.

As it is well known, time-frequency analysis is a very useful tool, since it allows for a study of all signal frequency components and their modifications over time. In the non-stationary case, the PSD consists of a function that represents the energy content of a series in the time-frequency domain. Several methods there exist to estimate it and the method best suited for the PSD evaluation depends on the particular application (often an empirical approach is followed for method choice) [55]. Among most commonly employed methods, parametric and non-parametric, we can mention Short-time Fourier transform (STFT); Auto Regressive methods (AR); Fast Recursive least square algorithms (RLS) [50][52][53][55].

The results described in this chapter were presented in different international congresses [56] and published on journal papers: "Time-frequency analysis of CTG signals" [57],

"Foetal heart rate variability frequency characteristics with respect to uterine contractions" [58] and "PSD modifications of FHRV due to interpolation and CTG storage rate" [59].

4.1 Time-frequency analysis of US-CTG signals

In foetal monitoring field, time-frequency analysis is often adopted as a simple, non-invasive tool for investigating the functional state of the autonomic nervous system (ANS) and specifically the autonomic control of the cardiovascular system [36][60]. For example, foetal HRV response to stimuli can reveal precious information about ANS reaction and compensation, which in turn depends on foetal well-being status. Studies of both term and pre-term infants suggest that new information may be obtained from accurate beat-to-beat HRV analysis.

Aim of the following study was to show some very useful examples of FHR time-frequency analysis purposes.

Indeed, time-frequency analysis of FHRV has been proved to be a good indicator for the evaluation of foetal well-being and reactivity in non-stress conditions. Foetal reactivity is considered a very important CTG characteristic to diagnose foetal health or distress but its interpretation is still somewhat uncertain. An improvement can be accomplished characterising foetal reactivity proposing new FHRV frequency-domain parameters to distinguish between reactive and non-reactive foetuses and therefore support a more exhaustive CTG analysis [53].

In foetal monitoring, furthermore, as above mentioned, it can be worth investigating eventual FHRV time-frequency modifications of PSD, which reflect foetal ANS activities in response to stimuli.

In particular, spectral analysis provides a tool for quantifying rather small changes in FHRV that may remain undetected if only visual interpretation of FHR tracings is used. Changes in FHR control, elicited by the ANS in response to foetal hypoxia, were for example reported in literature [8][48].

A UC is a strong compressive stimulus; it provokes an acute hypoxic stress to the foetus and generally elicits reactions in the FHR. It is well known that a FHR deceleration usually follows a UC and this sign is of great interest for physicians. Interest in studying UC reactions is also outlined by recent studies in which UC were elicited by an oxitocin challenge test to explore the consequent blood flow changes [52][61][62]. In conclusion, it is worth investigating eventual FHRV spectral modifications, which reflect foetal ANS reactions to UC.

Before FHR signal processing, it is worth mentioning that FHR signals are intrinsically uneven series; each FHR value is computed as inverse of the time between two consecutive R waves, so that FHR values are available only when new heart beats occur.

In general, to obtain evenly sampled series, commercial cardiotocographs (e.g. HP-135x) use a zero-order interpolation, that is each sample is held constant until the next heart beat occurs. Hence, with reference to FHR, if no new foetal beat is detected within a sampling interval (250 ms in HP cardiotocographs, corresponding to a storage rate of 4 Hz), the previous value is held (zero-order interpolation) [63]. This simple process provides FHR data at fixed sampling time instants (i.e. in the same time instants when UC values are

recorded), by delaying some samples and adding some duplicates (in the case of missed or undetected heart beats). This is an efficient solution for FHR time-domain or other rough analyses, e.g. to compute classical parameters, such as baseline, accelerations and decelerations, but it is not suitable for frequency analyses because interpolation introduces alterations in the FHR power spectrum [54]. In particular, this interpolation process produces possible artifacts and an attenuation of the high-frequency components of the PSD that, for example, affects the estimation of the sympatho-vagal balance (estimated as low-frequency/high-frequency power ratio), which represents an important clinical parameter [36][64][65].

Furthermore, some commercial software, employed for semi-automatic CTG analysis, in order to reduce required space memory and computational time, records US-CTG data at a lower storage rate (for example 2 Hz) involving data missing [29].

In order to eliminate the spectrum alterations due to zero order interpolation, and, more generally, to recover the true (unevenly spaced) FHR series from CTG data, the duplicated samples cannot be simply deleted, since duplicated samples can arise by equal subsequent beat-to-beat intervals, so a pre-processing algorithm was developed for this goal.

4.1.1   Processing (UCII)

Data collection

US-CTG signals were recorded during routine foetal monitoring, in an Italian public hospital, from 35 healthy pregnant women (singleton pregnancies), close to delivery (33-42 gestation weeks), who did not take drugs and having no known genetic malformations;

subjects laid down in a rest position. In line with clinical practice, US-CTG signals lasting less than 20 min or excessively noisy signals were excluded from the database (at the moment populated by about 600 CTG). 35 recordings were gathered for this study, 3 intra partum and the others with evident UC. On average, US-CTG recordings have a duration of about 30 minutes. At birth, Apgar scores, birth weights and other information were collected in order to involve in the analysis only CTG regarding healthy foetuses: in particular, enrolled infants had Apgar scores >=7 at 1st minute and >= 9 at 5th minute, birth weights (ranging from 2.7 to 4.25 Kg) appropriate for the gestational age and no one needed neonatal intensive care unit treatment.

US-CTG signals were acquired using HP-135x or Sonicaid cardiotocographs, equipped with an ultrasound Doppler probe to detect FHR signals (measured in beats per minute - bpm) and a pressure transducer to record UC signals (measured in mmHg). Both probes were placed upon maternal abdomen.

In HP cardiotocographs, FHR and UC signals are internally stored at 4 Hz (corresponding to a sampling interval of 250 ms). On the contrary, in Sonicaid cardiotocograph, FHR and UC signals are unevenly stored. Both devices provide a three-level signal which indicates the 'quality' of the received Doppler signal, which can result optimal, acceptable or insufficient (the latter corresponding to signal loss). In both cases, recorded data are transferred to the output serial port of the device that was connected to a laptop PC through a serial (RS232) connection.

Signal selection

US-CTG recordings with evident UC were chosen for the analysis; as done in previous works of the authors [6][66]. UC were selected respecting specific criteria in order to

reduce the physiological variability and to achieve a sort of uniformity for the UC stimuli. In particular, only uterine contractions of pronounced amplitude (at least 40 mmHg with respect to the resting tone), isolated (at least 130 s must elapse between the end and the start of two subsequent contractions), corresponding to good FHR and UC signal quality were considered for the analysis. About 100 UC, compliant with the above-mentioned specifications were enrolled in the analysis.

In order to carry out a quantitative comparison between the FHRV power spectrum modifications related to UC with respect to a reference condition, two kinds of time segments of the same length (231 samples, about 57 s) were selected (here called 'reference-segments'), chosen before the UC onset and 'UC-segments', chosen in correspondence of the UC (slightly retarded with respect to the UC apex) (please, refer to [6] for more detailed information).

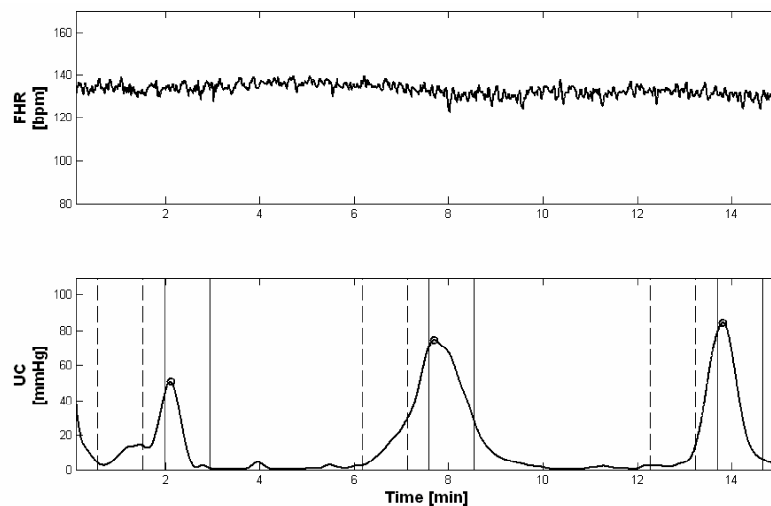Figure 12 offers an example of US-CTG signals and chosen segments.

Figure 12: example of US-CTG recording (from the top, FHR and UC signals) during labour, subject #12 - week 40th. It is possible to recognise three UC, which were selected according to the required criteria. Couples of vertical dashed lines represent start and end of reference segments and vertical solid lines represent start and end of UC segments.

FHRV time-frequency analysis

According to literature and previous works [6][29][66], we considered the FHR power spectrum mainly composed of a DC component (average of the FHR), a very low frequency (VLF) band (0-0.03 Hz) and FHR variability (FHRV) at higher frequencies. Therefore, FHRV signals were obtained evaluating (and then subtracting) components at lower frequencies by means of a smoothing cubic spline.

After that, because of the non-stationary behaviour of the FHRV signal, a time-varying frequency analysis by means of STFT had been carried out considering sliding Hamming windows of 128 samples (corresponding to 32 s) and using 99% overlap (window length was chosen according to literature [67]).

Finally, to concisely describe spectral modifications against time, the power associated with LF (0.03-0.2 Hz) and HF (0.2-1 Hz) bands was computed, for each time instant, PLF (t) and PHF(t), as expressed by [6]:

$$P_{LF}(t) = \frac{1}{T} \int_{0.03}^{0.2} |S(f,t)|^2 \, df$$

$$P_{HF}(t) = \frac{1}{T} \int_{0.2}^{1} |S(f,t)|^2 \, df$$

(1)

where, S (f, t) represents the time-varying spectral estimation of the FHRV signal and T is the time interval considered [6].

In order to highlight a common foetal ANS response to UC in a physiological situation, we also performed an average of LF and HF power signals (computed both for UC and references segments).

To further characterise PSD modifications of FHRV signals related to UC, we carried out an analysis to detect, at each time instant, the maximum frequency bin contained in the signal's spectrum. To this aim, we used the "Modified Crossing Threshold Method", based on D'Alessio's algorithm [66][67][68]. The method considers that the tail of the spectrum gives information on the level of noise present in the signal, since white noise is equally spread over all frequency. An estimation of the noise made in the tail of the spectrum is then used for setting a threshold. The magnitude of each bin of the spectrum is compared with the threshold and when the magnitudes of two successive bins are higher than the threshold, the first bin is considered as the maximum frequency bin. We evaluated the noise level using the bins from 14 to 32 of a 128 FFT array (corresponding to the frequency range from about 0.4 Hz to 1 Hz). The selected frequency range to evaluate the noise depends on the method used in evaluating the FHR and its spectrum array [68], which could substantially modify the far tail of the spectrum. The algorithm threshold is computed multiplying this estimation of noise for an integer factor; we heuristically chose a value of 5, which means that the probability value for which a sample crosses the threshold is less than 1% in presence of only noise [69].

A Student's t-test was employed to check the statistic separation between the analysed FHRV spectral populations (power in the different bands and frequency content of UC-segments and reference-segments; levels of statistical significance were always set at p value < 0.01).

For power estimation in HF band, we chose the fixed range 0.2 – 1 Hz, without considering the computed variable maximum frequency bin, in order to take into account noise contribution both for UC and ref segments.

4.1.2 Time-frequency analysis results (UCII)

As an example, figure 13 reports a spectrogram of a FHRV time-frequency distribution, obtained by STFT method, together with the corresponding US-CTG signal.
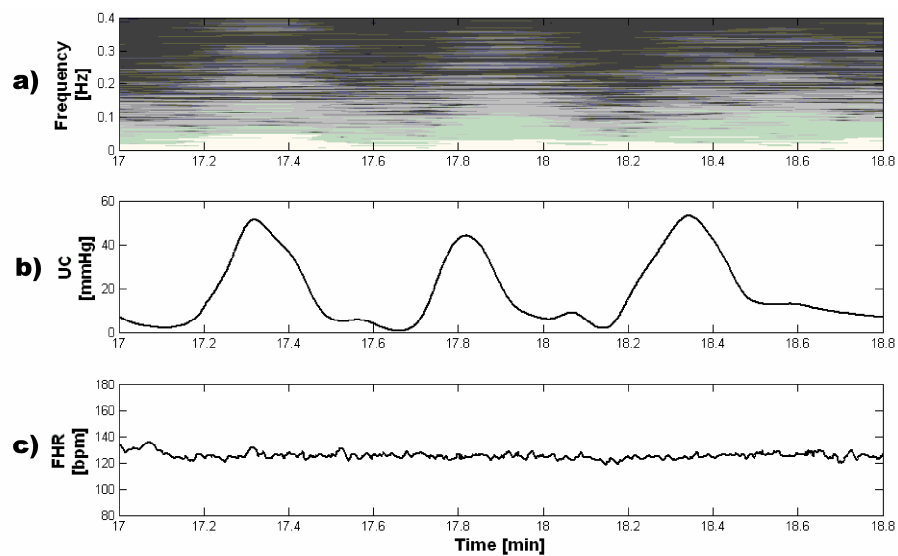

Figure 13: example of FHRV spectral modifications in correspondence of UC. From the top, spectrogram, evaluated by means of STFT, and US-CTG signal of the subject #24 (UC in 2b, FHR in 2c).

As illustrated by the previous figure, the FHRV power increases in correspondence of UC.

It is worth noting that this increase does not correspond, in the time domain, to a clear modification of the floating-line (id est, in the FHR signal there are no alterations, such as accelerations or decelerations, that could justify the power increase).

Furthermore, to present concise results, obtained average powers of LF and HF bands of FHRV power spectrum, estimated both for selected UC segments and reference segments, are reported in the following table.

	UC segments [bpm^2]	REF segments [bpm^2]
Power of LF band	459.44 (205.36)	183.72 (113.94)
Power of HF band	164.15 (85.36)	81.53 (62.15)

Table 3: powers in LF and HF bands, computed by means of STFT, are reported for the UC and reference segments in bpm2. Reported values represent average results computed on 108 segments, in brackets we report the standard deviation.

It is possible to note that average powers corresponding to UC-segments are higher than average powers corresponding to reference-segments. Moreover, UC-segments population resulted significantly different compared with reference-segments population for both FHRV power spectrum bands (*t*-test).

Concerning the analysis of FHR frequency content, results obtained by means of Modified Crossing Threshold Method highlighted that an enlargement of the band (shift to a higher value of signal maximum frequency bin) corresponds to the power increase of FHRV PSD. Figures 14 and 15 show an example of obtained results about the comparison between the power increase and the correspondent shift of signal maximum frequency bin.
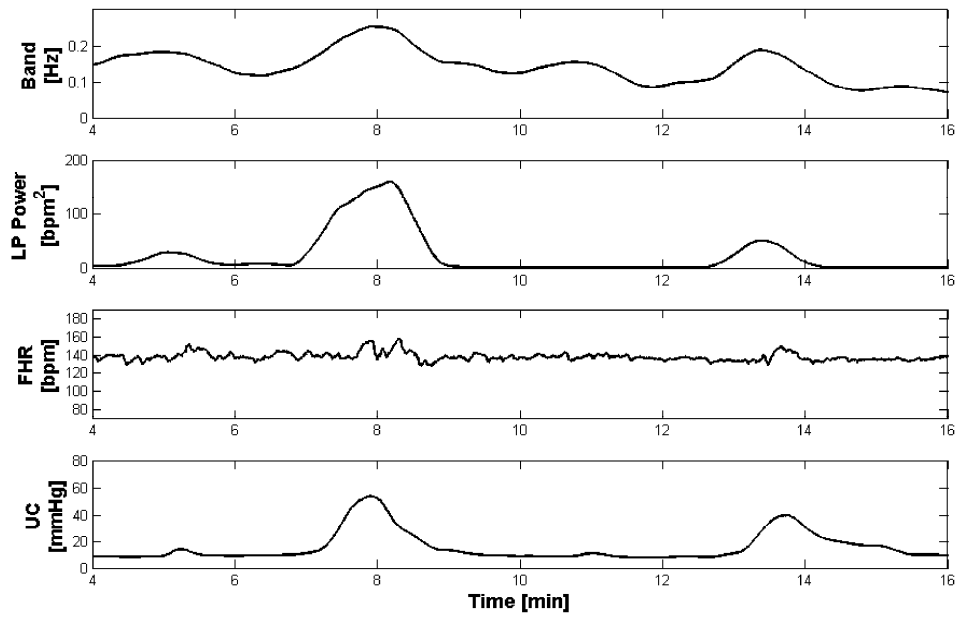
Figure 14: example of FHRV spectral modifications. From the top, frequency content, evaluated by means of the Modified Crossing Threshold Method, power of the LF band, and US-CTG signal of the subject #18.
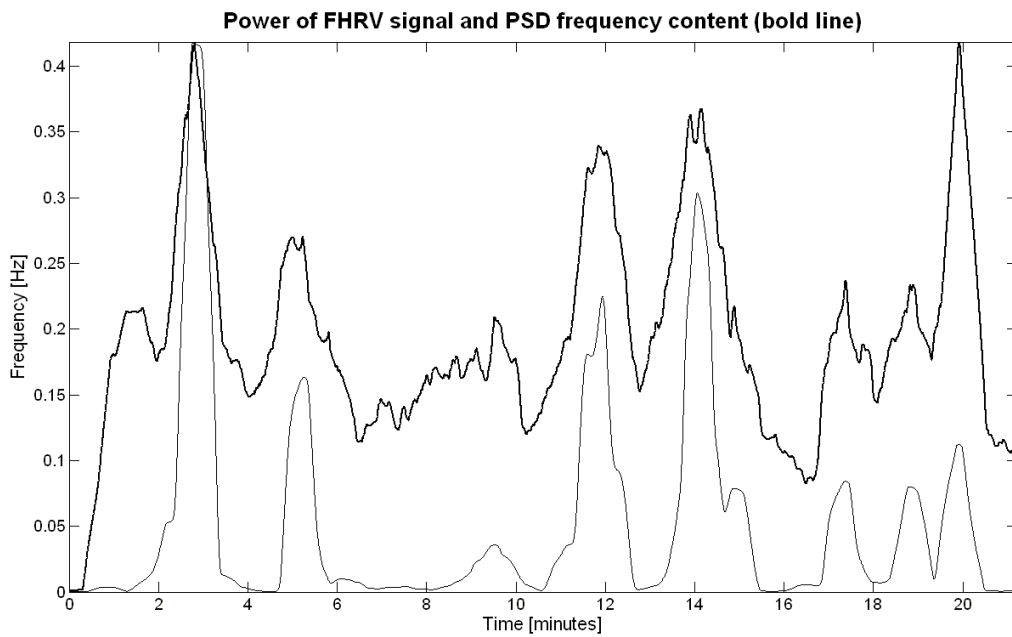

Figure 15: power of FHRV signal relative to US-CTG recording #37 is here represented in arbitrary units. In correspondence of a power increase a higher value of the signal maximum frequency (bold line), represented in Hz, can be found.

The average behaviour has been studied also in this case and obtained results are reported in the following table.

	UC segments [Hz]	REF segments [Hz]
Maximum frequency bin	0.218 (0.064)	0.172 (0.045)

Table 4: maximum frequency bin contained in the analysed signals both for UC segments and reference segments. Reported values represent average results computed on 108 segments, in brackets we report the standard deviation.

Average results highlighted, in correspondence of the UC, a percentage increase of the band, computed as:

$$\frac{\text{UC seg. value - REF seg. value}}{\text{REF seg. value}} \times 100 \qquad \textbf{(2)}$$

of about 27%. Also in this case, UC-segments population resulted significantly different compared with reference-segments population (*t*-test).

4.1.3   Foetal reactivity (CTG –TF)

Foetal reactivity was assessed, in ante partum period, by evaluating PSD characteristics of FHRV extracted from signals recorded in clinical environment. Once the FHR signals were pre-processed, 3 expert clinicians were asked to divide the selected US-CTG signals into two categories: reactive foetuses (RF) and non-reactive foetuses (NRF). A foetus is defined as reactive if two or more accelerations (an increase in the FHR of 15 bpm during at least

15 s) are identified within a 20 min US-CTG [70][71]. The foetus is declared non-reactive if the variability of the FHR is very tiny (less than 5 bpm) even in presence of foetal movements (detected as short, small spikes superimposed onto UC signal). The clinicians classified 75 CTGs as corresponding to RF and 20 to NRF.

According to literature and previous works [12][49] [72], the FHRV frequency analysis was carried out for each signal using only a 3 min segment (we decided not to use longer portions in order to collect a large number of comparable segments). The target was to emphasise eventual specific spectrum characteristics only related to steady physiological mechanisms and not to particular external or internal stimuli. Therefore, the 3 min segment was selected in absence of large FHR alterations (e.g. accelerations and/or decelerations) and other phenomena such as uterine contractions and/or foetal movements; segments were always corresponding to periods of low FHR variability.

After, the PSD grand averages relative to the two categories (RF and NRF) were evaluated. For each category, PSD peak values (expressed in bpm2/Hz) and their frequency positions were computed in LF and HF bands. For each frequency range, the mean power (expressed in bpm2), with SD of the powers corresponding to the different signals, were also evaluated.

A Student's t-test was employed to check the statistic separation between the analysed FHRV spectral power populations: RF and NRF categories in ante partum analysis (level of statistical significance was set at p value <0.05). The test was carried out separately for both LF and HF bands.

Characteristics of the average PSD of FHRV resulted strongly different between RF and NRF categories, confirming the usefulness of the frequency analysis as a support in

distinguishing foetal reactivity. The amplitude of the average PSD related to RF, its peak value and mean power resulted higher than those related to NRF, for each of the analysed frequency ranges (see figure 16 for results relative to LF band).

3D spectrum array

3D spectrum array
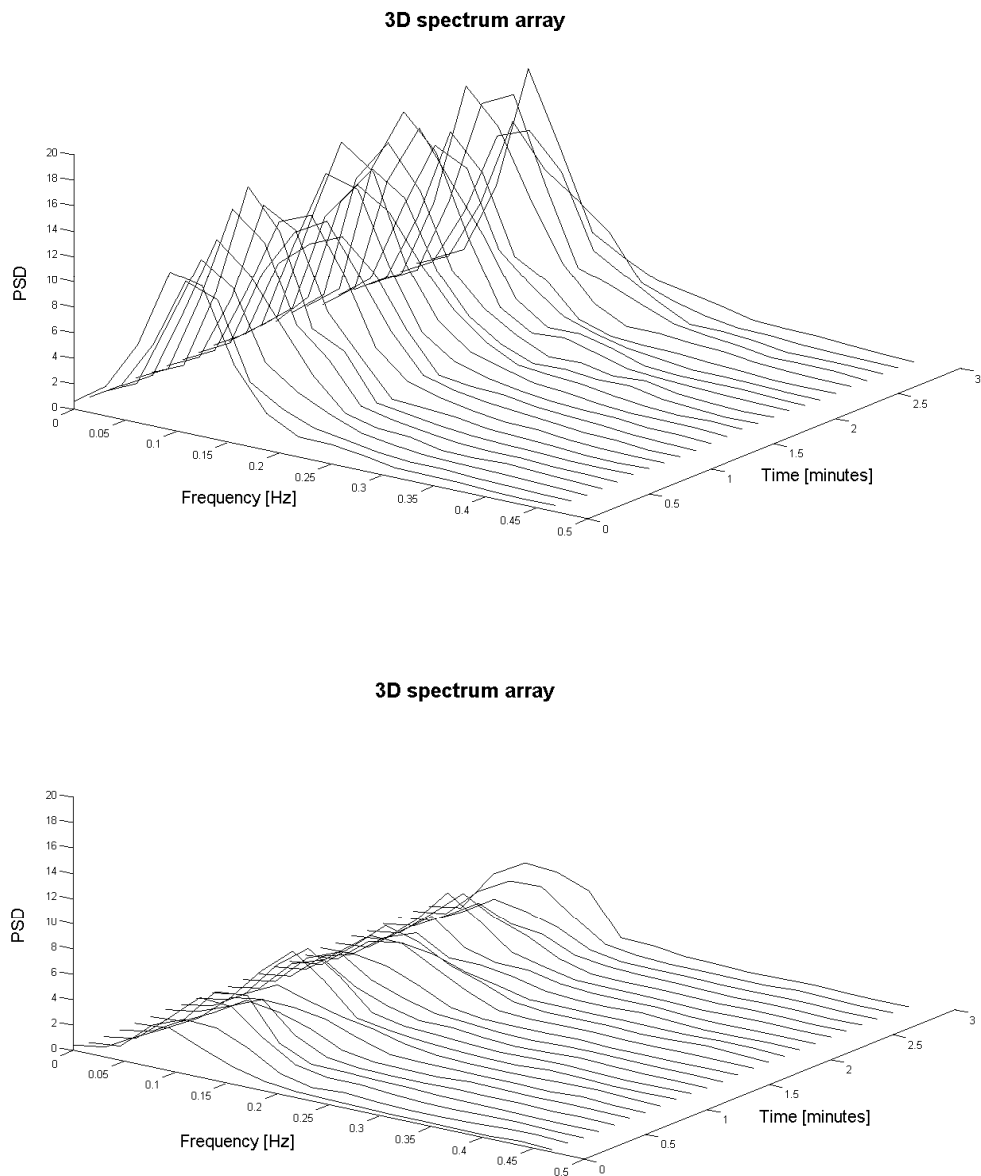
Figure 16: average PSD estimated on 75 FHR signals corresponding to reactive foetuses (top); average PSD estimated on 20 FHR signals corresponding to non reactive foetuses (bottom). Both PSD were computed on 3-minutes signal tracts.

No considerable difference was observed in the frequency peak position as shown in the following table.

	LF band				
	M=Maximum amplitude of PSD [bpm^2/Hz]	**Peak frequency [Hz]**	**Average power (AP) [bpm^2]**	**SD of AP**	**Number of segments**
RF	17,920	0,125	1,553	1,140	75
NRF	5,780	0,125	0,412	0,177	20

Table 5: PSD parameters evaluated for the LF band of FHRV relative to the two signal subsets (RF and NRF).

The populations of the average powers of the two categories (RF and NRF), computed in the LF band, resulted not completely separated, but partially overlapped. However, RF population resulted significantly different (*t*-test) compared with NRF population.

The average PSD was also computed, for each frequency range, in each week of gestation in the range 37-40. For each week of gestation, in the LF band, the PSD average corresponding to RF was higher than the PSD average corresponding to NRF (see next table).

LF band				
	Maximum amplitude of PSD [bpm^2/Hz]	Average power (AP) [bpm^2]	SD of AP	Number of segments
RF - 37th WG	30,510	1,532	1,014	16
NRF – 37th WG	11,828	0,434	0,177	3
RF – 38th WG	28,772	1,715	1,439	15
NRF – 38th WG	8,592	0,501	0,188	6
RF – 39th WG	24,342	1,609	1,387	15
NRF – 39th WG	9,188	0,364	0,266	3
RF – 40th WG	14,144	1,138	0,704	9
NRF – 40th WG	6,785	0,318	0,043	2

Table 6: PSD parameters evaluated for the LF band of FHRV relative to the two signal subsets (RF and NRF) and in each week of gestation. Total number of segments is different from that reported in Table 5: PSD parameters evaluated for the LF band of FHRV relative to the two signal subsets (RF and NRF). since some US-CTG involved in the average analysis were recorded in weeks of gestation not considered in this analysis.

Moreover, the average power shows a slight increase going from 37th to 38th week of gestation and then a slight decrease, both for RF and NRF categories. This result suites with previous literature findings [73].

4.2 PSD modifications of FHRV due to interpolation and US-CTG storage rate

Before any FHR signal processing, it is worth mentioning that FHR signals are calculated on an instantaneous basis (each FHR value is computed as inverse of the time between two consecutive R waves), so that FHR values are available only when new heart beats occur. So, FHR is intrinsically an uneven series and in order to perform spectral analysis using fast Fourier transform (FFT), the series should be interpolated and the resulting signal should be evenly sampled. Zero-order, linear or cubic spline interpolation can be employed. For example, to provide in output evenly sampled series, some commercial cardiotocographs (e.g. HP-135x) use a zero-order interpolation, that is each sample is held constant until the next heart beat occurs [63]. In particular, FHR and UC signals are internally recorded at a storage rate of 4 Hz (corresponding to a sampling interval of 250 ms). This process provides FHR data at fixed sampling time instants, by delaying some samples and adding some duplicates (in the case of missed or undetected heart beats). This is an efficient solution for computing classical parameters, such as baseline, accelerations and decelerations, but it is not suitable for frequency analyses because interpolation introduces alterations in the FHR power spectrum [54]. In literature the introduced error in the evaluation of PSD has not been widely documented [74][75]. However, it is known that the interpolation process produces possible artifacts and an attenuation of the high-frequency components of the PSD that, for example, affects the estimation of the sympatho-vagal balance (computed as low-frequency/high-frequency power ratio), which represents an important clinical parameter [64][65]. Furthermore, some commercial software, employed for semi-automatic US-CTG analysis, in order to reduce required

space memory and computational time, record CTG data at a lower storage rate (please see [29] for definition).

In order to estimate the frequency spectrum alterations due to interpolation and US-CTG storage rates, in this study uneven FHR series are simulated and their evenly spaced versions, as proposed in previous works [29][76], and estimated sympatho-vagal balance (SVB) values by PSD. The study considered do not analyse real signals since the real spectral characteristics are not known. To estimate PSD several methods there exist and the choice depends on the particular application (often an empirical approach is followed for method choice) [55]. Among most commonly employed methods to evaluated PSD, parametric and non-parametric, we can mention Short-time Fourier transform, Auto Regressive methods, Fast Recursive least square algorithms [50][52][55] and wavelet transform [76]. We decided to estimate the PSD for unevenly sampled FHR signals by means of Lomb method, as suggested by Laguna et al [54][77][78][79], since no explicit data replacement is made and PSD is calculated from only the known values. In order to compare obtained results, despite of high computational time, we adopted Lomb method also for PSD estimation of even FHR series.

This study presents a series of experiments to quantify the errors in FHRV spectral estimation due to zero-order, linear and cubic spline interpolations and sampling rates normally used to obtain typical CTG storage rates (2 and 4 Hz).

4.2.1 Simulation of FHR signals

Synthetic FHR signals were artificially generated, via software, using a slightly modified version of a method proposed for adults by other groups [67][80] and already employed in previous works of the authors [29][76]. Following that procedure, an artificial R-R tachogram with specific power spectrum characteristics was generated. Considering that in FHRV different relationships between the LF and HF bands are present, the following model parameters were adapted to resemble real foetal cases. LF and HF bands of the FHRV power spectrum were considered to lie between 0.04 and 0.2 Hz, and 0.2-1 Hz, respectively. LF/HF power ratio (considered a measure of the SVB) was fixed to 5 and Standard Deviation (SD) of HF band to 0.03. FHR mean value was initially set at 140 beat per minute (bpm), within the physiological range of 120-160 bpm; other values were chosen in the range 100-180 bpm. In addition, SD of FHR signal was heuristically set at 2 (for more details of the algorithm, please refer to the previous publication [76]). Finally, to obtain signals resembling other physiological conditions, accelerations were simulated by using Gaussian-like signal tracts (with SD heuristically chosen equal to 0.2); we adopted the classical definition: accelerations are transient increases of the FHR from the baseline of at least 15 bpm for at least 15 s [23][81]. For each FHR series, three accelerations were simulated.

All simulated FHR signals had duration of 25 minutes (see figures 17 for examples of simulated FHR signals).
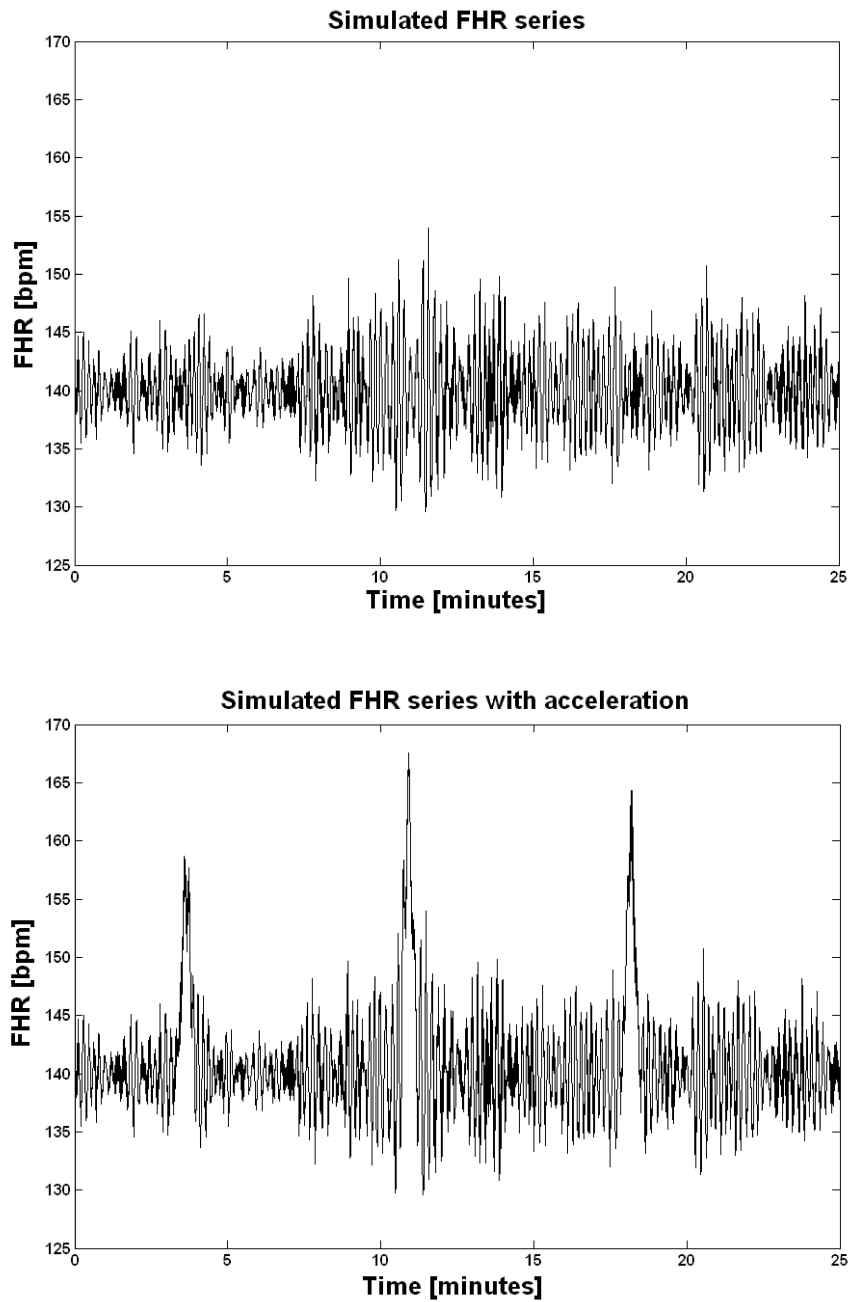
Figure 17: Simulated FHR signal # 13 (top); simulated FHR signal # 13 with 3 superimposed accelerations (bottom).

Another algorithm previously developed by the authors [29] was employed to provide evenly sampled series of the simulated FHR signals. Artificial signals were interpolated by

means of zero-order, linear and cubic spline interpolation and then sampled at 4 Hz (storage rate usually employed by the HP cardiotocographs) and decimated at 2 Hz (as done by some commercial software [82]).

4.2.2   Signal organization and processing

For each fixed FHR mean value, 350 FHR signals were generated and grouped in sub-sets of 50 signals; in particular, 50 uneven FHR signals (for simplicity, here also named series at 0 Hz) and 50 even FHR signals for each kind of interpolation (zero-order, linear and cubic spline) and storage rate (2 Hz and 4 Hz).

After that, to all these FHR series, 3 accelerations were added, as described in point 2.1.

Regarding evaluation of PSD alterations, according to literature [80], we considered SVB values as an index of eventual estimate differences. In particular, with regard to SVB computing, in order to highlight its common trend, average and standard deviation of all the SVB values were computed for each FHR signals sub-set. SVB values were computed for the same FHR signals without and with accelerations in order to evaluate the influence of these FHR alterations (accelerations) on SVB evaluation.

Furthermore, as in the real recordings the FHR mean value is not a-priori known, for each kind of interpolation and storage rate, we then grouped the signals differently: we obtained sub-sets of 250 synthetic signals merging the sub-sets corresponding to different FHR mean values. The differences between SVB values evaluated on these sub-sets and ones estimated on the subset of 250 uneven FHR synthetic signals were computed.

4.2.3 The Lomb Method

To estimate PSD of FHRV signals, we employed Lomb method [54][83].

The Lomb method is based on the minimization of the squared differences between the projection of the signal onto the basis function and the signal under study. Let x(t) be the continuous signal under study and bi(t) an orthogonal basis set that defines the transform. The coefficients c(i) that represent x(t) in the transform domain are:

$$c(i) = \int_{-\infty}^{+\infty} x(t)\, b_i(t)\, dt \qquad (3)$$

and these coefficients c(i) are those which minimise the squared error e(ci) defined as [7]:

$$e(c_i) = \int_{-\infty}^{+\infty} (x(t) - c(i)b_i(t))^2\, dt \qquad (4)$$

The Lomb method can be generalised to any transform estimation on unevenly sampled signals.

When the signal is accessible only at unevenly spaced samples, the solution has generally been to reduce it to an evenly sampled signal through sampling interpolation. However, as stated above, this process introduces some distortion in the spectrum (or transform). To avoid this problem, Lomb proposed to estimate the Fourier spectra of an unevenly sampled signal by adjusting the model:

$$x(t_n) + \varepsilon_n = a\cos(2\pi f_i t_n) + b\sin(2\pi f_i t_n) \qquad (5)$$

in such a way that the mean squared error (ε_n) is minimized with the proper a and b parameters [54].

4.2.4   Results

The results confirm that interpolation process and use of different storage rates affect PSD estimation, as roughly can be seen in figures 18 and 19, where examples of estimated PSD are reported. In particular, in figure 18, PSD estimations of simulated FHR signal # 10 with storage rate of 2 Hz and different orders of interpolation are reported. Figure 19 shows PSD of the uneven FHR series # 13 (plotted in figure 1a) and PSD of its evenly spaced versions, zero-order interpolated and sampled at 4 and 2 Hz.
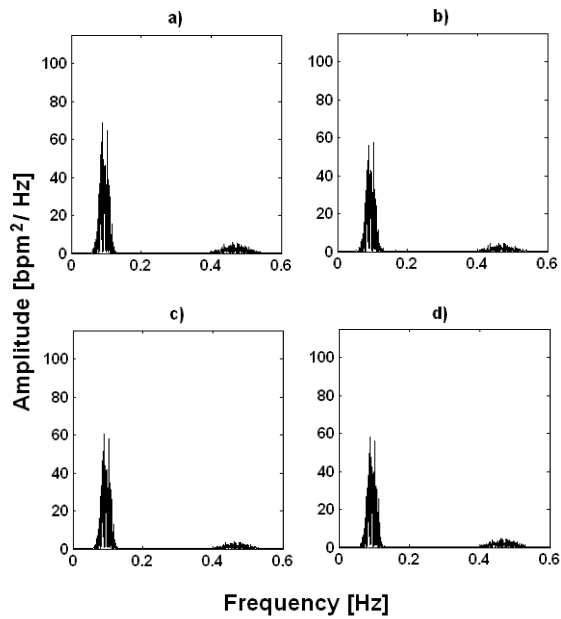
Figure 18: PSD estimations (amplitude measured in bpm^2/Hz), by means of Lomb method, of simulated FHR signal # 10 with storage rate of 2 Hz and different orders of interpolation: b)zero-order, c)linear, d)cubic. In a), PSD of the uneven FHR series.
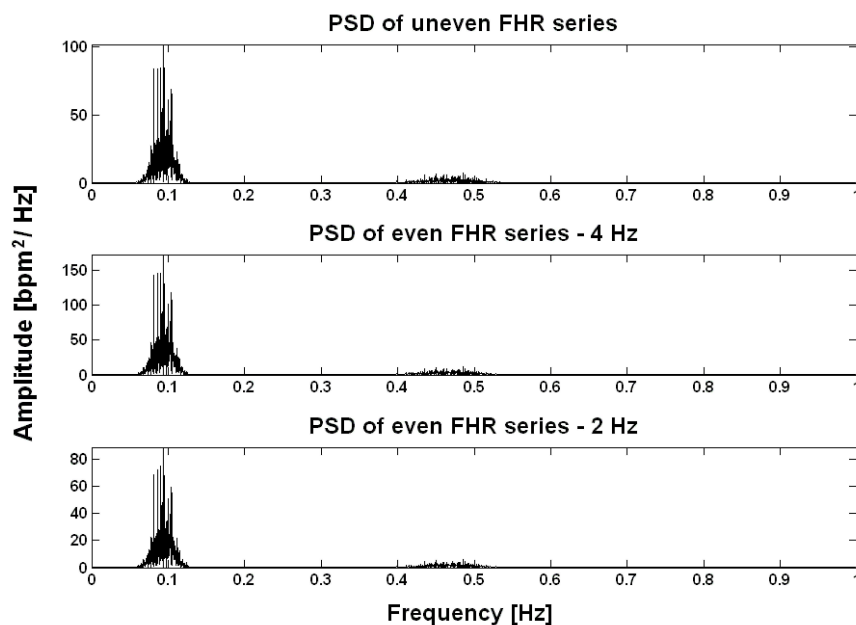
Figure 19: From the top, PSD estimations (amplitude measured in bpm^2/Hz), by means of Lomb method, of simulated uneven FHR signal # 13, its evenly spaced zero-order version at 4 Hz and at 2 Hz. Amplitude differences are visible in both LF and HF bands.

PSD modification has been here quantified by SVB computing, which resulted overestimated for even FHR series. Results are concisely presented in tables 7 and 8, where average values and standard deviations (in brackets) obtained on sub-sets of 50 synthetic signals are reported for each kind of interpolation and storage rate. Results in Tables 7 are relative to FHR series simulated without accelerations, while in table 8 are reported results relative to the same FHR series with superimposed accelerations.

SVB values were computed by means of Lomb method on the uneven FHR simulated signals (0 Hz) and on the corresponding even series (zero-order, linear and cubic interpolation, 2 and 4Hz). Just for sake of brevity, only results relative to some FHR mean values (100, 120, 140, 160 and 180 bpm) are reported.

Obtained results show that generally the observed overestimation is reduced when cubic spline interpolation is employed (see table 9). This result is verified at almost all the tested FHR mean values and storage rates except for some isolated cases (zero-order, 2 Hz, 100 and 120 bpm).

Interpolation	Storage Rate	100 bpm	120 bpm	140 bpm	160 bpm	180 bpm
Uneven	0 Hz	5.01 (0.06)	4.98 (0.06)	5.00 (0.06)	5.00 (0.06)	5.00 (0.05)
Zero- order	2 Hz	5.07 (0.08)	5.04 (0.06)	5.25 (0.11)	5.23 (0.08)	5.49 (0.07)
Zero- order	4 Hz	5.59 (0.08)	5.54 (0.08)	5.57 (0.07)	5.39 (0.07)	5.60 (0.08)
Linear	2 Hz	6.53 (0.08)	5.72 (0.20)	6.49 (0.08)	6.47 (0.08)	6.36 (0.09)
Linear	4 Hz	6.56 (0.08)	6.44 (0.10)	6.50 (0.07)	6.47 (0.08)	6.48 (0.07)
Cubic spline	2 Hz	5.13 (0.07)	5.04 (0.07)	5.08 (0.06)	5.07 (0.06)	5.06 (0.06)
Cubic spline	4 Hz	5.13 (0.07)	5.08 (0.06)	5.08 (0.06)	5.07 (0.06)	5.06 (0.06)

Table 7: Average values and standard deviations (in brackets) of SVB values obtained on sub-set of 50 synthetic signals without accelerations, for each interpolation method, for each storage rate and for different FHR mean values.

About storage rates, results show that, at low order of interpolation, storage rate of 2 Hz generally produces a lower overestimation with respect to 4 Hz.

Results reported in the next table show that accelerations cause a further little overestimation of SVB (maximum 2% with respect to the set value), also for uneven FHR series.

Interpolation	Storage Rate	100 bpm	120 bpm	140 bpm	160 bpm	180 bpm
Uneven	0 Hz	5.10 (0.09)	5.06 (0.09)	5.07 (0.07)	5.08 (0.07)	5.02 (0.13)
Zero- order	2 Hz	5.13 (0.09)	5.05 (0.07)	5.28 (0.11)	5.29 (0.08)	5.45 (0.15)
Zero- order	4 Hz	5.64 (0.09)	5.58 (0.08)	5.61(0.07)	5.43 (0.09)	5.60 (0.12)
Linear	2 Hz	6.60 (0.10)	6.34 (0.14)	6.54 (0.08)	6.51 (0.08)	6.48 (0.11)
Linear	4 Hz	6.63 (0.10)	6.54 (0.10)	6.55 (0.08)	6.52 (0.08)	6.48 (0.10)
Cubic spline	2 Hz	5.18 (0.08)	5.12 (0.07)	5.12 (0.06)	5.11 (0.06)	5.06 (0.08)
Cubic spline	4 Hz	5.18 (0.08)	5.13 (0.07)	5.12 (0.06)	5.11 (0.06)	5.06 (0.08)

Table 8: Average values and standard deviations (in brackets) of SVB values obtained on sub-set of 50 synthetic signals with accelerations, for each interpolation method, for each storage rate and for different FHR mean values.

The following tab reports the average and standard deviation of differences between SVB values computed on even and uneven series without considering the FHR mean values.

Interpolation	Storage Rate	Differences in SVB values	Percentage difference
Zero- order	2 Hz	0.22 (0.17)	4.4 (3.4)
Zero- order	4 Hz	0.54 (0.09)	10.8 (1.8)
Linear	2 Hz	1.32 (0.30)	26.3 (6.7)
Linear	4 Hz	1.49 (0.05)	29.9 (1.0)
Cubic spline	2 Hz	0.08 (0.03)	1.6 (0.6)
Cubic spline	4 Hz	0.09 (0.03)	1.8 (0.6)

Table 9: Average value and standard deviation (in brackets) of differences of SVB values computed on each sub-set of 250 synthetic signals, obtained by merging the sub-sets corresponding to different FHR mean values, respect to the values computed on the sub-set of uneven FHR series. The results are reported for each interpolation method and each storage rate and, in the last column, in percentage value.

The results suggest that 2 Hz vs. 4 Hz, leads to lower average differences but to a greater SD. Moreover, on average, cubic spline interpolation provides lowest difference and variability (in both cases less than 2%).

5. Foetal phonocardiography

5.1 FPCG signal

In the last years, many efforts have been paid by the scientific community to find a suitable alternative to the US-CTG. A valuable alternative can be the foetal phonocardiography, a totally passive (no ultrasounds are transmitted to the foetus) and low cost system for acoustic recording of foetal heart sounds (FHS) [32][33][34][38][84][85]. FPCG is a trace of acoustic energy produced by the mechanical activities of various foetus cardiac processes and is detected from the abdomen of the mother by means of a small acoustic sensor without the use of gel. Using this technique, long-term and frequent measurement of the FHR becomes possible. This provides valuable information concerning the physical state of unborn in the womb and has the potential for detection of cardiac functionality anomalies, such as murmur, split effect, extra systole, bigeminal/trigeminal atrial contraction, intrauterine growth retardation and other domain anomalies. Such phenomena are not obtainable with the traditional US-CTG technique or other methods [42][43][86].

Preliminary studies about phonocardiographic monitoring reported encouraging results and have inspired the possibility to employ FPCG to identify foetuses at risk. The preliminary evaluation done by Baskaran and Sivalingam [87] has shown, for example, that there are

significant differences in the characteristics of foetal heart sounds between intrauterine growth retarded and normal foetuses in the antenatal period.

However, before carrying on in analysis of FHS signal characteristics, it is important to remind some physiological notes. Even though the heart it is not fully developed in a foetus, since the 8th week of gestation (WG) it is already divided into two pairs of chambers and has four valves. During the foetal cardiac cycle, when the ventricles begin to contract, the blood attempts to flow back into the atrial chambers where the pressure is lower: this reverse flow is arrested by the closing of the valves (mitral and tricuspid), which produces the first heart sound (S1). After, the pressure in the ventricular chambers increases until the pulmonary valves open and the pressurized blood is rapidly ejected into the arteries. The pressure of the remaining blood in the ventricles decreases with respect to that in the arteries and this pressure gradient causes the arterial blood to flow back into the ventricles. The closing of the pulmonary valves arrests this reverse flow and this gives rise to the second heart sound (S2) [39].

In contrast to adult PCG, where a strong sound generator is close to the transducer, FPCG has to contend with a weak sound generator which is separated from the sensor by up to ten foetal heart diameters [88]. Generally, the foetal heart sounds can be heard in only a small area of the mother's abdomen of usually no more than 3 cm radius, although the range of this local area can encompass up to a 12 cm radius.
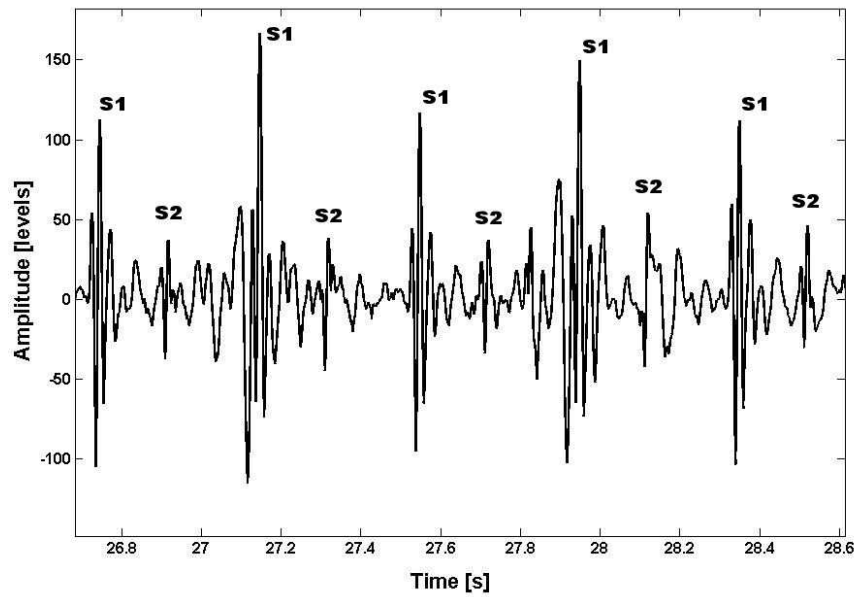
Figure 20: example of a FPCG signal.

In figure 20, examples of S1 and S2 events are shown. S1 contains a series of low frequency vibrations, and it is usually the longest and loudest heart sound; S2 typically has frequency higher than S1, and its duration is shorter; a third low frequency sound (S3) may be heard at the beginning of the diastole, during the rapid filling of the ventricles; a fourth heart sound (S4) may be heard in the late diastole during atrial contraction [89]. It is important to mention that in FPCG recordings, S3 and S4 sounds are practically undetectable [43] and that the power spectral density and relative intensity of these sounds is a function of foetal gestation age [90]. So, whenever the closing of cardiac valve creates a sound, sonic energy travels through a complex and dynamic system up to the maternal abdominal surface. The sounds transmission path comprises amniotic fluid, the muscular wall of the uterus, layers of fat, tissue, and possibly bony and cartilaginous material. Each of these substances attenuates the forward moving sound energy due to reflection arising

from the impedance mismatch that occurs at the boundary of each of these layers. The result is attenuation of signals, and the foetal heart sound becomes too weak causing a poor signal to noise ratio [43][91].
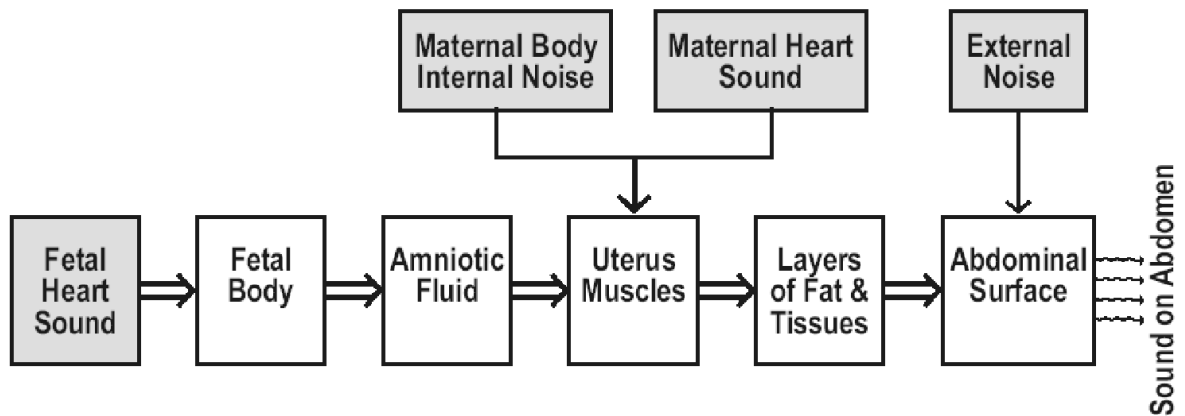
Figure 21: sounds transmission path.

Recorded FPCG signals are heavily loaded by different noise sources that can be so resumed [33][34][43][92]:

- acoustic noise produced by foetal movements;

- maternal digestive sounds;

- maternal heart activity sounds(MHAS);

- maternal respiratory sounds;

- movement of measuring sensor during recording – shear noise;

- external noise originating from the environment – ambient noise.

The above interferences are non stationary and have to be removed from a non stationary signal, i.e. foetal heart sounds signal. Thus, a crucial point is the correct recognising of

FHS associated to each foetal heart beat and then the reconstruction of the FHR signal [32][33][34] [86][93].

The most part of the early works in the area of FPCG monitoring were concentred on sensor development. More recent studies focused on FHR estimation and different signal processing algorithms were developed to perform foetal heart beats identification.

In literature it's possible to find different solution of enhanced signal processing strategy in order to detect foetal heart sound, such as: matched filtering (a technique commonly used to detect recurring time signals corrupted by noise); non-linear operator designed to enhance areas of local high energy like the Teager energy operator proposed by James F. Kaiser [94]; autocorrelation techniques in order to emphasize the periodic components in the foetal heart signal while reducing the non-periodic components; quadratic energy detectors that incorporate frequency filtering with energy detection [95]; neural networks; linear prediction that is commonly used in speech processing for the determination of fundamental frequency of voiced sounds by using the inverse linear prediction filter to remove the harmonic structure of the signal and only leaving periodic pulses.

However, except for some studies, the proposed methods have the main purpose of detecting occurrences, not precise locations, of the heart sounds. Moreover, no detailed quantitative results assessing the reliability of the proposed methods were given and completely dependable results were not yet obtained [32][33][34][86].

In this chapter, a new algorithm for FHR estimation from acoustic phonocardiographic signals, a software for simulating fPCG recordings (relative to different foetal physiological conditions and recording situations) and a home care phonocardiography application are presented. The obtained results, were presented in different international

congresses [96][97][98][99][100][101][102] and published on a journal paper: "An algorithm for FHR estimation from foetal phonocardiographic signals" [103].

5.2   Time-frequency analysis of FPCG signals

To realize the algorithm for FHR estimation and the simulator, it is needed to know all FHS characteristics; however, the literature in this field is poor, not rigorous and some results are not completely in agreement among them. Hence, we had to carry out a pilot study to gather all the necessary information both in time and frequency domain.

In healthy adult subjects, the frequency spectrum of S1 contains a peak in the low frequency range (10-50 Hz) and in the medium frequency range (50-140 Hz) [104]. S2 contains peaks in low (10-80 Hz), medium (80-220 Hz) and high-frequency ranges (220-400 Hz) [104].

Concerning the foetal heart sounds, some authors [105] declare that frequency spectrum has not been exactly measured because of dependence on the coupling condition between the transducer and abdominal wall. Additionally, they note that the frequency spectrum varies from one patient to another and also varies in the same foetus according to gestational age.

Nagel reports [90] that the spectrum of the foetal heart sounds varies considerably also with foetal gestational age. He suggests in fact the possibility of using the heart tone

spectrum as a means of estimating foetal maturity. According his studies, after the 34th WG, S1 and S2 main frequencies decrease with increasing of WG. In fact, due to maturation of autonomous nervous and cardiovascular systems and foetal morphology change (such as increasing dimensions and contractile strength of myocardium) during pregnancy, spectral characteristics of FHS are dependent on the stage of foetal maturity [106].

There are few studies about S1 and S2 frequency contents and they disagree on heart sounds main frequency, even if all state that spectra are about within 20 -100 Hz band and S1 frequency band is lower than S2 one at all times [90][105][107][108][109][110]. Since the available literature is not rigorous in this area a data collection pilot study was conducted on real recordings with the purpose of specifically identifying the S1 and S2 frequency characteristics.

5.2.1   Data collection

fPCG signals were recorded from 35 pregnant women, during the last month of their singleton physiological pregnancies (34th – 40th WG). We used a portable phonocardiograph, "Fetaphon Home", equipped with a microphone for FHS recording along with a traditional pressure probe for UC recording. The phonocardiographic device digitized audio signals by using a sampling frequency of 333 Hz and 8-bits ADC.

5.2.2 Pilot study

In fPCG recordings, S1 and S2 can be recognized. We analyzed 35 fPCG recordings (five for each WG considered). In each recording, ten S1 and ten S2 templates were manually chosen (by selecting start and end points) in fPCG recordings frames characterized by low noise and absence of artifacts, computed their power spectral density (PSD) and the maximum amplitudes of their peaks. Then, we evaluated: the average of fifty S1 and S2 PSD (respectively PSD1 and PSD2) obtained for each WG, the average of ratios between S1 peak amplitude and S2 peak amplitude (S1S2R) for each recording, the average of S1 and S2 time durations (respectively S1D and S2D).

It was also investigated the presence of a correlation between the frequency corresponding to the maximum value of S1 (and S2) PSD and WG. The correlation discovered was shown in the results section.

About mHS spectrum, there is little information in literature [43][90]. Nagel [31] found the maternal tones to be below 20 Hz. So in order to characterize maternal first and second heart sounds (respectively mS1 and mS2), a similar study was conducted by recognizing and selecting mS1s and mS2s from five fPCG recordings containing detectable mHS (in those recordings FHS are less pronounced or absents because of mHS grater amplitude), we evaluated: the average of about fifty mS1 and mS2 PSD (respectively mPSD1 and mPSD2) regardless of WG, the average of ratios between mS1 peak amplitude and mS2 peak amplitude (mS1S2R) for each recording, the average of mS1 and mS2 time durations (respectively mS1D and mS2D).

5.2.3 Analysis results

The results of the pilot study showed the existence of a correlation between the frequency corresponding to the peak of the PSD1 (and PSD2) and WG. In particular, a quadratic relationship with high correlation coefficients (R) was highlighted: for PSD1 R was equal to 0.93; for PSD2 R was equal to 0.96. Results reported in tableTable 10 and Figure 22 agree with literature [90]: after the 34th GW, S1 and S2 main frequencies decrease with increasing of WG.
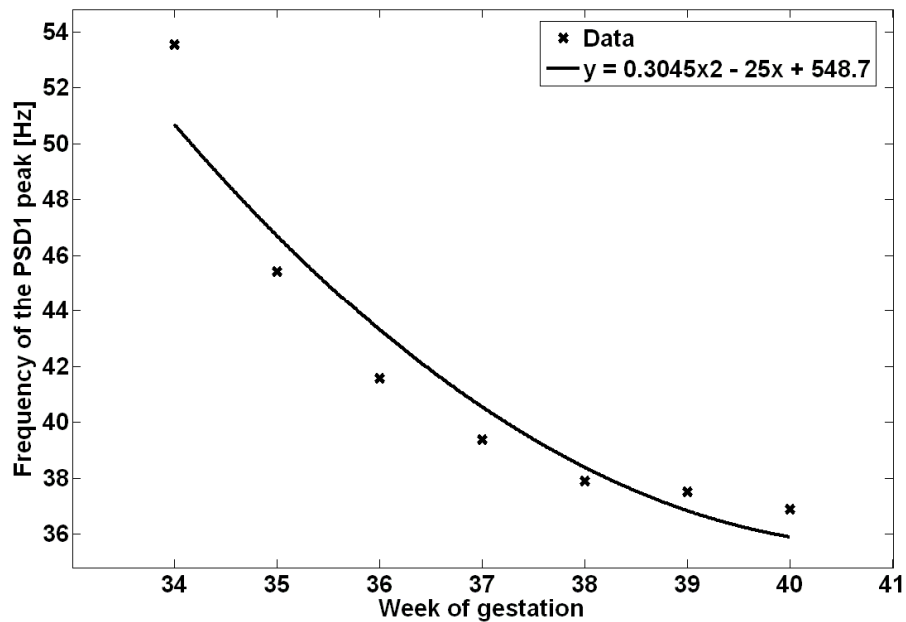
a)
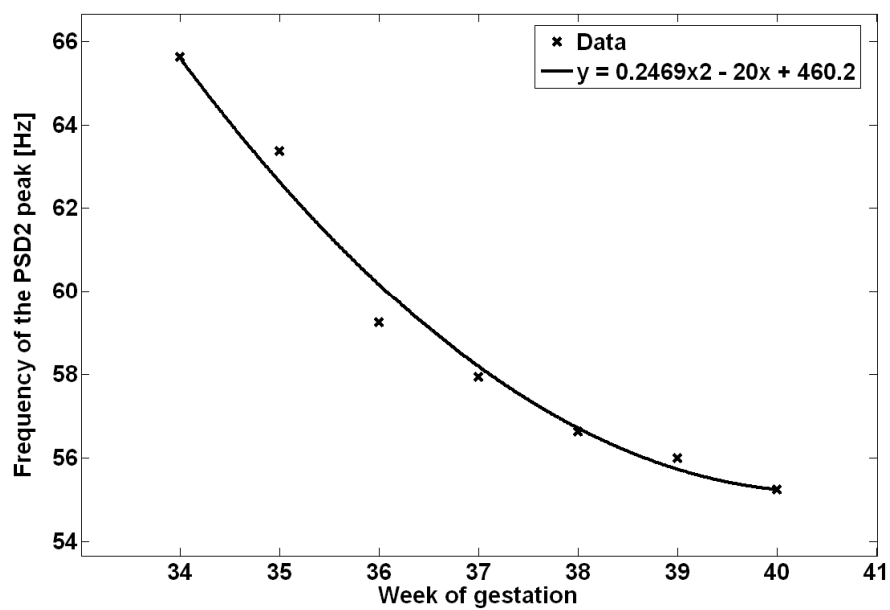
b)

Figure 22: quadratic regression F1 Vs WG (a) and F2 Vs WG (b)

WG	peak of the PSD1	peak of the PSD2
34	53.55	65.64
35	45.44	63.37
36	41.59	59.25
37	39.39	57.94
38	37.91	56.64
39	37.52	55.99
40	36.89	55.21

Table 10: correlation between the WG and the frequency corresponding to the peak of the PSD1 (and PSD2)

However, there wasn't found any correlation between the other parameters (S1S2R, S1D, S2D, SD1, SD2) estimated in the pilot study and the WG.

In figure 23, mPSD1 and mPSD2 show how mHS, according to literature [43][90], has a lower frequency spectrum than FHS.
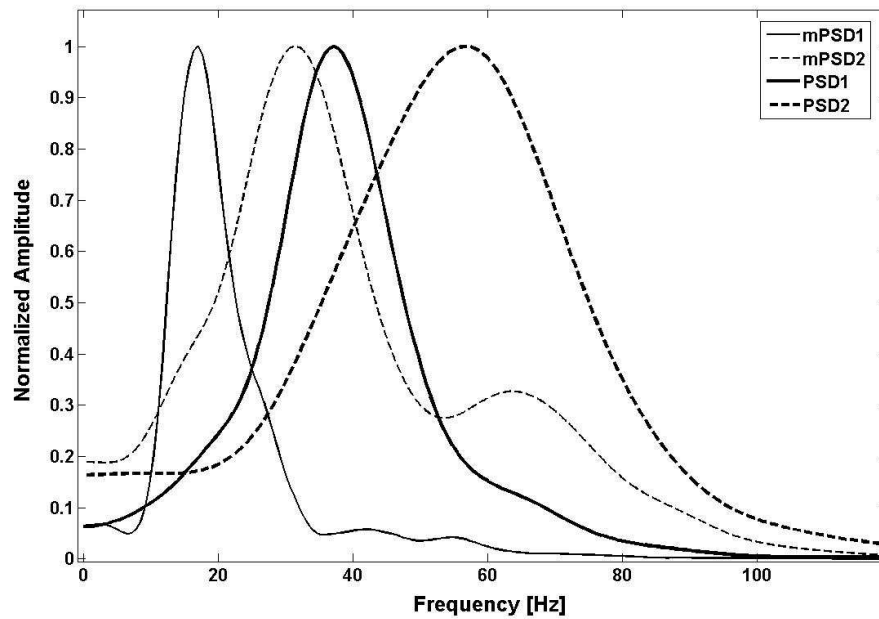
Figure 23: normalized amplitudes of PSD1 (38th WG), PSD2 (38th WG), mPSD1 and mPSD2

The next table reports the mean values and the standard deviations (in brackets) of the computed parameters from all the manually selected foetal and maternal first and seconds heart sounds, the frequencies mF1 and mF2 corresponding respectively to the maximum peaks of mPSD1 and mPSD2. In literature [43][90] it is possible to find the values of some parameters (in particular S1D, S2D, mS1D, mS2D, mF1 and mF2) that agree with the corresponding estimated mean values.

S1S2R	mS1S2R	S1D [ms]	S2D [ms]	mS1D [ms]	mS2D [ms]	mF1 [Hz]	mF2 [Hz]
1.70 (0.71)	1.54 (0.13)	85 (12)	58 (9)	136 (6)	95 (7)	16.93	30.44

Table 11: parameters estimated by the pilot study

5.3 Algorithm for FHR estimation

In this section a new algorithm for FHR estimation from acoustic phonocardiographic signals is presented. The algorithm was based on a "logic block" for reliable detection of heart beats. Owing to the extremely noisy nature of PCG signals, different filtering and signal enhancement techniques were applied, so that different signal processing paths (PP) were implemented. The performances of the different paths were tested comparing the estimated FHR signals with those of simultaneously recorded US-CTG (currently considered reference technique), in order to identify the most reliable path.

Obtained results showed that it is possible to obtain reliable FHR series, very close to US-CTG recordings, employing a multi-steps algorithm.

Techniques here tested but not judged to be good enough for FHR estimation are documented in this section in order to help in preventing useless duplication of tested strategies.

5.3.1 Patients' selection and equipment

PCG signals were recorded from pregnant women, during the last month of their singleton physiological pregnancies (34-40 weeks of gestation). It was used a portable phonocardiograph, "Fetaphon Home", equipped with a microphone for FHS recording along with a traditional pressure probe for UC recording. The phonocardiographic device digitized audio signals by using a sampling frequency of 333 Hz and 8-bits ADC.

The measurements were carried out simultaneously with Doppler cardiotocographic recordings (by means of HP or Sonicaid cardiotocographs) for further comparisons and assessments, during the daily clinical practice.

Simultaneous location of both US-CTG and FPCG probes, on the maternal abdomen, is difficult. Thus, recorded FPCG and US-CTG signals often showed a very lower SNR (with respect to either FPCG or US-CTG recording). Hence, before performing signal processing, recordings were visually inspected in order to select only those where both signals showed an acceptable SNR. We chose 35 couples of FPCG and US-CTG signals.

All the processing was developed off-line using Matlab version 7.0

5.3.2 Algorithm description

In FHS signals first and second foetal heart sounds (S1 and S2 respectively), shaped as bursts, can be recognized. S1 (closure of mitral and tricuspid valves) is considered a good

time indicator of heart beat, because of both its high energy, with respect to the other portions of the FHS, and less morphologic variability [33][45].

The developed algorithm was basically planed on S1 enhancement and detection. A logic block, based on mathematical rules mainly concerning mean heart beat characteristics, described in detail in the following section B.4 ("Logic block"), chose S1 among several "candidates". Finally, the time position of S1 was determined by a post-processing block. The flow chart in figure below represents the main steps of the signal processing.
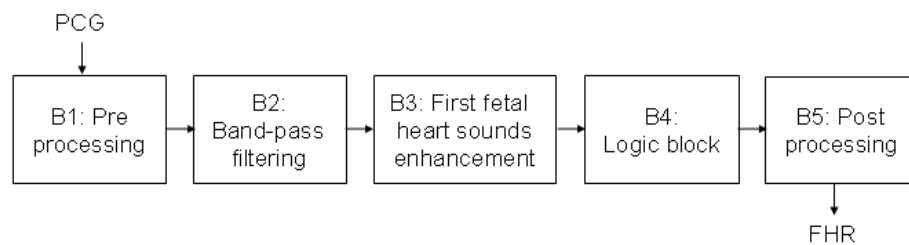
Figure 24: main blocks of the developed algorithm. Some blocks (B2 and B3) were implemented in different ways, as explained in details in the text.

Filtering and first foetal heart sounds enhancement blocks were implemented using different techniques (below summarized and explained in details in the following sections).

The filtering block was implemented by means of: matched filter with a template of S1 (chosen by the operator by selecting the start and the end points of a S1) or band-pass filter with set or variable centre-band frequency.

The S1 enhancement block was instead implemented by exploiting these different strategies: Teager Energy Operator (TEO), autocorrelation, autocorrelation + TEO or TEO + autocorrelation (because of the nonlinearity, TEO and autocorrelation operators are not commutative).

Therefore, considering all possible combinations of proposed blocks (for example matched filtering and TEO, or matched filtering and autocorrelation, etc), we tested 12 different signal PP.

All details concerning considered processing techniques are reported in the following sections.

B1. Pre-processing

At this step, we over-sampled PCG signals (re-sampling frequency equal to 1332 Hz) in order to reduce, at successive post-processing block (which performs time references positioning), errors due to low finite sampling rate [112][113]. Choosing a sampling frequency equal to 4 times the phonocardiographic device sampling frequency (333 Hz), we were able, in fact, to obtain errors below 1 ms.

B2. Filtering block

Signal filtering has generally the main goal to increase SNR. As above mentioned, band-pass filtering block was implemented in different ways, described in details in the following.

B2.1 Matched filtering

Matched filtering is a technique commonly used to detect recurring temporal events in signals corrupted by additive noise [114].

The matched filter can be represented by the following formula (FIR filter of order N):

$$y(n) = \sum_{k=0}^{N-1} h(k)x(n-k) \qquad \textbf{(6)}$$

where h(k) are the matched filter coefficients, x(k) are the samples of the input (FHS samples in this case), y(k) are the samples of the filter output and N is the selected template length in samples (which average value is 123 samples, about equal to 92 ms, coherent with literature [111]).

In matched filter design, the underlying assumption is that the time event has a known wave shape. There is an important difficulty in using matched filtering in FHS processing, the actual wave shape of the foetal heart beat is unknown, and so its estimation is necessary. This problem was here solved, for each PCG recording, using a template of S1, manually selected by the operator in a portion of FHS signal with high SNR. An example of FHS signal and chosen template is reported in figure 25.
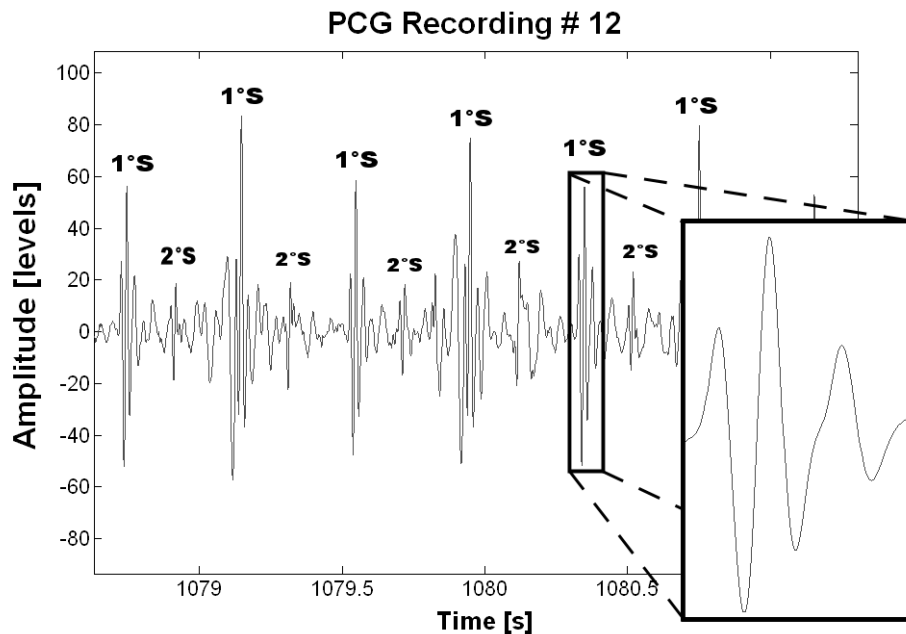

Figure 25: example of FHS signal (PCG recording # 12) in which visually recognized S1 and S2 sounds are marked as 1°S and 2°S. The zoom shows the S1 template chosen in this case.

B2.2 Set band-pass filtering

By literature it is known that, in PCG recording, interferences are confined below 20 Hz (mostly internal noise, for example maternal heart sounds and digestive sounds) and above 70 Hz (environmental noise) [32][33][34][43]. S2 spectrum, here considered as interference, is partially overlapped to S1 spectrum, so it is difficult to filter out; however, it is separable in time domain since time relationship between S1 and S2 is known; typical time distance between S1 and S2 peaks is about 150 ms [32][33][43][91].

The filtering was designed by using a digital band-pass filter having 3 dB band equal to 34-54 Hz and centred at 44 Hz.

B2.3 Variable band-pass filtering

Owing to maturation of autonomous nervous and cardiovascular systems as well as changing in foetal morphology during pregnancy, for example growing dimensions and increasing contractile strength of the myocardium, spectral characteristics of FHS are dependent on the stage of foetal maturity, that is on weeks of gestation [106]. In order to highlight the characteristics of this dependence, we carried out a preliminary study computing the average power spectral density (PSD) of S1. Results of this study showed a shift of S1 spectral features towards lower frequencies from the 34th week of gestation up to end of pregnancy (according to literature [90]); in particular, a quadratic relation was found (see section 5.2.3 for details). Therefore, to better enhance S1, we designed a digital band-pass filter with bandwidth equal to 20 Hz (as for step B2.2) and central frequency chosen according to week of gestation of PCG recording (see table 12).

Week of gestation	Central frequency
34	53.55 Hz
35	45.44 Hz
36	41.59 Hz
37	39.39 Hz
38	37.91 Hz
39	37.52 Hz
40	36.89 Hz

Table 12: chosen central frequency of the variable band-pass filter corresponding to each considered gestational age.

B3. First heart sound enhancement block

This step was necessary because disturbances still remain in the filtered PCG signals [34]. Hence, at this step, the algorithm had the main goal to discover the presence of bursts corresponding to S1 in FHS signals. As above declared, also for this block we tested different techniques, described in details in the following sections.

B3.1 Teager Energy Operator (TEO)

TEO is a time non-linear operator, defined in both the continuous and discrete time-domain, which has the property of identifying signal tracts of local high energy [115]. So, the rationale for using this block was that TEO would further enhance S1.

The following expression is used to describe the TEO in discrete time-domain:

$$E(n) = x2(n) - x(n+1) * x(n-1) \qquad (7)$$

where E(n) represents a measure of the Teager energy at time n; x(n), x(n+1) and x(n-1) are the values of the considered signal at time n, n+1, and n-1 respectively.

Owing to the residual noise [94], the B3.1 block output was low-pass filtered, by using a low-pass filter with a cut-off frequency of 30 Hz 1.

B3.2 Autocorrelation

PCG recordings can be considered consisting of two components: a set of periodic signals (among these the strongest is S1, being most of the others filtered out by B2 block) and a set of non-periodic signals which define background noise. Hence, autocorrelation technique was chosen because it has the property of emphasizing periodic components in noisy signals while reducing non-periodic components (like movement artifacts, foetal movements, casual environmental noise) [113][116].

The autocorrelation is computed as follows:

$$R(k) = \sum_{n=0}^{N-k-1} x(n)\, x(n+k) \qquad (8)$$

where x(n) is the signal to be processed with time length of N samples and R(k) is the autocorrelation result.

Each heart sound event corresponds to several oscillation peaks both in the FHS signal and in its autocorrelation, hence, for S1 searching we needed to study periodicity of the autocorrelation envelope. We computed the autocorrelation envelope (B3.2 output) by means of cubic interpolation of all local maxima (see Figure 26 for an example).

B3.3 Autocorrelation + TEO

This block was implemented because, theoretically, the combination of the two operators should highly emphasize the periodic components of FHS.

In this combination, the overall autocorrelation signal should increase SNR by suppressing the non-periodic noise in FHS; then, the TEO operator should further enhance heart sounds and slightly smooth the autocorrelation result.

B3.4 TEO + Autocorrelation

As addressed in paragraph B, this block was required mainly because of the nonlinearity of TEO and autocorrelation operators. However, in this combination, TEO should enhance the foetal heart beats and the autocorrelation should further highlight the periodicity of FHS, as for any periodic source.

In order to reduce remaining noise, outputs of these last blocks were further low-pass filtered.

Just for simplicity, we will call LP the output of B3 block.
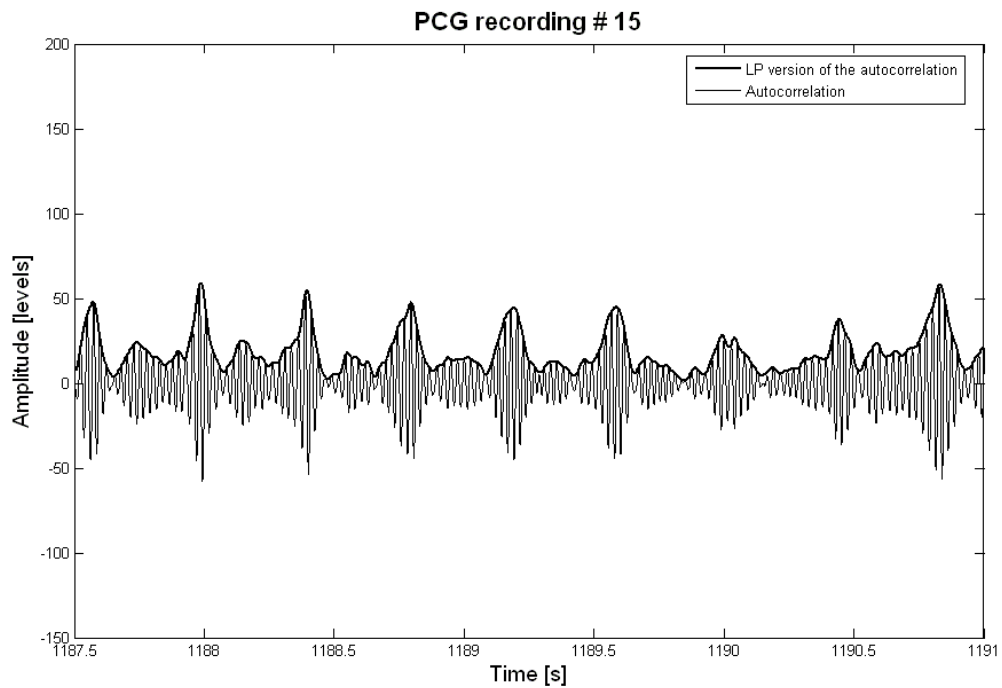
Figure 26: example of autocorrelation of the filtered FHS relative to PCG recording # 15. In bold, its LP version (envelope curve, B3.2 block output). For sake of clarity, the tract between lags 9.5 s and 13 s is presented.

<u>B4 Logic block</u>

This block had a crucial role for the developed algorithm. It had the aim to identify all (and only) the lobes of LP corresponding to the possible locations of S1.

It is worth stressing that, due to noise, there was not a one-to-one correspondence between LP lobes and S1 and that some lobe could show multiple peaks (see figure 27) [33].
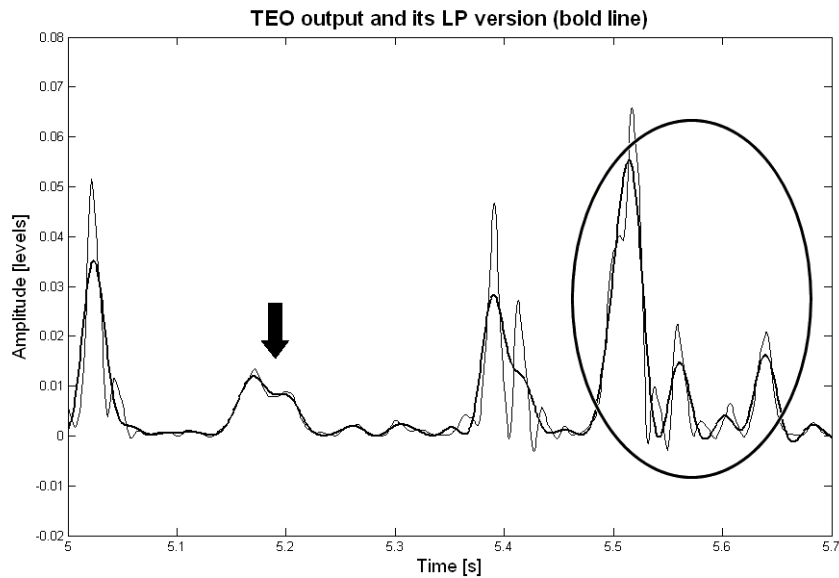
Figure 27: example of TEO output, with superimposed residual noise, and its smoothed version (LP, painted as bold line). The ellipse indicates multiple lobes in LP (corresponding to one S1 event) and the arrow shows a LP lobe with multiple peaks.

Roughly, when SNR of PCG recording is high, each lobe of B3 output corresponds to a S1; whereas, when PCG recording had not a good SNR, it was possible to find multiple lobes or lobes formed by multiple near peaks. If the wrong peak is chosen, some S1 could be incorrectly located. Hence, the algorithm had to select the right peak corresponding to S1 among multiple peaks and lobes.

To make this selection, the logic block analyzed LP peak by peak, following analysis strategies similar to those reported in literature [32][33][34][117]. Lobes were analyzed with regard to their inter-distance consistency (position criterion) and amplitude regularity (amplitude criterion). Peaks with a position into a fixed time interval (based on the mean value of peak inter-distances computed respect to the previous 8 detected beats) were considered as candidate beats. Among candidate beats, those with amplitude greater than a

fixed threshold (chosen with reference to the average of the maximum amplitudes of the previous 8 detected beats, value chosen according to literature [32][33]) were considered as probable heart beats, because peaks satisfying both criteria most likely preserve continuity of the FHR series.

In particular, called T0 the position of the last detected peak (recognized as S1), the algorithm searched the successive peaks (candidate beats) into the interval T defined as:

$$T = T0 + 0.65*MEAN, T0 + 1.35*MEAN \qquad (9)$$

where MEAN was the mean inter-distance value computed on the previous 8 recognized beats. This large interval (beyond the time where S1 was expected to occur) was chosen in order to consider acceptable instantaneous variations of FHR, automatically rejecting only extreme outliers (for example, if FHR mean value is 140 bpm, the chosen interval corresponds to a FHR interval equal to about 104 – 215 bpm).

In the T time interval could there be more, one or no peak. To select probable heart beats, the algorithm marked only peaks higher than the amplitude threshold estimated on the previous 8 detected beats (50% of the mean of their maximum amplitudes, here called high threshold: HT). If just one candidate beat satisfying the amplitude criterion was present in the interval T, the algorithm recognized it as detected beat and utilized its characteristics to update T0, MEAN and amplitude threshold values and then repeated the cycle (up to signal end).

Otherwise, if more peaks higher than HT were present in T (probable beats), called Pi their positions, the algorithm chose the peak that minimized the distance ||T0-Pi| - MEAN|; that

is we considered it like the most probable peak because its position was the closest to the previous mean value.

If in T there was not any peak greater than HT, the algorithm repeated the search setting the amplitude threshold at 30% of mean of maximum amplitudes of the previous 8 beats [32][33], (here called low threshold: LT).

If, also with this condition, in T there was not any candidate beat satisfying the amplitude criterion, in order to avoid missed beats, the algorithm fixed a peak in the time position P0 = T0 + MEAN and associated to this peak the lowest fiducial degree (see following paragraphs for details).

At the end, the logic block outputs are the recognized S1 associated with an index showing satisfied criteria; it will be used from the post-processing block.

See figures 28 and 29 respectively for a schematic representation of the operations of the logic block and for an example of positioning of candidate and detected beats.
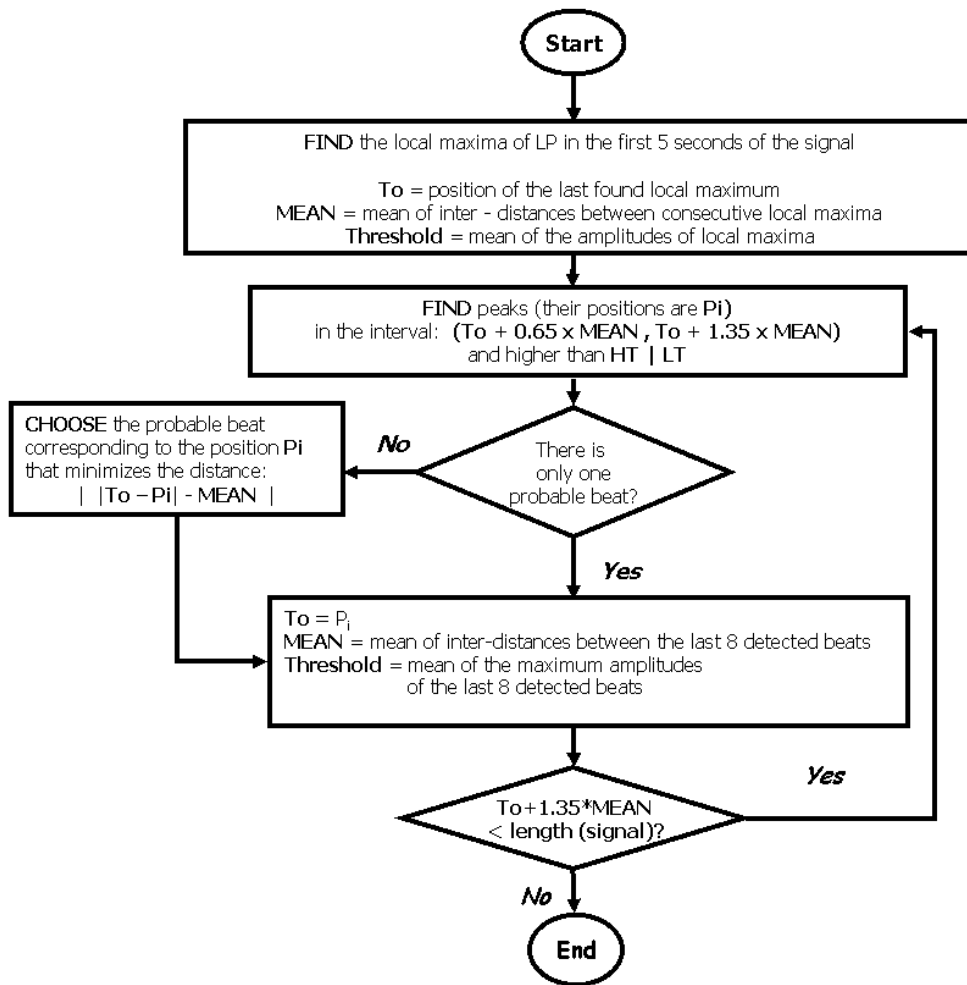
Figure 28: flow chart of the logic block .

In the previous, the first rectangular block represents the "training phase" of the algorithm. It, in fact, as first step, for the first 5 s of LP (value heuristically chosen after analysis of a large number of recordings), selected local maxima with a distance of at least 285 ms (corresponding to a FHR value of about 210 bpm, here considered as maximum possible value) and calculated their mean inter-distance value (considered as reference for the successive beats detection and named MEAN by the algorithm) and the average of their amplitudes.
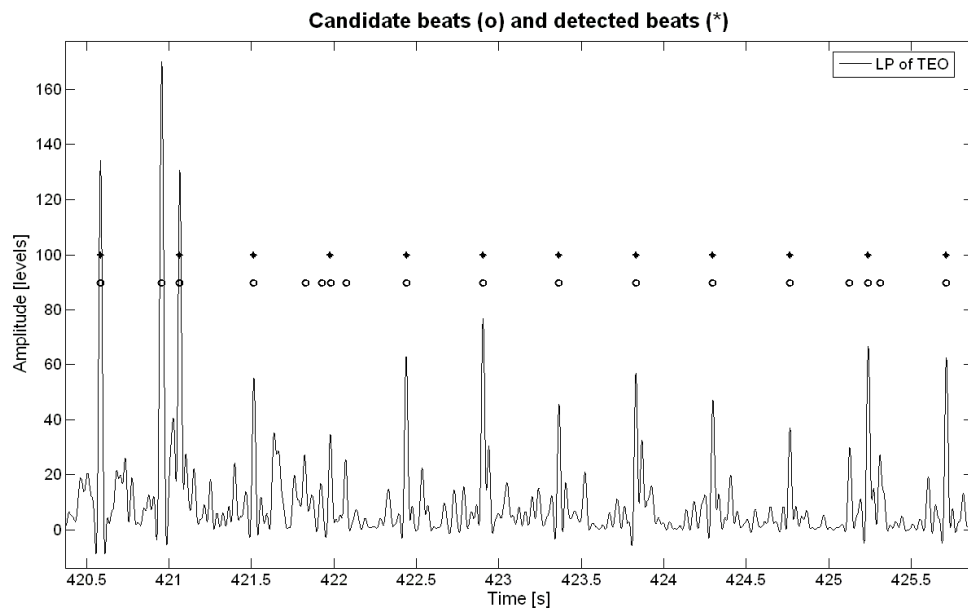
Figure 29: signal tract of B3 output, in particular low-pass filtered TEO output corresponding to PCG recording # 13. Circles indicate candidate beats, whereas stars point to detected beats.

As mentioned above, due to noise, many peaks, with very low amplitude, could there be in T. So that, in order to reduce the number of peaks to be analyzed, a local amplitude threshold (TH) was also considered. Of course, in presence of noise, the number of peaks in T could be high, thus making difficult and very time consuming the logic block working. To take into account SNR of the current processing interval, that is to identify and discard peaks more probably due to noise, the algorithm set a local, amplitude threshold, TH, equal to 1.2*M, where M was the LP mean value within the interval T. Only peaks greater than TH (see figure 30 for an example) were considered beats and analyzed by the logic block.
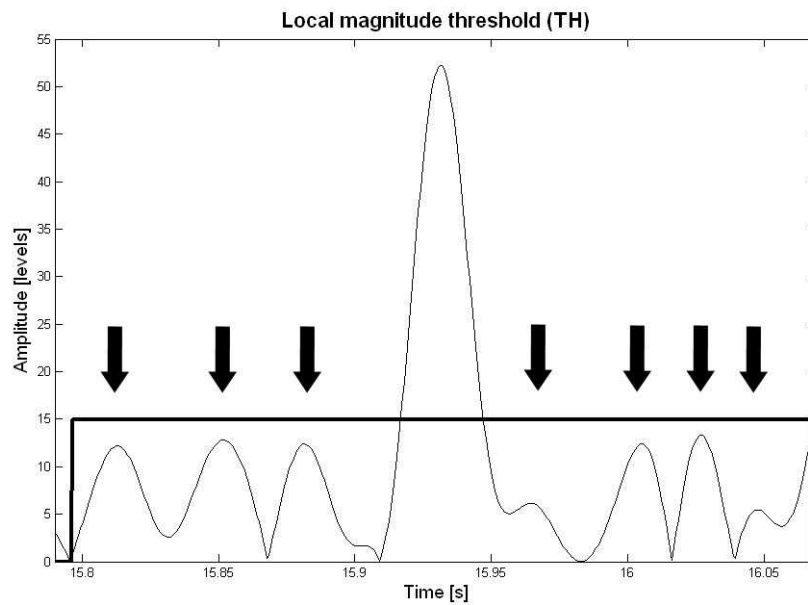
Figure 30: example of usefulness of local amplitude threshold TH (PCG recording # 11). Without TH, peaks indicated by the arrows would be considered as candidate beats. Considering SNR, and in turn TH (bold line), they were rejected (see text for details).

B5 Post-processing block

This block had different tasks: to locate time marks for detected S1, to estimate FHR signal, to compute a reliability index and to identify and substitute outliers.

B5.1 Time marks location

Once candidate peaks had satisfied the criteria for being S1 events, the timing of the occurrence had to be established. This task was particularly important to obtain a reliable series of beat to beat inter-distances and in turn a FHR signal with good quality.

Following an approach used also for QRS detection in ECG processing [118][119][120], for each chosen peak (corresponding to an identified S1), the post-processing block located

114

three kinds of time marks: 1) maximum of LP peak (M1); 2) centre of gravity of the rectified signal tract of filtering block output, corresponding to the chosen LP peak (M2); 3) maximum of the central peak of the rectified signal tract of filtering block output, corresponding to the chosen LP peak (M3). See figure 31 for an example.
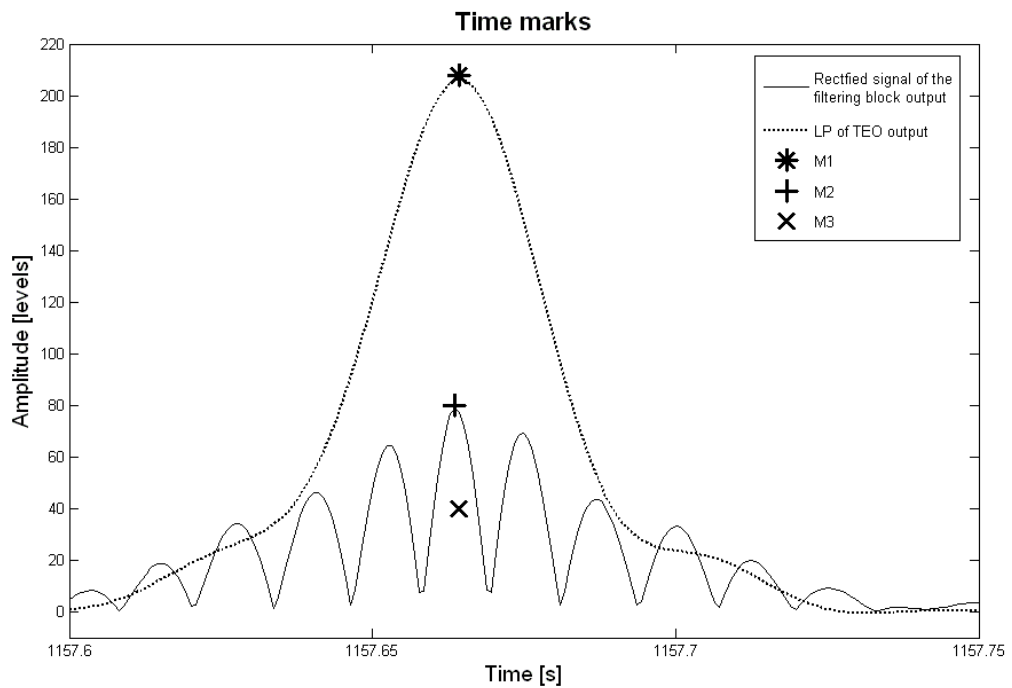
Figure 31: signal tract relative to PCG recording # 18. Solid line represents rectified B2 block output and dashed line represents B3 block output. Star corresponds to M1 time mark, fixed in respect to the signal painted as dashed line. Cross and "x" are, respectively, M3 and M2 time marks, chosen according to the signal shown as solid line.

B5.2 FHR estimation

Beat to beat inter-distances series (RR) was computed as differences between consecutive time marks (corresponding to detected heart beats) and expressed in ms. The correspondent FHR series was estimated as 60000/RR and expressed in bpm.

Considering all the implemented processing paths (twelve different combinations of filtering and first foetal heart sounds enhancement blocks) and the three kinds of time marks, 36 analysis procedures (AP) were achieved and 36 FHR signals for each PCG recording.

B5.3 Reliability index computation

Due to the highly non-stationary characteristics of the FHS itself and the unforeseeable noise state, some estimated FHR values may be more reliable than others. To express this condition, we provided a Reliability Index (here named RI) associated to each computed RR value (and in turn to each FHR value).

RI depended on other two indexes here proposed: Fiducial Degree (FDRR) and Quality Signal (QSRR) indexes.

The FD index expressed different fiducial levels associated to each detected beat using information stored by the logic block.

In particular, it was high if in the processed LP segment there was just one peak higher than HT; it scored a medium value if there were present two peaks higher than HT or one or two probable heart beats higher than LT and it scored low in all the other cases (see paragraph B4 for details about S1 detection).

The QS index was instead related to the quality of FHS signal. It was function of the ratio between RMS computed in an interval centred at the time mark and designed to include only S1 and RMS computed on an interval corresponding to about the whole heart period. Also QS could be high, medium or low in base on the ratio value.

Since, as explained in paragraph B5.2, a RR sample (RR(n)) was computed as difference between time positions of detected consecutive S1 (here named S1(n-1) and S1(n)), indexes linked to each RR interval were combination of FD and QS indexes associated to both S1 according to the following tables.

		$FD_{S1(n-1)}$		
FD_{RR}		HIGH	MEDIUM	LOW
$FD_{S1(n)}$	HIGH	High	Medium	Low
	MEDIUM	Medium	Medium	Low
	LOW	Low	Low	Low

Table 13: an RR interval was computed as difference between time positions of consecutive detected S1; so, for each RR value, FDRR was computed as combination of FD associated to previous and current S1 (respectively, FDS1(n-1) and FDS1(n)).

		$QS_{S1(n-1)}$		
QS_{RR}		HIGH	MEDIUM	LOW
$QS_{S1(n)}$	HIGH	High	Medium	Low
	MEDIUM	Medium	Medium	Low
	LOW	Low	Low	Low

Table 14: an RR interval was computed as difference between time positions of consecutive detected S1; so, for each RR value, QSRR was computed as combination of QS associated to previous and current S1 (respectively, QSS1(n-1) and or QSS1(n)).

Finally, RI value, associated to RR(n) and then to FHR(n), was high if both FDRR and QSRR were high; it was medium if FDRR or QSRR was high and medium the other index; it was low in all the other cases (see next table).

RI		QS$_{RR}$		
		HIGH	**MEDIUM**	**LOW**
FD$_{RR}$	**HIGH**	High	Medium	Low
	MEDIUM	Medium	Low	Low
	LOW	Low	Low	Low

Table 15: computation of RI associated to each RR value in base on FDRR and QSRR indexes.

B5.4 Outliers detection and substitution

Nevertheless the developed algorithm was planned to be "intelligent and robust", residual estimate errors (outliers) can be in FHR signals. They should be removed before any analysis can be carried out, so we realized another step for outliers detection and substitution [34].

At this step, the algorithm reviewed all FHR samples associated to high and medium RI values. FHR samples associated to low values of RI were not processed because they were not considered in further analyses. For outliers detection, the algorithm combines the statistical definition of outlier [121] with the RI value (which qualitatively expresses the probability of logic block error).

In particular, if RI associated to FHR(n) was high (low probability of logic block's error), the algorithm set a threshold to 15 bpm; if RI was medium, it set the threshold to 10 bpm (lower value).

To recognize FHR(n) sample as outlier, the algorithm compared the set threshold with the two following differences |FHR(n) – M - | and |FHR(n) – M +|; where M – is a fifth order median value computed on the five previous FHR samples and M + is computed on the five following FHR samples. The FHR(n) sample was considered an outlier if both differences were higher than the set threshold.

For outliers substitution, the algorithm used the median value computed on 7 consecutive FHR samples (heuristically chosen value) associated to RI high or medium around the outlier sample. For an example see figure 32. In any case, the substituted sample was marked with a low value of RI.
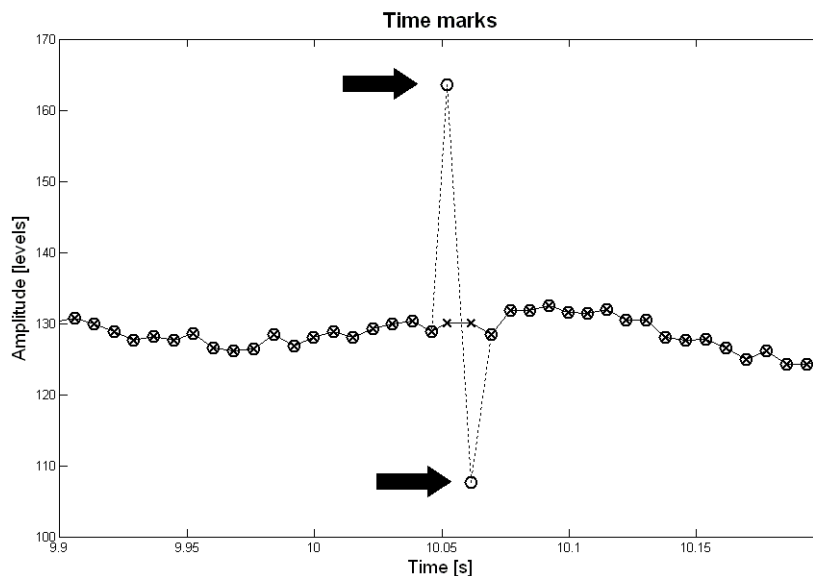
Figure 32: FHR estimated from PCG recording # 10 printed as dotted line. The arrows show extreme values of FHR detected as outliers. These samples were substituted from the developed algorithm by samples painted as "x". The re-computed FHR signal is shown as solid line.

5.3.3 PCG and CTG comparison

FHR signals estimated by the developed algorithm (FHR-FHS) were compared with FHR signals simultaneously recorded by means of CTG (FHR-CTG).

To this purpose, also in line with literature [32], we considered only signal tracts for which FHR-FHS showed high or medium RI and the corresponding FHR-CTG showed good quality on the device. The comparison between two FHR series (FHR-FHS and FHR-CTG) was carried out by computing the differences point by point. So, as the algorithm for each PCG recording provided 36 FHR series (see section B5.2), 36 differences series (DS), expressed in bpm, were computed.

<u>Software Quality Index</u>

For each patient, all the DS, obtained from the different recordings, were analyzed in order to estimate the following concise statistic parameters: mean absolute value (ME in bpm), standard deviation (SD in bpm) and a combination of percentages (PRI) of high (%H), medium (%M) and low (%L) RI values:

$$PRI = 1 * \frac{\%H}{100} + 0.3 * \frac{\%M}{100} + 0 * \frac{\%L}{100} \qquad (10)$$

where, of course, it results:

$$\%H + \%M + \%L = 100 \qquad (11).$$

Beside, the algorithm computed the mean value (estimated on all the patients and weighted according to the analyzed number of beats) of above mentioned parameters:

$$\overline{X} = \sum_{n=1}^{N}(b_n \cdot X_n)\bigg/\sum_{n=1}^{N}b_n \qquad (12)$$

where bn is the number of analyzed beats for the nth patient, Xn is the considered parameter computed for the nth patient, N is the number of all the patients and $\overline{X}$ is the mean value.

According to literature [32][33][122], where FHR series closest to CTG recordings are considered more reliable, to compare the different AP performances, we decided to identify the AP characterized by the smallest differences. For that goal, a software quality index (SQI), calculated as linear combination of the mean of 3 statistic parameters ($\overline{ME}, \overline{SD}, \overline{PRI}$), was introduced:

$$SQI = \sum_{i=1}^{3}S_i = \sum_{i=1}^{3}(k_i \cdot \overline{X}_i + a_i) \qquad (13)$$

For each mean parameter $\overline{X}$, a linear transformation was imposed to obtain values between 0 and 1; ki and ai values were reported in the table below.

	$\overline{ME}$	$\overline{SD}$	$\overline{\%H}$ /100	$\overline{\%M}$ /100
ki	-0.4	-0.5	1	0.3
ai	1.2	2	0	0

Table 16: coefficients imposed to the linear transformations applied to the chosen parameters.

Values out of a pre-selected range were saturated 3. The saturation levels were reported in the table below.

Saturation level	0	1
$\overline{ME}$	≥ 3	≤ 0.5
$\overline{SD}$	≥ 4	≤ 2

Table 17: selected ranges of variability were [0.5, 3] for $\overline{ME}$ and [2, 4] for $\overline{SD}$. Values out of these ranges were saturated at 0 and 1 values.

5.3.4   Results

Regard algorithm performances assessment, we analyzed 34 PCG recordings. After discarding of values with low RI, analyzed signal tracts lasted 8 minutes on average, so that, for each DS, more than 30000 beats were compared.

For a schematic representation of the obtained results (Table 18), each AP was identified by means of a 3 numbers code, where the first number represents B2 block (1 = matched filter with manual template, 2 = set band-pass filter, 3 = variable band-pass filter); the second, B3 block (1 = TEO, 2 = autocorrelation, 3 = autocorrelation + TEO, 4 = TEO + autocorrelation); the third, the kind of time mark (1 = M1, 2 = M2, 3 = M3).

The analysis of the DS indicated that some AP was able to provide a FHR series very similar (almost all confined between +/- 3 bpm) to that provided by a commercial US cardiotocographic device, currently employed in clinical routine (see figure 33 for an example).
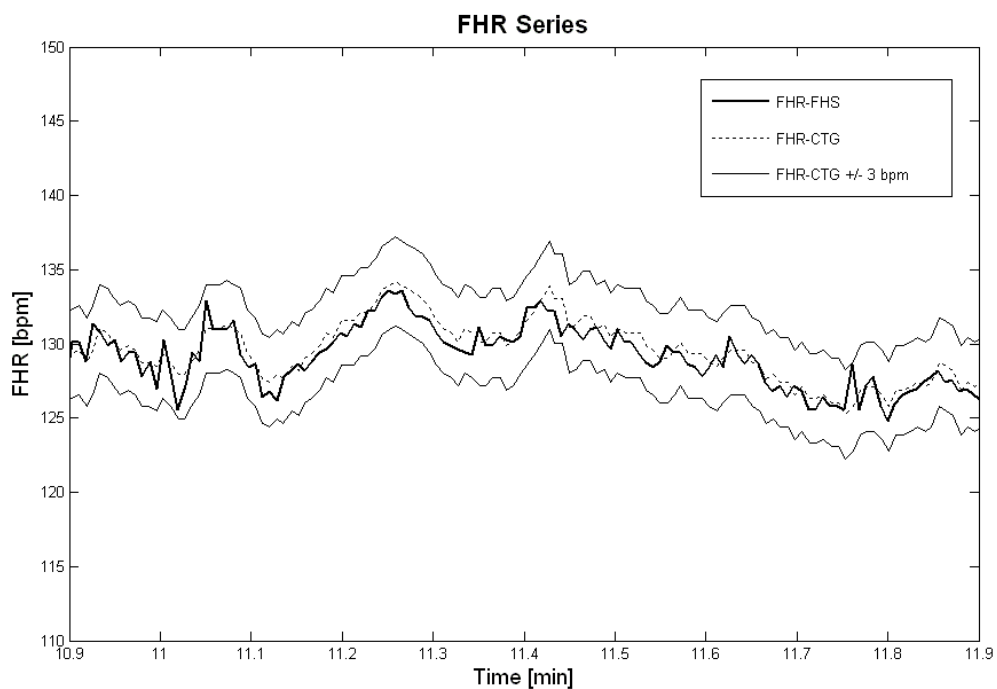
Figure 33: comparison between a FHR estimated from FHS signal (FHR-FHS, bold line) and FHR simultaneously recorded by means of CTG (FHR-CTG, dotted line); PCG recording # 13. Thin lines represent limits of FHR-CTG   3 bpm within which FHR-FHS resulted confined.

From Table 18, it is possible to highlight which PP and time mark had better performances. In particular, the 1.1.1 AP corresponded to the highest SQI value.

Besides, we can observe that for B3 block, TEO operator seemed to be the best choice (results of all the PP which employ only TEO operator are: $\overline{ME}$ values $\leq$ 0.52 bpm; $\overline{SD}$ values in the range 2.72 – 4.49 bpm and high SQI values), with every filtering and time mark (rows 1-3, 13-15 and 25-27). Moreover, about B2 block, so significant differences among filtering kinds were not found. However, fixed the other variables, the use of matched filtering seemed the best choice, but the other two choices (band-pass filtering with set or variable centre-band frequency), which have the advantage of avoiding the manual template selection, gave acceptable results too. In the PP employing the TEO operator, time mark M1 gave the highest SQI values while M3 the lowest ones.

	AP	$\overline{ME}$	$\overline{SD}$	$\overline{PRI}$	SQI
1	1.1.1	0.30	2.72	0.71	2.35
2	1.1.2	0.30	3.20	0.71	2.12
3	1.1.3	0.34	3.95	0.71	1.74
4	1.2.1	0.96	5.24	0.18	1.00
5	1.2.2	0.79	5.35	0.18	1.06
6	1.2.3	3.69	8.85	0.18	0.18
7	1.3.1	0.79	5.02	0.17	1.06
8	1.3.2	0.63	5.22	0.17	1.12
9	1.3.3	3.53	8.95	0.17	0.17
10	1.4.1	0.80	3.79	0.34	1.33
11	1.4.2	0.78	3.61	0.34	1.43
12	1.4.3	0.79	4.43	0.34	1.23
13	2.1.1	0.33	3.31	0.69	2.04

14	2.1.2	0.33	3.55	0.69	1.92
15	2.1.3	0.52	4.49	0.69	1.68
16	2.2.1	1.04	6.44	0.14	0.93
17	2.2.2	0.97	6.45	0.14	0.95
18	2.2.3	6.00	11.41	0.14	0.14
19	2.3.1	1.01	6.32	0.13	0.93
20	2.3.2	0.80	6.32	0.13	1.01
21	2.3.3	5.34	11.37	0.13	0.13
22	2.4.1	1.01	4.07	0.35	1.15
23	2.4.2	1.00	3.96	0.35	1.17
24	2.4.3	0.99	4.63	0.35	1.16
25	3.1.1	0.30	3.37	0.71	2.02
26	3.1.2	0.29	3.64	0.71	1.89
27	3.1.3	0.34	4.46	0.71	1.71
28	3.2.1	1.05	6.20	0.15	0.93
29	3.2.2	0.86	6.29	0.15	1.01
30	3.2.3	5.24	11.09	0.15	0.15
31	3.3.1	0.91	6.10	0.13	0.97
32	3.3.2	0.96	6.10	0.13	0.95
33	3.3.3	5.12	11.56	0.13	0.13
34	3.4.1	0.95	3.97	0.37	1.20
35	3.4.2	0.90	3.84	0.37	1.29
36	3.4.3	0.95	4.56	0.37	1.18

Table 18: obtained SQI values for all the DS. In the second column, a numerical code corresponds to each AP: the first number represents the filtering block (1 = matched filter with manual template, 2 = set band-pass filter, 3 = variable band-pass filter); the second, the first heart sound enhancement block (1 = TEO, 2 = autocorrelation, 3 = autocorrelation + TEO, 4 = TEO + autocorrelation) and the third, the kind of time mark (1 = M1, 2 = M2, 3 = M3).

5.3.5   Further considerations

Signal processing time was about 4 minutes, depending on computer characteristics (Dual CPU Pentium, 1.80 GHz, 2 GB RAM).

Owing to the extremely noisy nature of PCG signals and the overlap of different components spectra, standard filtering approaches or autocorrelation methods alone are not successful in determining the period of the foetal heart signal reliably [90]. Different filtering and enhancement techniques, to enhance the first foetal heart sounds, were applied, so that different signal PP were implemented. Then, in order to extract reliable time references from FHS, a "logic step" and a post processing block were included in the signal processing flow chart.

For algorithm performances validation, a comparison with a gold standard technique is necessary. Currently, CTG is generally considered as reference, due to its wide diffusion in clinical environments (in some countries it has also legal value). So, a comparison between FHR signals estimated by employed PP and simultaneously recorded CTG measurements was carried out. To simultaneously record PCG and CTG signals, we placed on maternal abdomen both probes (microphone and Doppler). Simultaneous location of both CTG and PCG probes, on the abdominal surface, is difficult. Thus, recorded PCG and CTG signals often showed a very lower SNR (with respect to either PCG or CTG recording). However, in cases where we could not hear the sound, we observed that the pregnant women were very obese. This is not surprising as we experienced the same problem even when we recorded only CTG.

Besides, it is known that due to non-stationary characteristics of noise and foetal heart sound itself, the calculated FHR in some interval may be more reliable than in others. Hence, we proposed a RI associated to the estimated FHR, provided by the developed algorithm itself.

Moreover, in order to compare the performances of the different tested PP, we decided to identify the PP characterized on average by the smallest errors (differences between corresponding samples of FHR-FHS and FHR-CTG series). For that goal, a software quality index (SQI), calculated as linear combination of the 3 chosen mean statistic parameters ($\overline{ME}, \overline{SD}$ and $\overline{PRI}$), was computed.

From the obtained results, as global consideration, it seemed that a correct FHR signal can be extracted by the acoustic signal, despite some unreliable FHR values obtained in case of highly noisy recordings.

A more in depth observation of obtained results yields also some other comments.

About B3 block, it is known that a problem with using TEO could be that it is sensitive to noise (noise bursts are enhanced along with the foetal heart sounds) [123]. However, by combining the TEO with an appropriate previous step of filtering, the foetal heart beats resulted enhanced and the noise reduced. In fact all the PP involving TEO operator showed the best performances.

Although the matched filter is resulted the best choice, it involves the manual selection of an accurate template of S1. When it is preferable to make automatic the overall processing, the band-pass filtering (with both set and variable characteristics) can be chosen obtaining satisfactory results (see rows 13-15 and 25-27 of table 18).

As expected, for FHS processing, autocorrelation technique resulted the worst choice (obtained results scored always very law values, SQI ≤ 1.06, slightly higher in few cases, relative to the use of both TEO and autocorrelation, see for example rows 10-12 and 34-36). It was due to the nature of FHS signal. In fact, it is not a real periodic signal and periodic sources of noise (for example mother heart sounds) corrupt the FHS leading to peaks in the autocorrelation result that do not correspond to foetal heart beats.

Concerning parameters chosen for SQI evaluation, it is important to underline that $\overline{PRI}$, basically related to reliability of detected beats, did not distinguish between different time marks. Beside, it was not sufficiently sensitive to differentiate the best filtering. Probably, this low sensitivity could be due to the high percentage of PCG signals with sufficient SNR (when the filtering process was not so significant).

$\overline{ME}$ and $\overline{SD}$ parameters are valuable to statistically characterize the DS and to estimate the error introduced by the time mark positioning. In some case, in fact, in correspondence of the same PP, DS have the same $\overline{ME}$ value but different $\overline{SD}$ values (compare rows 1 and 2, rows 13 and 14, row 25 and 26 of table 18).

Finally, about S1 time marks, it is known that use of the event peak can be plagued by problems because the actual peak may not be sampled, whereas the centre of gravity approach intuitively seems to be the most immune from noise, in fact since it uses the area under the curve to find the centre of the beat, small variations due to noise should effect it very little.

In contrast, with regard to the PP best performing, obtained results showed that M1 gave the highest SQI values (rows 1-3, 13-15 and 25-27). The result confirms, according to literature, the usefulness of the signal over-sampling.

5.4 Simulation of foetal phonocardiographic recordings

In this chapter, it is presented a software for simulating fPCG recordings relative to different foetal physiological conditions and recording situations. As it will be better explained in the following section, whole software processing, consists of 3 main steps: FHR simulation, FHS simulation, noise simulation.

In FHR simulation, by choosing different values of sympatho-vagal balance (SVB), number of accelerations and decelerations of FHR signals, it is possible to simulate various foetal conditions (i.e. sleep, minor or major foetal activity, tachycardia, bradycardia, stress). On the other hand, in the second step, by modifying the S1 and S2 frequency bands, it is possible to simulate different gestational ages and, by changing their amplitude, different conditions of signals acquisition (FHS amplitude depends for example on the foetal heart – acoustic sensor distant). Finally, the third step consents to generate different internal noise sources (i.e. foetal and mother's movements, mother's breathing) and external noise sources (environment noise), in order to simulate recordings with different SNR.

The developed software can be useful both for testing and assessment of FHR extraction algorithms from fPCG and as a teaching tool for demonstration to medical students and others. In this context, we have used fPCG software simulator to test the algorithm [103] for FHR extraction in cases of different SNR recordings.

Obtained results showed the usefulness of the developed simulator software as test tool and confirmed the good performances of the previously developed algorithm.

5.4.1 Signal simulation

About the fPCG signal, it can be summarized by the following expression:

$$x(t) = s(t) + n(t) \qquad (14)$$

where x(t) is the composite signal consisting of FHS signal, s(t), superimposed on background noise, n(t) [124].

For fixing sounds timing, an FHR signal was formerly simulated.

So, as mentioned in the section Introduction, the software processing consists of 3 main steps: FHR simulation, FHS simulation, noise simulation.

5.4.2 FHR signal simulation

To simulate FHR signals a slightly modified version of a method proposed by other authors was used; for detailed info please refer to [67][80][125]. Following that procedure, an artificial R-R tachogram with specific power spectrum (S(f)) characteristics is generated

by taking the inverse Fourier transform of a sequence of complex numbers with amplitudes $\sqrt{S(f)}$ and phases which are randomly distributed between 0 and 2π.

The following model parameters were adapted to resemble real foetal cases [125]. Low frequency (LF) and high frequency (HF) bands of the foetal heart rate variability (FHRV) power spectrum were considered to lie between 0.03 and 0.2 Hz, and 0.2 – 1 Hz, respectively (values adapted from [9][36][126][127]). LF/HF power ratio was fixed to 5 and Standard Deviation (SD) of HF band to 0.03. Mean FHR was initially set at 140 bpm - beats per minute - (within the range of normality, 120-160 bpm [1][23][23] and its SD was in the range 1-4. Then, more extreme values (from 80 bpm up to 200 bpm), simulating bradycardia and tachicardya, were simulated.

Baseline fluctuation was introduced adding to the signal a very slowly varying sine wave [67].

In addition, to obtain signals resembling physiological conditions, also accelerations were simulated by using Gaussian-like signal tracts (with standard deviation heuristically chosen equal to 0.2); the classical definition was adopted: accelerations are transient increases of the FHR from the baseline of at least 15 bpm for at least 15 s [23][81]. For each FHR series that had duration of about 25 minutes, three accelerations were simulated.

An example of a simulated FHR series is shown in figure 34.
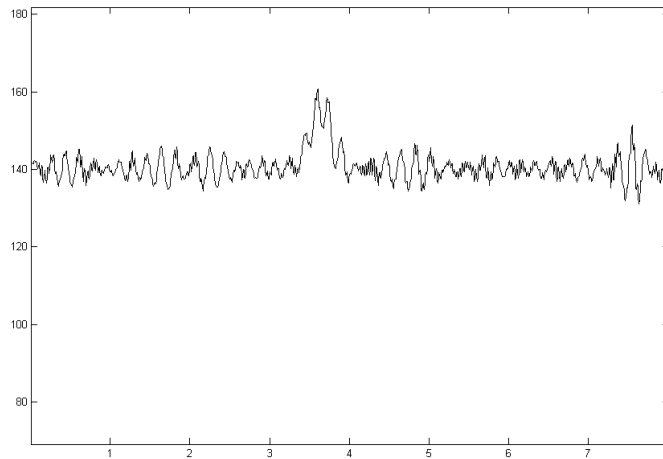
Figure 34: a part of a simulated FHR series: it is possible to observe an acceleration starting at about 3.5 minutes

5.4.3   FHS signal simulation

The FHS signal can be modelled as a sum of almost periodically recurring deterministic transients or "wavelets" [124][128]. In particular, S1 and S2 wavelets were modelled by gaussian-modulated sinusoidal pulses by Mittra [43]: in figure 35 it's shown how the PSD of a single S1 or S2 wavelet is very similar to a gaussian curve. The centre frequencies of the gaussian pulses simulating S1 and S2 (respectively F1 and F2) were chosen according to the results of the pilot study and depending on the WG while their standard deviation values (respectively SD1 and SD2) were set, regardless of WG, by computing the SD1 (and SD2) particular value of the gaussian curve that minimizes the mean quadratic error between the normalized PSD1 (and PSD2) and the gaussian curve that simulate S1 (and S2).

132
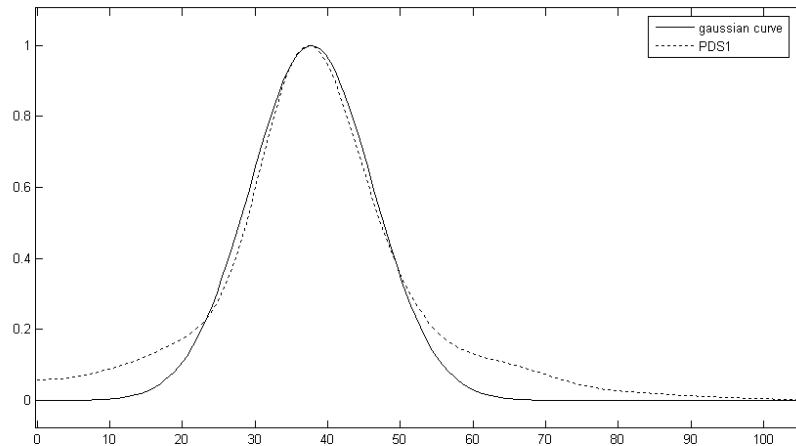
Figure 35: normalized PSD1 (38th WG) and the gaussian curve that minimizes the mean quadratic error

The following table reports the SD values computed by minimizing the mean quadratic error between the gaussian curves, which modelled foetal and maternal S1 and S2 wavelets in the frequency domain, and the correspondent normalized PSD .

SD1 [Hz]	SD2 [Hz]	mSD1 [Hz]	mSD2 [Hz]
8.64	17.81	4.62	14.41

Table 19: SD values computed (where mSD1 and mSD2 are the standard deviation values used to simulate the maternal S1 and S2)

FHS signals were simulated by a series of frames including the couple S1 and S2 wavelets (two gaussian-modulated sinusoidal pulses): a frame simulates foetal heart sounds corresponding to one heart beat. S1S2R was set according to the pilot study.

133

Because of their small energy, S3 and S4 sounds are practically undetectable [43] and so they were not simulated.

S1 – S2 inter-distance (SSID) in ms is a function of the FHR value [32]:

$$SSID = 210 - 0.5 * FHR \qquad (15)$$

Since each frame of the simulated FHS signal, corresponds to a single FHR value: the frame length (in minutes) is the inverse of the FHR value.

About wave's amplitude, because the software is supposed to simulate recordings of a generic fPCG device characterized of an unspecific gain, all the amplitudes are relative to a conventional value equal to 1, here considered corresponding to the saturation value of the generic fPCG device.

5.4.4   Noise simulation

In foetal phonocardiography, noise can be divided in two main categories: internal noise (produced by mHS, maternal digestive sounds, maternal respiratory sounds, foetal movements) and external noise (movement of measuring sensor during recording, ambient noise).

The amplitude of mHS may is much variable depending on recording conditions. In any case, mHS separation is possible in frequency domain, since it is characterized by a lower frequency range as confirmed by the results of the pilot study that agree with literature [43][90].

mHS is simulated exactly by the same methodology as FHS but, of course, with different values of the parameters, according to the pilot study: maternal heart rate (mHR) was simulated as the method discussed above for the foetus [67][80]; in the same way, mS1 and mS2 wavelets were modelled by gaussian-modulated sinusoidal pulses with different centre frequencies (respectively mF1 and mF2), SDs (respectively mSD1 and mSD2) and amplitude peaks according to the pilot study but regardless of WG. Like the FHS, mS1 – Sm2 inter-distance (mSSID) in ms is a function of the mHR value [129]:

$$mSSID = 0.2 * (60000/mHR) + 160 \text{ ms} \qquad (16)$$

Examples of simulated FHS and mHS frames are shown in the figure 36.
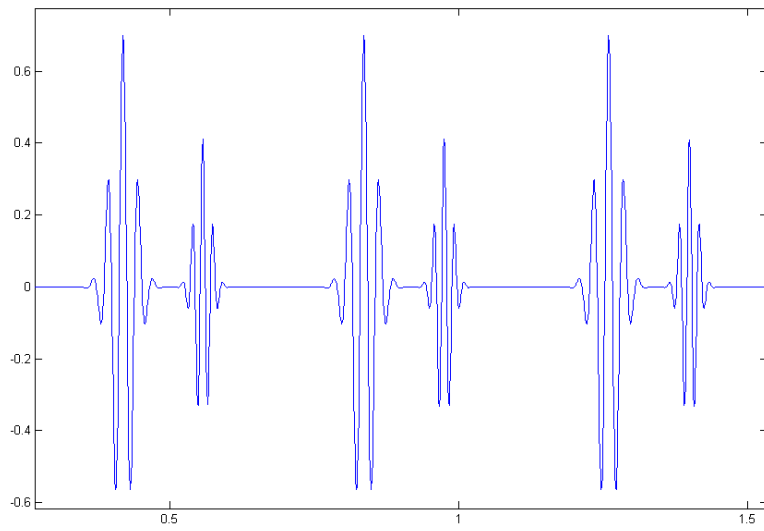
a)
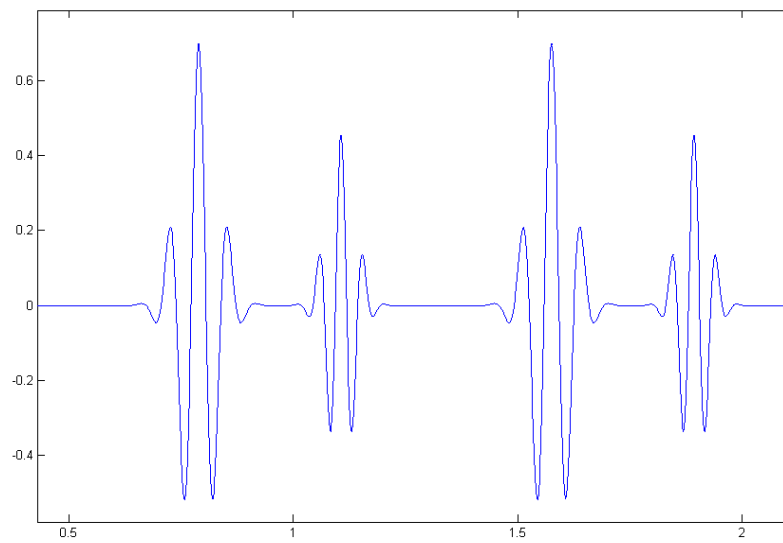
b)

Figure 36: examples of three simulated FHS frames (a) and two simulated mHS frames (b)

In addition to mHS, other internal noise contributes are sounds created by vibrations of maternal body organs (due to maternal digestion, respiratory muscular movements, placental blood turbulence) and of foetal movements.

According to literature [32][43][130], those internal noise (IN) contributes have low amplitude with main frequency spectrum components from 0 Hz to 25 Hz while external noise (EN), due to unwanted sounds from surrounding environment, is comparatively of high frequency (100 – 20.000 Hz) with large amplitude. IN and EN were simulated by passing a white noise through respectively a fifth order Butterworth low-pass filter with cut-off frequency limit of 25 Hz and a fifth order Butterworth high pass filter with a cut-off frequency limit of 100 Hz.

Finally, other two noise contributes were also considerate.

The first is an additive white gaussian noise (WGN) with zero mean [91] which simulates a generic noise such as the one due to amplifiers of a fPCG device.

The second is a noise source of limited duration impulses (LDI) that saturate the fPCG signal and simulate different kinds of acoustic bursts due to maternal fast body movements, maternal coughing, acoustic sensor displacements and generic high magnitude external noises. This noise source was simulated by generating random spikes along the whole length of simulated fPCG recordings. Those spikes were characterized by a random limited duration in the range 0.5 – 1.5 s and by the conventional maximum amplitude equal to 1 (here considered saturation value of the generic fPCG device).

All the noise contributes were linearly added to FHS signals to obtain the final simulated fPCG signals.

It is important to note that different recording conditions (such as distance between foetal heart and acoustic sensor, amniotic fluid volume, layers of fat and muscles thickness [43]); correspond to different SNR values. To simulate different SNR, all the noise contributes amplitudes (amS1, aWGN, aEIN that are the maximum amplitude values respectively of mS1, WGN, both IN and EN) were set to different values relative to the S1 peak amplitude of FHS (aS1) that was fixed to a value equal to 0.7 (relative to the conventional maximum value equal to 1), except LDI which amplitudes (aLDI) were set equal to 1.

So, different combinations of those amplitudes were simulated (see table 20) and were estimated different corresponding SNR values in dB according to the following formula:

$$SNR = 10\log_{10}\left(\frac{P_s}{P_n}\right)$$
(17)

where Ps and Pn are respectively the power of FHS signal and the power of the noise n(t).

aS1	amS1	aEIn	aWGN	SNR [dB]
0.7	0.1	0.05	0.025	-4.3
0.7	0.15	0.1	0.05	-6.6
0.7	0.35	0.1	0.05	-8.1
0.7	0.15	0.1	0.25	-10.2
0.7	0.15	0.3	0.05	-11.2
0.7	0.15	0.1	0.25	-14.7
0.7	0.35	0.1	0.25	-15.3
0.7	0.55	0.1	0.25	-16.4
0.7	0.75	0.1	0.25	-17.7
0.7	0.95	0.1	0.25	-19.1
0.7	0.75	0.3	0.25	-21.0
0.7	0.55	0.3	0.35	-22.6
0.7	0.75	0.3	0.35	-23.2
0.7	0.95	0.1	0.45	-24.5
0.7	0.95	0.3	0.45	-26.1
0.7	0.95	0.5	0.45	-28.7

Table 20: different SNR obtained by different combination of all the noise contributes maximum amplitudes.

Finally, to verify the similarity between simulated and real signals, a data set including fifty simulated and fifty true fPCG recordings was gathered. Two expert gynaecologists inspected visually 10 seconds segments randomly chosen from the data set, without knowing which were simulated, and sorted them as simulated or true recordings. So, two contingency tables (see next section) were created and also Cohen's Kappa values were calculated as a measurement of concordance in categorical sorting.

5.4.5   Simulation results

The developed software allowed simulating fPCG signals akin to acoustical signals recorded on the abdomen of the mother.

	True recordings	Simulated recordings
Recordings sorted as true recordings	24	16
Recordings sorted as simulated recordings	26	34

Table 21: first gynaecologist's contingency table; Cohen's Kappa value equal to 0.16

	True recordings	Simulated recordings
Recordings sorted as true recordings	28	19
Recordings sorted as simulated recordings	22	31

Table 22: second gynaecologist's contingency table; Cohen's Kappa value equal to 0.18

The two calculated Cohen's Kappa values (0.16 and 0.18) were both lower than 0.20 that means poor agreement in the sorting: two expert gynaecologists were not able to distinguish simulated signals from the true fPCG recordings.

In next figure, an example of a simulated S1 superimposed on a real recording shows how well a gaussian-modulated sinusoidal pulse fits a heart sound.
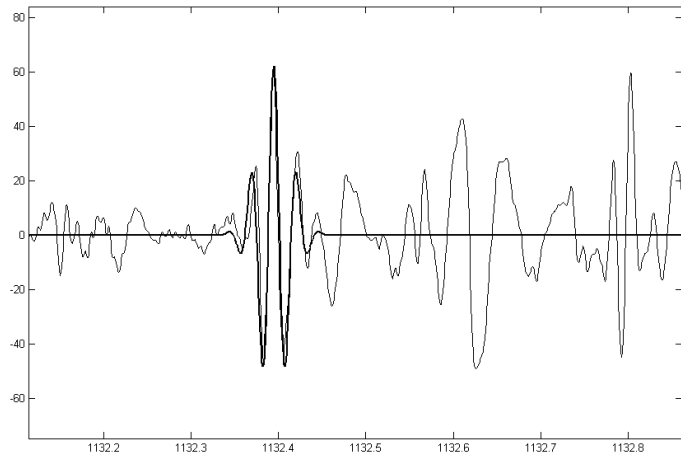
Figure 37: an example of a simulated S1 superimposed on a real recording (38th WG)

Two simulated fPCG signals with different SNR values are shown as examples in figure 38. It's possible to note that if the SNR is enough low, FHS signal will be heavily hidden by the different noise contributes.
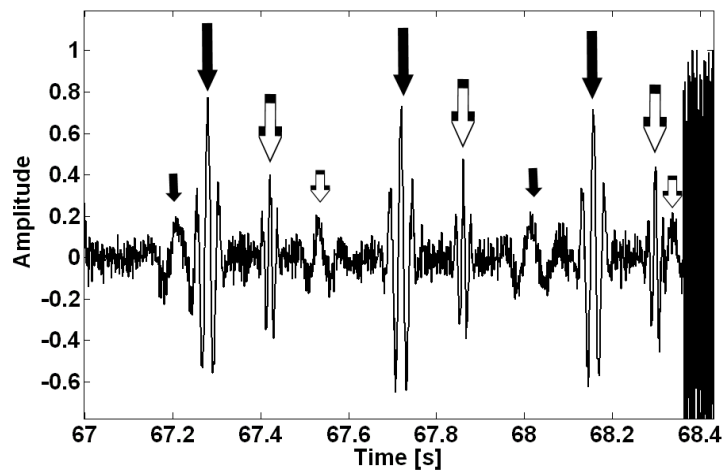
a)
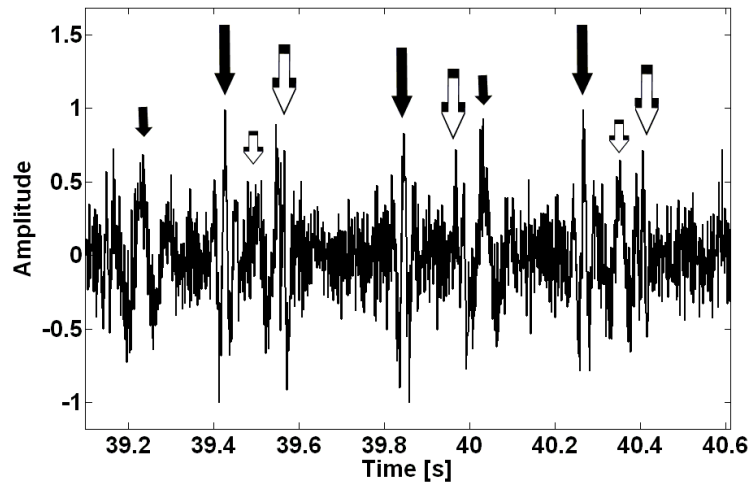
b)

Figure 38: Examples of tracts of simulated fPCG recordings with SNR = - 5.8 dB (a) and SNR = -9.9 dB (b). Long black arrows indicate S1, short black arrows indicate mS1. Long white arrows indicate S2, short white arrows indicate mS2. At the end of (a) it is shown an example of a random LDI

5.5 Assessment of FHR extraction algorithm

fPCG recordings simulated with different parameters and SNR (see the previous section for details) were used to test and assess the performances of the developed FHR extraction algorithm from fPCG [103] by means of an error analysis. In particular the PP number 13 was considered since it was the best choice that avoids the template selection. Although the matched filter is resulted the best choice, it involves the manual selection of an accurate

template of S1. When it is preferable to make automatic the overall processing, the band-pass filtering can be chosen obtaining satisfactory results.

Simulated FHR series were compared to the corresponding FHR series extracted by the algorithm according to the following scheme:
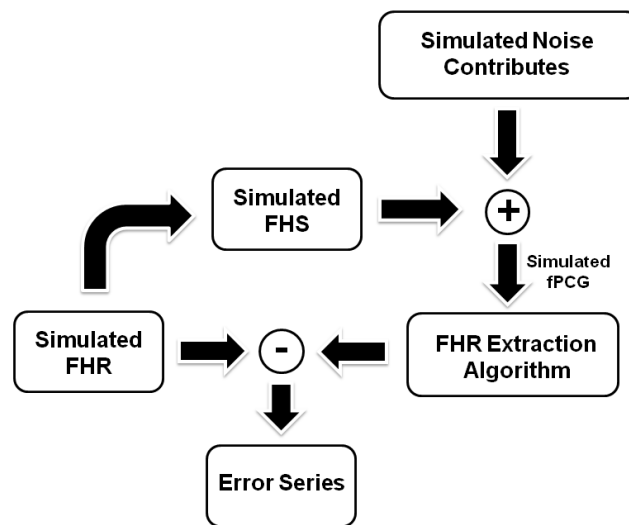
Figure 39: error analysis blocks scheme.

Beat-to-beat differences between the corresponding values of the two FHR series were calculated and an error series was obtained and analysed for each simulated fPCG recording.

5.5.1 Statistical analysis

For each error series mean absolute value (aM in bpm) and standard deviation (eSD in bpm) were initially estimated.

By literature [131][132] it is known that different indexes can be considered to assess an algorithm such as: true positive (TP), number of beat occurrences correctly detected; false positive (FP), number of artifacts detected as beat occurrences; false negative (FN), number of beat occurrences not detected. We chose accuracy (ACC), a metric summarizing the positive and negative diagnostic values of a test or method [60], and the percentage of missed beats (PMB) as performance indexes to carry out the error analysis. ACC and PMB are respectively defined as:

$$ACC = TP / (TP + FP + FN) \qquad (18)$$

$$PMB = 100 * FN / TP \qquad (19)$$

Moreover, the difference (eSVB) between SVB indexes of the two FHR series (simulated and extracted) was estimated. SVB indexes were computed as LF/HF ratio [57][80][133][134].

To calculate the power spectrum of the two FHR series, it was used the Lomb method that was proposed as a more appropriate spectral estimation technique respect to classical methodologies for unevenly sampled signals (like FHR series) [54][57][80].

All the processing was developed off-line using Matlab version 7.0

5.5.2   Assessment results

In the reported table, the error analysis results were reported for different SNR simulated recordings processed by the FHR extraction algorithm. The different SNR values were obtained by means of different combinations of maximum amplitude values of all the noise contributes according to table 20.

SNR [dB]	aM	eSD	eSVB	PMB	ACC
-4.3	0.0	0.4	1.2	1	0.99
-6.6	0.0	0.8	2.7	1	0.99
-8.1	0.0	0.8	3.0	1	0.99
-10.2	0.0	2.2	6.3	2	0.98
-11.2	0.0	2.2	6.3	2	0.98
-14.7	0.0	3.5	7.1	11	0.90
-15.3	0.0	3.5	7.1	11	0.90
-16.4	-0.1	3.5	7.1	12	0.89
-17.7	0.0	3.5	7.1	16	0.86
-19.1	0.0	3.5	7.1	17	0.85
-21.0	0.0	3.5	7.1	18	0.85
-22.6	0.5	4.8	7.3	29	0.78
-23.2	0.0	5.1	7.3	30	0.77
-24.5	0.2	6.3	7.0	41	0.71
-26.1	0.0	6.4	7.0	43	0.69
-28.7	0.2	6.8	7.6	44	0.68

Table 23: error analysis results

The analysis shows that how performance of the under test algorithm decrease if the SNR increases. If SNR > -10 dB, the algorithm extracts FHR series with a very low error (eSD <

1 bpm, PMB < 2%, ACC > 0.98). If -22 dB < SNR < - 10 dB, beat-to-beat differences between the two FHR series is still limited eSD < 3.6 bpm, PMB < 20%, ACC > 0.84) even if the algorithm provides a SVB value quite different from the simulated value (eSVB > 5). Finally, if SNR < - 22 dB, the algorithm performance fall down quickly.

These results showed the usefulness of the simulator to test the performances of the developed algorithm and confirmed its good performance.

5.6   Home care phonocardiography

In the past decade and until now several research groups are working on techniques like electrocardiography or phonocardiography, which are passive in nature, low-cost, easy to use, particularly suitable for long-term monitoring and optimally performed for a telemedicine system. The patient could easily record FHR at home using an electronic monitor based on these techniques and transmit the signal to a specialized centre for interpretation and evaluation. Recently, technological advances have led to small, lightweight, portable FHR and contraction monitors, which are highly reliable, simple to use, and well-accepted by patients [135]. Nevertheless, in spite of technological and signal processing advances just some sporadic pilot telemedicine network has been developed [136].

The aim of the present study was to evaluate the feasibility of home antenatal surveillance in high-risk pregnancies using these new monitors. In the initial phase of the research, here

presented, it was specifically tested the system, to train the personnel involved and to determine patient satisfaction with this technology.

For this study, it was used a highly reliable compact telemedicine system based on the passive phonocardiographic equipment developed by Pentavox manufacturer (Budapest, Hungary) [32][85]. To make compact this portable equipment, the developers decided to split the computational effort, some part is carried out on the low-cost, battery operated home unit, while the detailed analysis is performed at the computer centre. The local unit transfers data using a standard mobile telephone technology and a highly efficient compression method. The gynaecologist could consult patient record on the database, make his trace recording evaluation and send a text message to patient, which will read it directly on the equipment display.

The study group consisted of 6 patients without effective risk pregnancy at 39-42 weeks' gestation being followed at an ambulatory service in Naples. Informed consent was obtained from the patients before their participation in the study.
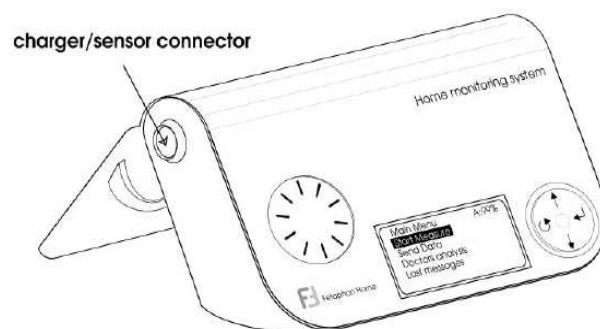
Figure 40: the portable Fetaphon-Home product by Pentavox. It is possible to see the charger/sensor connector in the upper part of the lateral side, the alphanumeric display in the central bottom part of the front panel, the multiple selector on the right bottom part of frontal panel and the loudspeaker.

Each patient was supplied with a lightweight ambulatory phonocardiotocograph, Fetaphon-home (Pentavox Ltd Budapest, Hungary), equipped with two probes, a microphone and a pressure transducer. The foetal monitoring device sends pre-processed and compressed signals to a server through the GSM network. Recorded signals can also be displayed on a specially enabled mobile phone of the doctor examining the pregnant woman. The period of tracing was 20 min. An internal clock controls the recording duration and after 20 minutes automatically stops the recording. Monitoring covers the measurement of foetal heartbeat, uterine contractions and foetal movements. In this study three fetaphon devices have been used.

Trained personnel instructed all patients in the use of the monitoring device. To assure correct placement of the transducers and transmission capability, patients performed a trial without assistance in gynaecologist office and transmitted data to the receiving centre (see figure 41).
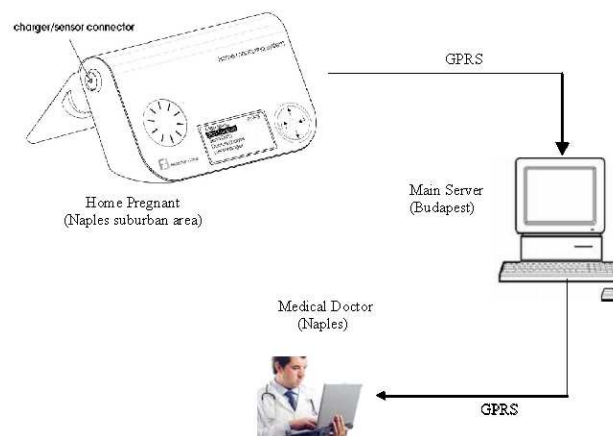
Figure 41: the Fetaphon transmission system. From the Fetaphon equipment the phonocardiographic recorded trace is sent to the main server located in the Pentavox, Budapest. Medical doctor, from its office located in Naples, could consult the patient database and carry out the trace evaluation.

It was used the manufacturer experimental server, located in Hungary, as computer server. Thereafter, patients were asked to perform the recording at home two times a week and to transmit it to the computer sever of reference centre. The transmission takes only few minutes.

After that, the gynaecologist could consult patient record stored on the computer server. The medical doctor could visualize the last sent recording, insert measure evaluation in the patient data record and send a text message to patient (of course, all the patient records are available at website).

As an example, figure 42 shows a recording as displayed by the web server.
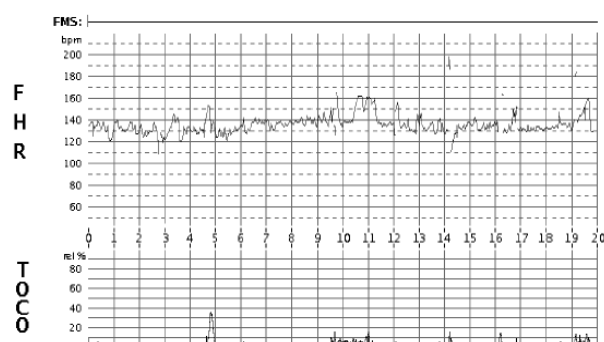
Figure 42: example of phonocardiographic recording displayed on the web server.

The patient will read the message directly on the equipment display. The message texts were standardized to ensure a clear comprehension. In case that the trace re-corded was considered pathologic the medical doctor sent a message recommending urgent hospitalisation of pregnant. In case of a trace considered "non-reassuring" the medical

doctor suggested repeating the recording at its ambulatory. In case of mistaken trace recording the doctor suggested to repeat the trace recording. In case of a reassuring recording the doctor sent a message of foetal well-being.

To determine satisfaction with care, patients were re-quested to complete a quality-of-life and anxiety-state questionnaire before and at the end of the study, which was adapted from the questionnaire suggested by Kerner [135]. Each item was rated on a scale of 1–4, and the sum of the scores was defined as the satisfaction index.

Questionnaire addressed to the patient for quality of life evaluation is below reported.

- Do you regularly submit to foetal monitoring by means of phonocardiographic device?

- Do you feel that the surveillance during the pregnancy is too intense?

- Are you receiving practical help from the medical staff?

- Are you satisfied with our help and support?

- Do you feel relaxed?

- Do you feel safe?

- Do you believe you are having a harder time with the pregnancy compared to other women?

- Do you feel anxious?

- Do you feel comfortable?

- Are you afraid?

- Do you feel satisfied about the home foetal monitoring?

- Do you wait too long for the results concerning your home recording?

- Did your trust on your own doctor diminish in consequence of your participation in the foetal home care project?

The home monitoring sessions were performed in addition to the routine surveillance at the clinic; thus, in this initial phase, the study monitoring did not replace clinic visits.

All patients assigned to home monitoring were able to perform the trace recording and correctly transmit the data. Overall, about 40 tracings were received from 6 patients, of which 2 (5%) were characterized as suspicious or non-reassuring (see the table below).

N. traces	N. reassuring	N. suspicious traces	N. non-reassuring traces
41	39	2	0

Table 24: classification of traces from a diagnostic point of view

After this, women repeated the test at home, and all the tracings were read as reassuring. No patient was then discharged for further surveillance with home monitoring and no patient was hospitalized for further observation.

From a technical point of view (see the following table), the quality of the recorded traces was correlated with maternal weight and a high correlation between this parameter and lowest quality traces was found.

N. traces	N. good quality traces	N. repeated traces
41	39	2

Table 25: classification of traces from a technical point of view

About patient response to this methodology, analysis of the questionnaire responses showed high patient satisfaction with care. Quality-of-life was considered improved by pregnant women. Satisfaction did not vary between patients who used the monitoring for shorter or longer periods of time.

6. Foetal Electrocardiography and combined FECG-FPCG monitoring

In this chapter, the use of foetal phonocardiographic and electrocardiographic methodology and their combination, are presented in order to detect the foetal heart rate and other functioning anomalies. The developed software processing methodologies, suitable for longer-term assessment, were able to detect heart beat events correctly, such as first and second heart sounds and QRS waves. The detection of such events provides reliable measures of foetal heart rate, potentially information about measurement of the systolic time intervals and foetus circulatory impedance.

All the obtained results were presented in a chapter "Non invasive foetal monitoring with a combined ECG - PCG system" of the book: "Biomedical Engineering, Trends, Researches and Technologies" [137].

6.1 FECG signal

Abdominal ECG measures the electrical signals generated by the foetal heart with multi-channel electrodes placed on the mother's body surface. The waveform of foetal ECG is similar to that of mother signal. The three main characteristics that need to be obtained from the FECG extraction for useful diagnosis include [47]:

- Foetal heart rate

- Waveform amplitudes

- Waveform duration.

Unobtrusive, long-term and risk-free monitoring are obviously the major requirements for obtaining the FECG. However, now there is not a good stated and reliable method for FECG extraction.

The major disadvantages with this technique are that the acquisition of the FECG cannot be guaranteed and often has a very low SNR because of the interference caused by maternal ECG (mECG). To overcome the above problems, some multiple-lead algorithms use the thoracic mECG to cancel the abdominal mECG.

Another disadvantage of the FECG is that around the 28th to 32nd weeks of gestation, the amplitude of the FECG is markedly attenuated due to the electrically insulating effect of the vernix caseosa covering the foetus and the existence of preferred conduction pathways between the foetal heart and maternal abdomen around this time [27].

The electromyography (EMG) signal, due to an uncomfortable position of the patient or to the uterus contraction, together with motion artifact, lead to difficulties in determining the FHR from the FECG signal.

The foetal ECG reflects the summation of electrical events within the myocardial cells as seen from the body surface [132]. Cardiac events on an ECG are associated with the alphabetical labels as shown in figure 43. A cycle of normal heart beat, consists of waves, complexes, intervals, and segments representing as follows:

- P wave: the firing of the sinoatrial (SA) node and atrial depolarization;

- PR interval: the atrial depolarization and atrioventricular (AV) delay;

- QRS complex: the ventricular depolarization;

- Q wave: the initial negative deflection resulting from ventricular depolarization;

- R wave: the first positive deflection resulting from ventricular depolarization;

- RR interval: the amount of time between consecutive R waves;

- S wave: a second negative deflection of ventricular depolarization following the R wave;

- ST segment: a part of the ventricular depolarization process;

- T wave: the ventricular repolarization;

- QT interval: the amount of time which ventricular depolarization and repolarization take.
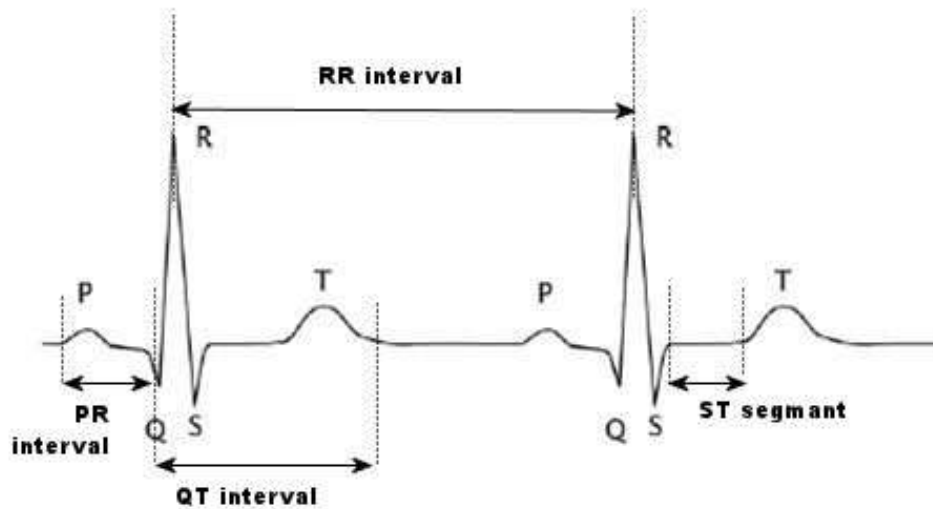
Figure 43: An example of ECG signal and its components.

The analysis of FECG permits the determination of cardiac parameters and, in turn, the identification of cardiac pathologies, such as acidosis [27]. It can also give other information about premature ventricular contractions (PVC), activity of the autonomic nervous system by spectral heart rate analysis, cardiac arrhythmia, uterine contraction, etc.

Oxygen deficiency is a known cause of neurological damage. The ST interval reflects the function of the foetal heart muscle (myocardium) during stress tests. Intervention according to ST waveform analysis has been found appropriate and it results in a significant reduction in the number of acidotic babies. At the same time, unnecessary interventions are avoided. Rosen and Kjellmer [138] observed progressive changes in the ST interval prior to the bradycardia in the FECG tracings in experimental hypoxia. The ST waveform can be assessed qualitatively by its shape, and quantitatively by the height of the T wave in relation to the height of QRS (T/QRS ratio). Greene et al. [139] found a correlation between high T/QRS with persistently elevated ST waveforms and anaerobic

metabolism in chronically instrumented lambs. In adults, ST depression with T wave elevation (a biphasic ST waveform) is also seen in myocardial ischemia, and may represent an earlier stage in the development of myocardial ischemic hypoxia when the action potential change is not uniform throughout the myocardium. It is used to diagnose myocardial infarction or coronary insufficiency [140].

The acquired FECG signals are characterised by a great amount of overlapped noise such as [46]:

- *Base-line wander*: respiration and body movement that can cause electrode-skin impedance changes result in baseline drift interference [27]; the drift of the baseline with respiration can be represented as a sinusoidal component at the frequency of the respiration combined with the ECG signal; the baseline drift interferences are considered to be low frequency components

- *Power line interference*: induced by the electrical power source (60 or 50 Hz)

- *mECG*: the main interference is maternal electrical activity since its amplitude is considerably higher than that of the foetus (in an abdominal register, the amplitude of the QRS commonly oscillates around 1mV for the maternal recording and up to 60µV for the FECG); in addition, the spectra of both maternal and foetal signals overlap; it is consequently not possible to separate them through conventional frequency selective filtering [27]

- *EMG:* it is the artefact of muscular contractions and is characterized by relatively high frequency noise that can be assumed to be transient bursts of zero-mean Gaussian noise although its amplitude is usually insignificant [27]; the situation is far worse during the uterine contractions of the mother, when the ECG will be

corrupted by the uterine EMG or electrohysterogram (EHG), which are due to the uterine muscle rather than due to the heart; the response of the foetal heart to the uterine contractions is an important indicator of the foetal health, so it could be useful monitoring FECG during uterine contractions, but it is a difficult task because of very poor SNR [47]

- *Inherent noise in electronics equipment*: all electronic equipments generate noise; this noise cannot be eliminated; using high-quality electronic components can only reduce it.

In addition, inter- and intra-subject variability is mainly increased by factors related to the gestational age and the position of the electrodes during the acquisition of the signal.

6.2   FHR extraction from FECG

The extraction of the FHR from FECG to monitor the general foetus well-being raises serious signal processing issue. In literature it's possible to find different techniques to extract FHR from abdominal FECG recordings: neural Networks [141][142], Dynamic Neural Network [141][143], Least Mean Square [143][144], Orthogonal Basis Function [145], Subtraction of an Average Pattern [146], Wavelet Transform [46][147][148], State

Space Projection [149] [150], Temporal structure [151][152], Polynomial networks [153], Independent Component Analysis [154][155].

However, there is not agreement about which is the best one. In particular, we have focused on Independent Component Analysis (ICA). It is essentially a method for extracting individual signals from mixtures of signals. Its power resides in the physically realistic assumption that different physical processes generate unrelated signals. The simple and generic nature of this assumption ensures that ICA is being successfully applied in a diverse range of research fields [154].

There are some different algorithms used to implement the ICA.

Aapo Hyvärinen in 1997 introduced a family of algorithms that are grouped under the epithet fixed-point or FastICA algorithms [156]. The members of this family are differentiated firstly by the algorithmic approach and secondly by the contrast function used. The key to all the variations is finding independent components by separately maximising the negentropy of each mixture [157].

A basic ICA assumption is that the source components are statistically independent. In this case we suppose the foetal and maternal signals as independent, which is a physically realistic assumption.

In order to extract FHR from FECG, a FastICA algorithm was chosen since ICA offers a fast and efficient approach for the pre-processing of FECG with multiple signals of interest, in particular when the SNR is low. Beside, no specific a priori knowledge is required in order to identify components generated from different sources. However, the main disadvantage of the techniques based on Blind Source Separation (BSS) approach, like ICA, is that it requires different ECG leads [154][155].

At present, the position of the electrodes placed on the body depends by the method used for the extraction of FECG from the abdominal record [158].

Furthermore, as the foetus moves, it is clear that a standard location for the sensors does not exist.

However, the number of electrodes should not be excessive because it could be uncomfortable for the mother; on the other hand, it must be suitable to ensure a good informative content for the foetal extraction. Thus, we used four electrodes placed on the maternal abdomen and an additional electrode as the reference.

One of the known limitations of ICA is that the number of the output channels cannot be larger than the number of input signals. Since the independent sources of the recorded signals could be more than the number of the abdominal recordings, it is important to reduce, as much as possible, the known sources of noise (such as maternal ECG, baseline wander, power-line interference, motion artifacts).

Sharp notch filters (with Q-factor equal to 30) at 50 Hz and its possible higher harmonic components (100, 150 and 200 Hz) were used to suppress the power line interference.

After a band pass filter with 3 dB band equal to 3 - 40 Hz was used because the frequencies of interest of QRS waves (used as reference for FHR extraction) lay mainly inside this frequency range. This filter reduced high frequency noises, motion artifatc and also the baseline wander.

In order to reduce the maternal ECG, maternal QRS waves were detected by means of a threshold (proportional to the local root mean square value of the signal); for each detected maternal QRS, an average wave, computed on the previous detected 5 waves, was subtracted to the current detected QRS wave.
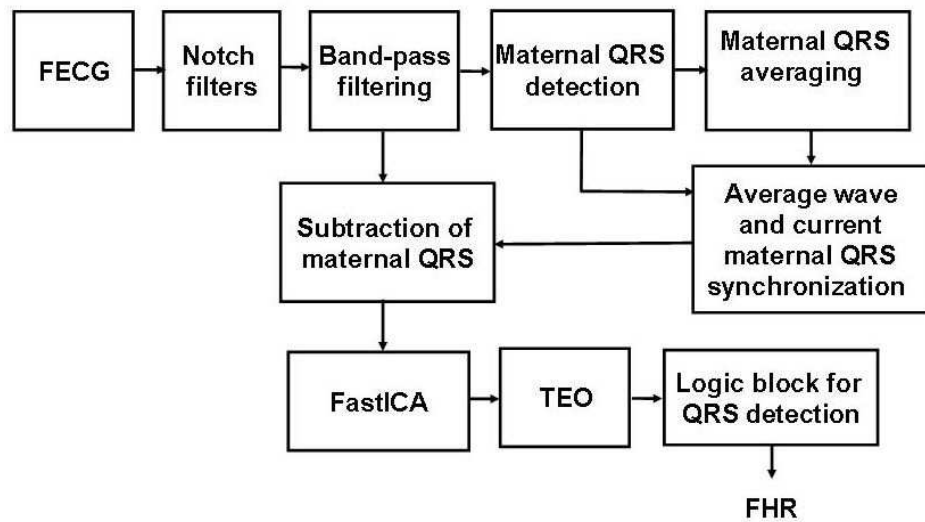
Figure 44: Flow chart of the algorithm for FHR extraction.

The fastICA algorithm was applied to the all abdominal channel processed as previously described.

The previous shows how the algorithm elaborates FECG. The independent component where FECG resulted better projected was chosen manually.

In order to extract FHR, the foetal QRS waves were detected using the same strategy used for the FPCG. Foetal QRS waves were enhanced by means of TEO and after detected by using the same logic block used for S1 events that is an approach used also for QRS detection in ECG processing [118][159][160].
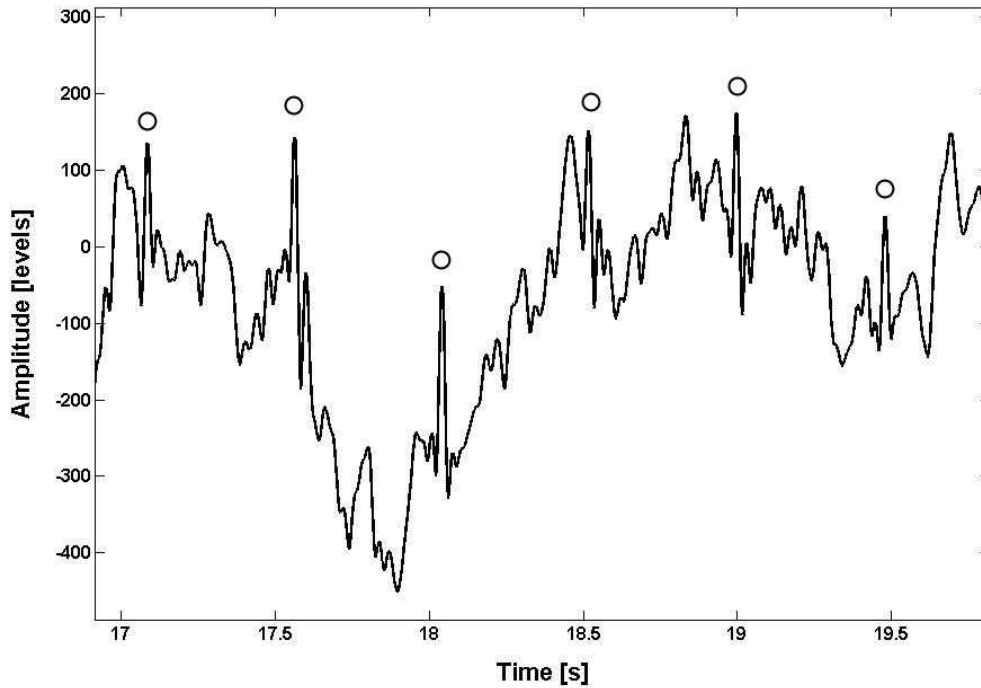
Figure 45: Examples of detected QRS events (circles).

6.3   Combined FECG-FPCG monitoring

Measurement of the systolic time intervals of the foetal heart (FSTI) may provide a suitable not invasive methods to evaluate foetal distress and beside a longer-term assessment of the foetus [161].

The most satisfactory available technique for FSTI measurement is the simultaneous recording of the FECG and of valve movements from a Doppler ultrasound system [162][163][164][165].

However the FPCG could be a possible alternative to ultrasound for the detection of foetal cardiac valve movements [161]. This would have the real advantage of overcoming the problem caused by the directionality of the ultrasound beam. Furthermore, as FPCG is a passive technique it avoids the controversial issue of acoustic exposure which concerns users of diagnostic ultrasound despite the absence so far of proven hazards [166].

In order to make FSTI measurements using the FPCG and FECG signals it is necessary to extract different heart beat events. In particular, from FPCG, it is necessary to detect the relatively high-frequency vibrations which identify the mitral valve closure and aortic valve closure and the lower-frequency component resulting from the ejection recoil which indicates aortic valve opening at the commencement of systole while, from FECG, it is necessary to extract the pre-ejection period (PEP, which is defined as the interval from the onset of the Q-wave to) [161].

The proposed algorithms provides all the required information; the occurrence of PEP can be estimated by means of the QRS waves detection while the other needed time occurrences can be estimated by the detection of the S1 and S2. In both the first and second sounds, the main part of the complex consists of large irregular vibrations, caused in the main by valvular events [111]. Therefore, division of each sound into different phases (corresponding to different valvular events such as mitral valve closure and opening and aortic valve closure) is relatively easy [161].
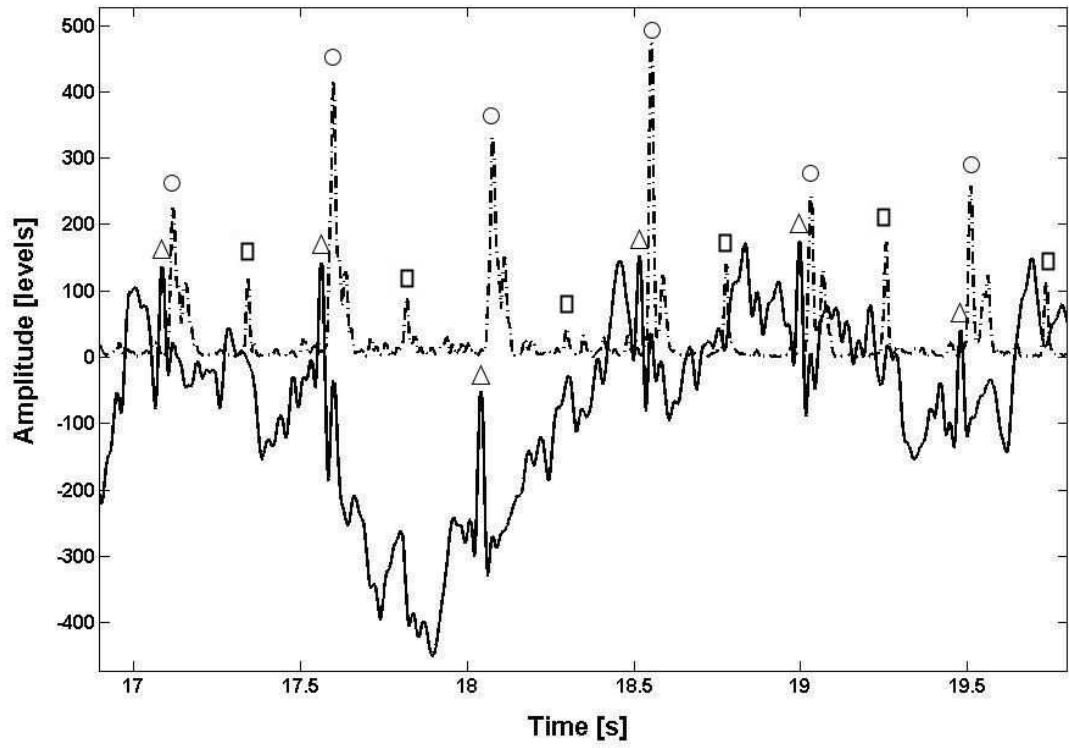
Figure 46: Examples of detected QRS events (triangles), S1 events (circles) and S2 events (squares) in a combined recording.
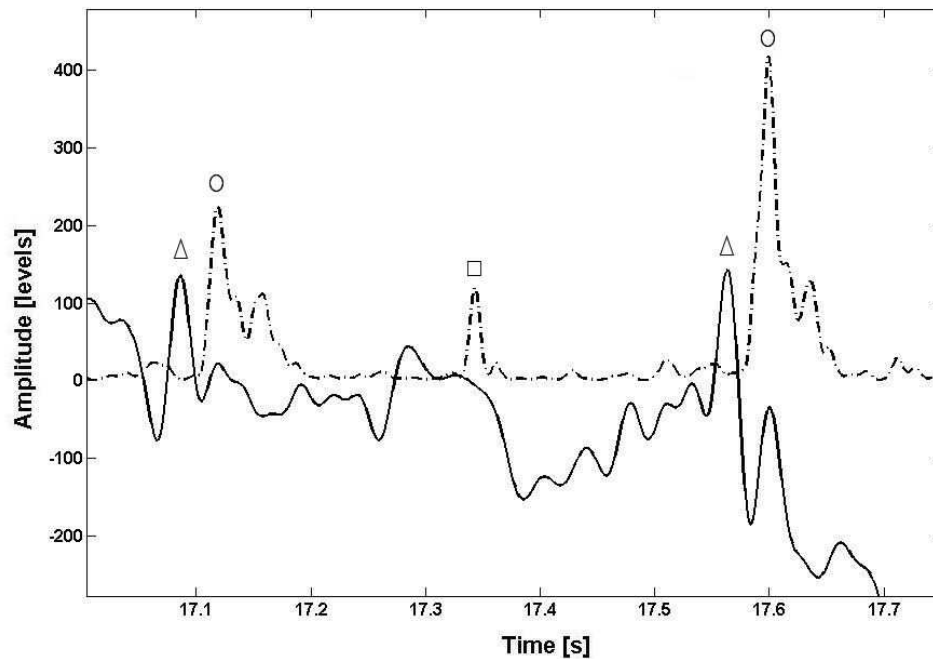
Figure 47: A particular of figure 46.

CTG monitoring is limited to only recording duration (typically 20-30 minutes) in any one day and it does not provide information about the foetal circulatory impedance on a continuous basis or on longer period (greater than 20-30 minutes). Obtained results will encourage the further development of appropriate processing techniques to obtain further information about the foetal circulatory impedance. By monitoring of the time difference between occurrence of a point on the FECG (such as P wave) and the corresponding foetal heart sounds, it is possible to provide information about the measure of the circulatory impedance. For example when the placental resistance rises due to placental insufficiency, greater pressure must be developed in the foetal ventricles; this leads to a lengthening of the time interval between the P wave and occurrence of the first heart sound. Any increase of this time interval, can be monitored over a period of time allowing the determination of a foetus at risk due to a placental insufficiency or other reason.

7. Discussion and conclusion

7.1 Analysis of US-CTG signals

Cardiotocography is an established part of daily obstetric practice, to monitor foetal health, mostly in the last weeks of gestation. Clinicians regularly monitor FHR and UC for signs of at-risk (or compromised) foetal conditions. During labour, to assess foetal reactivity, attention is focused on FHR alterations (such as decelerations) in correspondence to UC.

US-CTG usefulness is undoubted; nevertheless, there is, still nowadays, substantial intra- and inter-observer variation in the assessment of FHR patterns, due mainly to the visual inspection of US-CTG, which can lead to intervention when it is not required or lack of intervention when it is. Hence, several analysis methodologies (in time domain, in frequency domain, with semi-automatic software which compute specific time-domain parameters, etc.) were proposed in recent years to improve reliability and objectivity of US-CTG signals interpretation [29][48].

This is still insufficient to certainly identify suspect or ambiguous conditions. So, great interest was dedicated to the FHRV. It is commonly accepted that the use of a convenient technique for measuring and displaying beat to beat fluctuations is of value for estimating the maturation of ANS and the integrity of the nervous control of heart rate [167]. In

particular, frequency analysis of FHRV could be a useful, additional tool [3][50][73] both in ante partum and in intra partum period.

A careful surveillance has to be dedicated to the intra partum period; in fact, while labour is of short duration in comparison to pregnancy, this period is of great risk for the foetus [168]. Intra partum stress can provoke adaptive changes in foetal metabolic process that can impact the future health of newborn [169]. Therefore, clinicians regularly check FHR and UC to try to identify foetal distress symptoms and adapt the extracting procedure for signs of at risk foetuses. In particular FHR alterations in correspondence to UC are evaluated, to assess foetal reactivity. However, it is well known that there is still controversy over the interpretation of different FHR patterns and that objective clinical criteria to recognise foetal distress by CTG data are still poorly defined, especially during labour [170] and no clear conclusions are available so far. Positive predictive value of abnormal intra partum FHR patterns for foetal acidemia is only around 30% [8], whereas detection of foetal distress, early in labour, may significantly improve newborn's health. Besides, literature regarding intra partum CTG is much less rich than that about ante partum CTG, mainly due to registration difficulties. Therefore, it is important to try to obtain more reliable and objective methods for CTG interpretation and for neonatal outcome prediction [171][172][173][174][175][176][177].

In this scenario, analysis of FHRV can provide additional, useful information related to the foetal ANS control of the heart and its compensation capability. Analogously as for adults, specific stimuli can alter heart autonomic regulation and in turn generate specific modifications in the HR, particularly evident in frequency domain. Indeed, a UC is a strong compressive stimulus [178] (intra-uterine pressure can become four times stronger than basal pressure) that severely solicits the immature foetal ANS. This stress causes

reactions in the FHR; one of the most evident is a FHR deceleration that often is associated with a UC, which is an important sign for physicians. Therefore, a more detailed study of the reaction of foetal ANS to UC, such as FHRV spectral modifications analysis, may help in the understanding of specific foetal reactivity, capability and modality of foetal compensation to hypoxic stress.

This thesis presents a study to investigate spectral modifications of the FHRV in response to the external stimulus represented by UC, for healthy foetuses, in order to find, during labour, possible predictive information about risky foetal conditions, before foetuses become injured.

It was not consider the gestational age (related to ANS maturation), even if it is well known that considerably affects the foetal hemodynamic responses to stimuli and distress, because weeks of gestation, in all recordings, were in a range where it is possible to disregard this factor as an additional cause of considerable FHR changes [54][69][179].

Clinical intra partum UC and FHR are very noisy signals prone to frequent sensor disturbances; however, despite these conditions, the segment length required for frequency analysis, as proposed in this study, is short enough to overcome this problem.

Obtained results showed that a FHRV power spectrum modification can be observed in response to UC stimulus. In particular, a significant increase of the average power (confirmed by a t-test, $p < 0.01$) during UC-segments with respect to reference-segments is noted.

Moreover, it was observed a shift to higher values of the maximum frequency contained in the signal in correspondence of the power increase. So that, it is possible to conclude that

the power increase is not due to a specific band enlargement but is spread over all frequencies.

By literature it is known that, in general, a large variability reflects a healthy ANS and also chemoreceptors, baroreceptors and cardiac responsiveness; while foetal hypoxia, congenital heart anomalies and stress, cause a decreased variability [23][48][180][181]. So, in healthy foetuses, we expected an evident modification in FHRV frequency characteristics corresponding to a good capability of reaction to UC stimulus.

Obtained results, according to that finding, should indicate a foetal reactivity (in terms of FHRV power spectrum modifications with respect to the rest condition) to mechanical compressive stimulus represented by UC for healthy foetuses. Therefore, such spectral modifications, being a sign of ANS reaction, could represent additional, objective information about foetal reactivity and in turn about foetal health during labour.

About foetal reactivity in ante partum period, this thesis presents also a study for improving the understanding and the interpretation of cardiotocographic data, by means of analysis of PSD characteristics. Sometimes, the foetus is in a healthy status but the US-CTG doesn't show, in time-domain, characteristics corresponding to the definition of RF. In these situations, clinicians base their diagnosis almost exclusively on their experience. Therefore, it should be advantageous to have a new tool to support diagnosis in such doubtful cases. Preliminary results are satisfying, because they seem to indicate a certain differentiation between RF and NRF categories in frequency domain. This information could be useful to improve the knowledge of foetal condition. However, these results must be confirmed by a more extensive analysis.

In a future perspective, it should be very interesting to analyse not only the average behaviour of FHR spectral modifications but also its trend during labour course in order to evaluate the individual status of a foetus and possibly to set an alarm threshold. Since foetal response is probably due to number and frequency as well as intensity of UC, it is important to establish a criterion for an objective and standardised measure of the stimulus intensity, reminding that in cardiotocography only a relative measure of UC is known.

However, these issues deserve a more detailed and exhaustive analysis, mainly involving problematic pregnancies and cases of ascertained foetal distress, in order to, considering foetal health situations as point of reference, to recognise specific spectral characteristics to distinguish foetal well-being and foetal distress in order to propose such methodology in daily clinical practice.

In conclusions, the Variability of the Foetal Heart Rate around its baseline provides extremely significant information concerning the cardiac and ANS activities and their functional development during pregnancy up to labour. Obtained results demonstrated important modifications in the PSD of FHRV signals related to physiological stimulus represented by UC, both as power and frequency content, proving that the FHRV time-frequency analysis could be a very useful tool for a more objective and depth evaluation of the foetal health. We would not expect to find such modifications in cases of foetal distress; therefore, if these results will be confirmed by the study of FHRV signals recorded during risky pregnancies, information about the capability of a foetus to react to stress during labour course could be obtained by means of this approach.

7.2   PSD modifications of FHRV due to interpolation and US-CTG storage rate

Several analysis methodologies of CTG data were proposed in recent years for improving objectivity of CTG interpretation. FHRV spectral analysis, in particular, is accepted as a powerful technique for monitoring foetal health and ANS maturation. However, in spite of the great importance of obtained results in field of FHRV spectral analysis, it is worth stressing that spectral analysis of FHRV often employs methods (such as for example FFT) which require an evenly sampled time series. The FHRV series is computed from the variations in the beat-to-beat interval timing of the cardiac cycle, R-R series, which is determined at R-wave moments and so intrinsically involves non equidistant samples. Therefore, in order to achieve an evenly sampled time series from the R-R series, an interpolation and sampling is usually adopted. This technique results in unwanted effects in the power spectrum [64][80] and then alters the results of frequency analyses [54]. To avoid this problem, some researchers proposed the Lomb-Scargle periodogram as a more appropriate spectral estimation technique for unevenly sampled time series. It is shown to provide a superior PSD estimation respect to FFT or autoregressive methods with linear or cubic interpolation and uses only the original data [54][64].

In foetal monitoring, the cardiotocography is the most commonly technique employed in clinical routine. Many commercial cardiotocographs store FHR signals as evenly spaced series using a zero-order interpolation.

Zero-order, linear and cubic spline interpolations can produce significant errors in the PSD estimation, which can cause an alteration of important clinical parameters, such as the SVB. In this thesis, it was studied the errors in FHRV spectral estimation due to zero-order, linear and cubic spline interpolations and to sampling rates normally used by some commercial cardiotocographs to obtain even FHR series (2 and 4 Hz) and found, in general, an overestimation of SVB value, respect to the set value.

By obtained results, it is possible to observe in particular that, for different FHR mean values and storage rates, although in some isolated cases zero-order provides smallest overestimation of SVB, cubic spline interpolation produces more robust and accurate results. By analyzing the results obtained on sub-sets of 250 synthetic signals, without considering the FHR mean values, cubic spline interpolation confirms to be the best choose. Those results agree with results of a similar study for heart rate series analysis in adult subjects [80]. However, it is important to point out that heart rate variability characteristics are quite different in foetuses and in adults and that cited studies did not consider zero-order interpolation, which is critical since it is employed from widely diffused commercial cardiotocographs.

About storage rates, the overestimation obtained at 2 Hz is lower than that at 4 Hz. This result is in disagreement with what happens in short time variability analysis, for which a storage rate of 2 Hz provides less reliable results [29].

Concerning FHR signals simulated with superimposed accelerations, we noticed a further slight overestimation in SVB values, probably due to the frequency content of accelerations that partially overlaps to the low frequency band of FHR signal so increasing its power.

Obtained results suggest also that, to obtain more accurate SVB estimations, it should be preferable to analyse uneven FHR series employing Lomb method. However, since some commercial cardiotocographs do not provide real uneven FHR series, a pre-processing data tool to recover it from cardiotocographic data is necessary. If the employed cardiotocograph uses the zero-order interpolation, the algorithm previously proposed by the authors [125] could be utilised.

7.3 The algorithm for FHR estimation

The acoustic foetal heart beat signal results from vibrations produced in the opening and closing of the valves which control blood flow through the heart and from vibrations of the foetal heart muscle. It can be recorded by means of a microphone. Phonocardiography, based on this technique, due to its passive nature, is a suitable alternative tool to record FHR. Besides, physiological considerations together with medical experience show that the diagnostic potential of foetal PCG is much higher than generally supposed, and worth further intensive investigation. However, the first goal of PCG analysis is usually FHR estimation. To estimate FHR, it is necessary to extract reliable time references of the heart sounds. This is not an easy goal because of the poor SNR of the foetal PCG and the cardiac sound morphology. Furthermore, characteristics of FHS signal are variable, since the morphology of heart sounds changes with physiological processes (such as respiration). However, these variations mostly affect S2 while the appearance of S1 is quite robust and its energy is higher [117].

In this thesis, a new, fast algorithm developed for FHR extraction from PCG signals, based on S1 detection and timing and involving different processing paths, was presented.

From the obtained results, as global consideration, it seemed that a correct FHR signal can be extracted by the acoustic signal, despite some unreliable FHR values obtained in case of highly noisy recordings.

Different filtering and enhancement techniques, to enhance the first foetal heart sounds, were applied, so that different signal PP were implemented. Then, in order to extract reliable time references from FHS, a "logic step" and a post processing block were included in the signal processing flow chart.

For algorithm performances validation, a comparison with a gold standard technique is necessary. Currently, CTG is generally considered as reference, due to its wide diffusion in clinical environments (in some countries it has also legal value). So, a comparison between FHR signals estimated by employed PP and simultaneously recorded CTG measurements was carried out.

Besides, it is known that due to non-stationary characteristics of noise and foetal heart sound itself, the calculated FHR in some interval may be more reliable than in others. Hence, we proposed a RI associated to the estimated FHR, provided by the developed algorithm itself.

Moreover, in order to compare the performances of the different tested PP, it was decided to identify the PP characterized on average by the smallest errors (a software quality index was proposed).

A more in depth observation of obtained results yields also some other comments. Although the matched filter is resulted the best choice, it involves the manual selection of

an accurate template of S1. When it is preferable to make automatic the overall processing, the band-pass filtering (with both set and variable characteristics) can be chosen obtaining satisfactory results. As expected, for FHS processing, autocorrelation technique resulted the worst choice. It was due to the nature of FHS signal. In fact, it is not a real periodic signal and periodic sources of noise (for example mother heart sounds) corrupt the FHS leading to peaks in the autocorrelation result that do not correspond to foetal heart beats. Finally, about S1 time marks, it is known that use of the event peak can be plagued by problems because the actual peak may not be sampled, whereas the centre of gravity approach intuitively seems to be the most immune from noise, in fact since it uses the area under the curve to find the centre of the beat, small variations due to noise should effect it very little. In contrast, with regard to the PP best performing, results showed that M1 gave the highest SQI values. The result confirms, according to literature, the usefulness of the signal over-sampling.

In conclusion, a correct FHR signal can be extracted by the FPCG recordings and to achieve that goal, a reliable algorithm should include the following main steps: filtering for increasing SNR (reducing artifacts and mothers heart sounds), and TEO operator for enhancing signal tracts corresponding to S1 (areas of maximum local energy). Even after above mentioned steps, multiple lobes and peaks in correspondence of S1 and/or outliers caused by residual noise could be observed; hence, a logic block and a post processing block should also be included. The logic block selects the peak which most likely reflects the FHR trend among many candidates and the post-processing block exactly recognizes time references of S1 (corresponding to foetal heart beats), and detects and substitutes outliers [34].

7.4 FPCG simulation and assessment of the FHR extraction algorithm

The target was to provide a software for simulating fPCG recordings relative to different foetal physiological conditions and recordings situations and to use it as a test tool for FHR extraction algorithms.

There are few studies about foetal heart sounds frequency content and they disagree on heart sounds main frequency and since the available literature is not rigorous in this area a data collection pilot study was conducted with the purpose of specifically identifying both foetal and maternal heart sounds characteristics.

The results of the pilot study allowed to detect the main frequency components of FHS and mHS, and also the existence of a correlation between the frequency corresponding to the peak of the PSD1 (and PSD2) and WG.

The developed fPCG recordings simulator software allows to simulate the FHR, FHS, mHS and the noise sources typical of a fPCG recording. It is important to note that the generation of FHS and mHS with different pathological conditions is possible by merely altering the values of system parameters (such as HR, FHR, number of accelerations and decelerations, S1 and S2 shapes, SVB).

This software can be useful not only as a teaching tool for demonstration to medical students and others but also for testing and assessment of FHR extraction algorithms from fPCG. Owing to the extremely noisy nature of fPCG signals and the overlap of different components spectra, the first goal of fPCG analysis is usually FHR estimation. On this

purpose, we have used fPCG simulator software to test the developed algorithm [103] for FHR extraction in cases of different SNR recordings. Obtained results showed the usefulness of the simulator to test the performances of our algorithm and confirmed its good performance.

Future developments will aim to enrich the simulator software with new features for simulation of cardiac functionality anomalies such as murmur, split effect, extra systole, bigeminal/trigeminal atrial contraction.

7.5   Foetal home monitoring experience

About the experience of foetal home monitoring, the results obtained in this preliminary test, performed on healthy foetuses, suggest that, after a short training, pregnant women are able to identify the foetal heart beat and distinguish it from their one. Furthermore, the use of telemedicine system was well accepted by pregnant as far as it is a useful tool to reduce the need to travel for patients living away from adequately equipped medical centres, increasing their quality of life. The system fulfils patient expectations without posing an excess burden or causing unnecessary concern. This positive acceptance increases the possibility of foetal long-term home surveillance which in turn could increase the efficiency of the service offered to pregnant women.

Patient data and recorded traces are stored on a central server, in an easily accessible form consultable over the network, in order to allow gynaecologist to evaluate it. The possibility

of message exchange was appreciated both by gynaecologist and patients as far as it makes easy their daily contact.

It is important to underline that storing recorded traces and other related patient data on a central server makes easy to organize a second opinion service. Sharing data between international multi-centre databases could help in developing library of cardiac foetal diseases.

Beside, as an important goal of telemedicine is to improve both patient and physician satisfaction, it was used a simple questionnaire to evaluate it. The analysis of pregnant women responses showed a high patient satisfaction.

The result of response questionnaire suggests also that even if only high-risk patients really might benefit from frequent monitoring, the home foetal surveillance reduces pregnant women stress and increases their quality of life. In conclusion, this preliminary result suggests that foetal home self-monitoring with appropriate support systems and services is useful for pregnancy surveillance. However, the reduced number of patients involved in this preliminary test suggests the need to carry out larger studies.

7.6   Combined FECG-FPCG monitoring

The development of new electronic systems and sensors now offer the potential of effective monitoring of foetal phonocardiography (FPCG) and foetal electrocardiography (FECG) with passive, fully non-invasive low cost digital recording systems that could be

suitable also for home monitoring. These advances provide the opportunity of extending the recordings of the current commonly used CTG from relative short to long term, and provide new previously unavailable measures of cardiac function.

In this thesis, highlights of research lines in non-invasive foetal monitoring, in particular the use of foetal phonocardiographic and electrocardiographic methodology and their combination, are presented in order to detect the foetal heart rate (FHR) and other functioning anomalies. The developed software processing methodologies, suitable for longer-term assessment, were able to detect heart beat events correctly, such as first and second heart sounds and QRS waves. The detection of such events provides reliable measures of heart rate, potentially information about measurement of the systolic time intervals and foetus circulatory impedance.

In particular, by monitoring of the time difference between occurrence of a point on the FECG (such as P wave) and the corresponding foetal heart sounds, it is possible to provide information about the measure of the circulatory impedance. For example when the placental resistance rises due to placental insufficiency, greater pressure must be developed in the foetal ventricles; this leads to a lengthening of the time interval between the P wave and occurrence of the first heart sound. Any increase of this time interval, can be monitored over a period of time allowing the determination of a foetus at risk due to a placental insufficiency or other reason.

Further information to assess the foetus well-being can be estimated from the FECG and FPCG signals separately. FECG processing allows ST interval analysis. Synchronized averaged fECG can improve the SNR. Once being aligned R-peaks detected in a given time windows (e.g. 30 seconds or more), all the recognized FECG can be averaged (the expected improvement of the SNR is proportional to the square root of the number of

FECG considered in the average operation); in this way it could be possible to reduce the noise and analyse the ST interval which reflects the condition of the heart muscle under load and therefore it increases the clinicians' capability in decision for and timing of obstetric interventions [184].

7.7   Further considerations and future developments

In this thesis, new parameters or methods of interpretation and alternative methodologies for non-invasive foetal monitoring are presented in order to further support physicians' decisions. Indexes related to variability of foetal heart rate are particularly studied, from US-CTG recordings, by applying a time-frequency approach. FHRV around its baseline provides extremely significant information concerning the cardiac and ANS activities and their functional development during pregnancy up to labour. Obtained results demonstrated important modifications of FHRV signals PSD related to physiological stimuli represented by UC, both as power and frequency content, confirming that the FHRV time-frequency analysis could be a very useful tool for a more objective and depth evaluation of the foetal health and capability to react to stress.

To estimate FHR, phonocardiography is a suitable tool alternative to US-CTG. Besides, physiological considerations together with medical experiences show that the diagnostic potential of foetal FPCG is much higher than generally supposed, and worth further intensive investigation.

The developed FPCG recordings simulator software allows to simulate the FHR, FHS, mHS and the noise sources typical of a fPCG recording, offering a wide variety of conditions. The software presented can be useful as a teaching tool for demonstration to medical students and others and for testing and assessment of FHR extraction algorithms from FPCG.

Future developments will aim to enrich the simulator software with new features for the simulation of cardiac functionality anomalies such as murmur, split effect, extra systole, bigeminal/trigeminal atrial contraction.

Monitoring of foetal well-being using a passive technique such as FPCG is still a challenging task, mainly due to the low SNR of sound signals recorded through maternal abdomen. Although this limit, the presented algorithm for FHR estimation from phonocardiographic signals shows that it is possible to obtain very reliable FHR series employing a multi-step algorithm. However, to achieve the best performances, future development will aim to improve the algorithm by adding further processing steps to detect new features for the simulation of cardiac functionality anomalies.

Concerning the use of foetal phonocardiographic and electrocardiographic methodology and their combination, obtained results will encourage the further development of appropriate processing techniques to obtain further information about the foetal circulatory impedance. By monitoring of the time difference between occurrence of a point on the FECG (such as P wave) and the corresponding foetal heart sounds, it is possible to provide information about the measure of the circulatory impedance. On the other hand, further information to assess the foetus well-being and cardiac functioning anomalies can be estimated from the FECG and FPCG signals separately and from their combination.

Finally, obtained results are very promising, mainly in field of phonocardiography: in particular, results of the pilot study have been useful to characterise heart sounds better and more completely and developed software have showed good performance to be a suitable and alternative tool in monitoring of foetal well-being.

REFERENCE

[1] Royal college of obstetricians and gynaecologists. *The use of electronic foetal monitoring. The use and interpretation of cardiotocography in intrapartum foetal surveillance*. London: RCOG; 2001

[2] *J.S.H. Curnow, L.b. barron, J. Westgate, K.g. Greene. Four channel foetal ECG data collection system. Med. Eng. Phy., Marzo 1995.17(2):122-125*

[3] C.B. Martin, JR. *Physiology and Clinical Use of Foetal Heart Rate Variability*. Clinics in Perinatology, June 1982, 9 (2): 339-352

[4] S. GRACZYK, K. HOROBA, J. JEREWSKI, J. WROBEL, A. GACEK. *Use of running statistical evaluation in analysis of electrohysterographic signals.* Proceedings of Medicon 98 Cipro June 14-17

[5] Caldeyro-Barcia R. *Fenômenos ativos do parto: Contratilidade uterina*. Rezende, J. Obstetrícia, Vol 1, Guanabara Koogan, Rio de Janeiro, 1962.

[6] KLAUS GOESHEN. *Cardiotocografia pratica*. Roma, V edizione CIC Edizioni Internazionali, 1998

[7] Luis A. Bracero, Harold Schulman, Laxmi V. Baxi. *Frequenza cardiaca foetale. Parametri che possono contribuire alla diagnosi di benessere foetale.* La Clinica Ostetrica e Ginecologica. Edizione Italiana di Clinical Obstetrics and Ginecology. Piccin editore Padova 1980; XIII(1): 3-16

[8] H.P. van Geijn. *Developments in CTG analysis*. Baillieres Clin Obstet Gynaecol 1996 Jun, 10 (2): 185-209

[9] L.W. Oppenheimer, R.M. Lewinsky. P*ower spectral analysis of foetal heart rate.* Baillère's Clinical Obstetrics and Ginecology. Settembre 1994, 8 (3): 643-661

[10] Bruce Rosen, Dinah Soriano, Tom Bylander, Hunmerto Ortiz-Zuazaga, Barry Schifrin. *Training a Neural Network to Recognize Artifacts and Decelerations in Cardiotocograms*. 1996 AAAI Spring Symposium on Artificial Intelligence in Medicine

[11] R. Mantel, H.P. van Geijn, F.J.M. Caron, J.M. Swartjes, E.E. van Woerden and H.W. Jongsma. Computer *Analysis of Antepartum Foetal Heart Rate:1. Baseline Determination*. International Journal of Biomedical Computing, 1990;25:261-260

[12] R. Mantel, H.P. van Geijn, F.J.M. Caron, J.M. Swartjes, E.E. van Woerden and H.W. Jongsma. *Computer Analysis of Antepartum Foetal Heart Rate: 2. Detection of Accelerations and Decelerations*. Internetional Journal of Biomedical Computing,1990;25:273-286

[13] Dawes GS, Meir YJ, Madruzzato GP. *Computerized evaluation of foetal heart-rate pattern*. J Perinat. Med. 1994; 22: 491-499

[14] Mantel R, Van Geijn HP, Ververs IAP, Copray FJA. *Automated analysis of near term antepartum Foetal Heart Rate in relation to foetal behavioural states: The Sonicaid System 8000*. Am J Obstet. Gynecol 165 (1991) 57

[15] Guzman E, Vintzileos A, Martins M, Benito C, Houlihan C. *The efficacy of individual computer heart rate indices in detecting acidemia at birth in growth-restricted fetuses*. Obstet Gynecol 1996; 87: 969-974

[16] Donker D.k., van Geijn H.p., Hasman A. *Interobserver variation in the assessment of foetal heart rate recordings*. European Journal of Obstetrics, Gynecology & Reproductive Biology, 1993; 52: 21-28

[17] R. Depp, K. Kuhlman. *Identification and management of the fetus at risk for acidosis. Intensive Care of the Fetus and Neonate*. Ed. Alan R. Spitzer, Cap. 9, pagg. 105-122

[18] C.M.A.van Rovenswaaij-Arts, L.A.A.Kollèe, J.C.W.Hopman, G.B.Stoelinga, H.P.van Geijn. *Heart Rate Variability*. Annals of Internal Medicine 1993; 118(6): 436-447

[19] N. Montano, T.G. Ruscone, a. porta, F. Lombardi, M. Pagani, A. Malliani. *Power Spectrum Analysis of Heart Rate Variability to assess the Changes in Sympathovagal Balance During Graded Orthostatic Tilt*. Circulation 1994; 90: 1826-1831

[20] O. Sibony, J.P. Fouillot, M. Benaoudia, A. Benhalla, J.F. Oury, C. Sureau, P. Blot. *Quantification of the heart rate variability by spectral analysis of foetal well-being and foetal distress*. European Journal of Obstetrics & Gynecology and Reproductive Biology, 1994,54:103-108

[21] J. Karin, M. Hirsch, S. Akselrod. *An Estimate of Foetal Autonomic State by Spectral Analysis of Foetal Heart Rate Fluctuations*. Pediatric Research, 1993, 34 (2): 134-138

[22] J. Bernardes, A. Costa-Pereira, H. van Geijn, L. Pereira-Leite. *A more objective fetal heart rate baseline estimation.* British Journal of Obstetrics and Gynaecology, Giugno 1996, 103: 714-715

[23] Peter P. Toth, D. and A. Jothivijayarani. *Obstetrics: Intrapartum Monitoring and Management.* University of Iowa Family Practice Handbook, 3rd Edition, Chapter 8; 20/07/1999.

[24] A. Sweha, T.W. Hacker. *Interpretation of the electronic fetal heart rate during labor.* American Academy of Family Physician 1 Maggio 1999, (9);

[25] Romanini C, Rizzo G. *Fetal behaviour in normal and compromised fetuses. An overview.* Early Hum Dev 1995 Oct 2; 43(2): 117-31

[26] Nijhuis JG. Behavioural states: concomitants, clinical implications and the assessment of the condition of the nervous system. Eur J Obstet Gynecol Reprod Biol 1986 May; 21(5-6):301-8

[27] Janjarasjitt S., *A new QRS detection and ECG signal extraction technique for foetal monitoring*, Department of Electrical Engineering and Computer Science Case Western Reserve University, May 2006.

[28] N. E. Babbitt. *Antepartum foetal surveillance. nonstress test, contraction stress test, and biophysical profile*. S D J Med, 49(11):403–8, 1996.

[29] M. Cesarelli, M. Romano, P. Bifulco, Comparison of short term variability indexes in cardiotocographic foetal monitoring, Computers in Biology and Medicine vol. 39 issue 2 (2009), 106-118

[30] Karlsson B., Pourcelot D., Pourcelot L., Berson M., Miniature sensor for Doppler ultrasound Fetal Heart Rate monitoring. Increased patient comfort and ergonomy in use, IEEE Instrumentation and Measurement Technology Conference Brussels, Belgium, June 4-6. 1996.

[31] H. Kieler, S. Cnattingiust, B. Haglund, J. Palmgren, O. Axelsson.. Ultrasound and adverse effects.. Ultrasound in Obstetrics and Gynecology. Vol. 20, Issue 1, pp. 102-103, 2002

[32] F. Kovacs, M. Torok, I. Habermajer. A rule-based phonocardiographic method for long-term fetal heart rate monitoring. IEEE Trans. on Biomed. Eng., vol. 47, no 1, January 2000

[33] Peter Varady, Ludwig Wildt, Zolta´N Benyo´, Achim Hein. An advanced method in fetal phonocardiography. Computer Methods and Programs in Biomedicine 71 (2003) 283/296

[34] Hany E. Bassil, James H. Dripps. Real time processing and analysis of fetal phonocardiographic signals. Clin. Phys. Physiol. Meas., 1989, Vol. 10, Suppl. B, 67-74. Printed in UK

[35] R.T. Wakai. Assessment of fetal neurodevelopment via fetal magnetocardiography. Experimantal Neurology 190 (2004) S65-S71

[36] Y.E. Zhuravlev, D. Rassi, A.A. Mishin, S.J. Emery. Dynamic analysis of beat-to-beat fetal heart rate variability recorded by squid magnetometer: quantification of sympatho-vagal balance. Early Human development 66 (2002): 1-10

[37] D. Mantini, S. Comani, G. Alleva, G.L. Romani. Fetal cardiac time intervals: validation of an automatic tool for beat-to-beat detection on fetal magnetocardiograms. IJBEM. Vol. 7, No. 1, 2005

[38] B.H. Tan, M. Moghavvemi (2000) Real time analysis of fetal phonocardiography. IEEE

[39] McDonnell, J.T.E. (1990) 'Knowledge-based interpretation of foetal phonocardiographic signals', IEE Proceedings, Vol. 137, No. 5, pp.311–318

[40] J. Abrams. Essentials of Cardiac Physical Diagnosis. Lea & Febiger, Philadephia, 1987.

[41] L. Sherwood. Human Physiology From Cells To Systems, chapter Cardiac Physiology, page 319. Thomson - Brooks / Cole, Belmont, 2004.

[42] D. Chen, L.-G. Durand, H. C. Lee. Time-frequency analysis of the first heart sound. Part 1: Simulation and analysis. Med. Biol. Eng. CompuL, 1997, 35, 306-310

[43] A.K. Mittra, N.K. Choudhary, A.S. Zadgaonkar. Development of an artificial womb for acoustical simulation of mother's abdomen. Int. J. Biomedical Engineering and Technology, Vol. 1, No. 3, 2008

[44] Echeverria Jc, Ortiz R, Ramirez N, Medina V, Gonzalez R. A reliable method for abdominal ECG signal processing. IEEE – Computers in Cardiology 1998 Vol 25

[45] J.F. Pieri, J.A. Crowe, B.R. Hayes-Gill, C.J. Spencer, K. Bhogal. Compact long-term recorder for the transabdominal foetal and maternal electrocardiogram. Med. Biol. Eng. Comput., 2001, 39: 118-125

[46] Hasan M. A., Reaz M. B. I., Ibrahimy M. I., Hussain M. S., and Uddin J., Detection and Processing Techniques of FECG Signal for Fetal Monitoring, Biological Procedures Online, Publisher Springer New York, Vol. 11, no 1, pp. 263-295, 27 March 2009.

[47] Peddaneni H., Comparison of algorithms for fetal ECG extraction, University of Florida, 2004.

[48] M. G. Signorini, G. Magenes, S.cerutti, D. Arduini, Linear and nonlinear parameters for the analysis of fetal heart rate signal from cardiotocographic recordings, IEEE Trans Biomed Eng. 2003 Mar; 50 (3), 365-75

[49] M. Romano, M. Cesarelli, P. Bifulco, M. Sansone, M. Bracale, Development of an algorithm for homogeneous FHR signals identification, Proceedings of Embec'02 2nd European Medical and Biological Engineering Conference., December 04-08, 2002, Vienna, Austria; II/1542

[50] S. Cerutti, S. Civardi, A. Bianchi, M.G. Signorini, E. Ferrazzi, G. Pardi, Spectral analysis of antepartum heart rate variability, Clin. Phys. Meas. , 10 (1989), (suppl. B) 27-31

[51] M.Y. Divon, Y. Muska, L. D. Platt, E. Paldi, Increased beat to beat variability during uterine contractions: a common association in uncomplicated labor, American Journal of Obstetrics and Gynecology,149 (1984), 893-896

[52] M. Romano, P. Bifulco, M. Cesarelli, M. Sansone, M. Bracale. Fetal heart rate power spectrum response to uterine contraction, Medical & Biological Engineerin & Computing, Vol.44, N.3, March 2006, 188-201 (Epub 2006 Feb 21)

[53] M. Romano, M. Bracale, M. Cesarelli, M. Campanile, P. Bifulco, M. De Falco, M. Sansone, A. Di Lieto, Antepartum cardiotocography: a study of fetal reactivity in frequency domain, Computers in Biology and Medicine, 2006 Jun; 36 (6), 619-633. (Epub 2005 Jul 11)

[54] P. Laguna, G.B. Moody, R.G. Mark, Power spectral density of unevenly sampled data by least-square analysis: performance and application to heart rate signals, IEEE Transactions on Biomedical Engineering, vol.45, no.6, June 1998

[55] S. Pola, A. Macerata, M. Emdin, C. Marchesi, Estimation of the power spectral density in nonstationary cardiovascular time series: assessing the role of the time-frequency representation (TFR), IEEE Transactions on Biomedical Engineering, Vol. 43, no 1, January 1996

[56] M. Cesarelli, M. Romano, M. Ruffo, P. Bifulco, G. Pasquariello, A. Fratini: PSD modifications of FHRV due to CTG storage rate. 9th International Conference on Information Technology and Applications in Biomedicine- ITAB 2009, November 5-7, Larnaca, Cyprus

[57] M. Romano, M. Cesarelli, P. Bifulco, M. Ruffo, A. Fratini, G. Pasquariello: Time-frequency analysis of CTG signals. Current Development in Theory and Application of Wavelets, Vol. 3, Issue 2, August 2009, pp. 169 - 192

[58] M. Cesarelli, M. Romano, M. Ruffo, P. Bifulco, G. Pasquariello; Foetal heart rate variability frequency characteristics with respect to uterine contractions. Journal of Biomedical Science and Engineering, Vol. 3, Issue 10, Oct. 2010, pp. 1014 – 1021

[59] M. Cesarelli, M. Romano, M. Ruffo, P. Bifulco, G. Pasquariello, A. Fratini; PSD modifications of FHRV due to interpolation and CTG storage rate. In press by Biomedical Signal Processing and Control (Available online 18 November 2010)

[60] M.V. Kamath, E.L. Fallen, Power spectral analysis of heart rate variability: a noninvasive signature of cardiac autonomic function, Critical Reviews in Biomedical Engineering, 21 (3), (1993), 245-311

[61] S. Gudmudsson, P. Olofsson, Acute changes of cerebral venous blood flow in growth-restricted human fetuses in response to uterine contractions, Ultrasound Obstet Gynecol, 24 (2004), 516-521

[62] H. Li, S. Gudmundsson, P. Olofsson, Acute increase of umbilical artery vascular flow resistance in compromised fetuses provoked by uterine contractions, Early Human Development 74 (2003), 47–56

[63] HP operating manual, Series 50 XMO, Viridia

[64] H. G. Van Steenis, J. H. M. Tulen, L. J. M. Mulder, Heart rate variability spectra based on non-equidistant sampling: the spectrum of counts and the instantaneous heart rate spectrum, Med. Eng. Phys. , Sept. 1994, 16, 355-362

[65] Z. Xianchao, W. Yingyu, C. Guoliang, A new approach for implementing the Arithmetic Fourier Transform (AFT), Proceedings of the 4th International Conference "High Performance Computing in the Asia-Pacific Region 2000; (2), 633-634

[66] G. Magenes, M. G. Signorini, D. Arduini, S. Cerutti, Fetal heart rate variability due to vibroacoustic stimulation: linear and nonlinear contribution, Methods of Information in Medicine, 43 (1) (2004), 47-51

[67] P. E. Mcsharry, G.D. Clifford, L. Tarassenko, L. A. Smith, A dynamical model for generating synthetic electrocardiogram signals, IEEE Trans. on Biomedical Engineering, vol. 50, no. 3, march 2003

[68] R. Moraes, N. Aydin, D. H. Evans, The performance of three maximum frequency envelope detection algorithms for Doppler signals, Journal of Vascular Investigation (1995) 1:3, 126-134

[69] T. Ohta, K. Okamura, Y. Kimura, T. Suzuki, T. Watanabe, T. Yasui, N. Yaegashi, A. Yajima, Alteration in the low-frequency domain in power spectral analysis of fetal heart beat fluctuations, Fetal Diagnosis and Therapy, 14 (1999), 92-97

[70] B. Rosen, D. Soriano, T. Bylander, H. Ortiz-Zuazaga, Barry Schifrin, Training a neural network to recognize artifacts and decelerations in cardiotocograms, 1996 AAAI Spring Symposium on Artificial Intelligence in Medicine

[71] S. M. Menticoglou, The fetal biophysical profile. Intenisve Care of the Fetus and Neonate, Ed. Alan R. Spitzer, Publisher Mosby, January 1996, St.Louis, MO, Chapter 10, 123-129

[72] H. Van Geijn, Van Ravenswaaij-Arts, J. Hopman, L. Kollee, G. B. Stoelinga, Spectral analysis of heart variability in spontaneously breathing very preterm infants, Acta Paediatrica, 83 (1004), 473-480

[73] L. W. Oppenheimer, R. M. Lewinsky, Power spectral analysis of fetal heart rate, Baillère's Clinical Obstetrics and Ginecology, 1994 Sept; 8 (3), 643-661

[74] G. B. Moody, "Spectral analysis of heart rate without resampling," Comput. Cardiol., pp. 715–718, 1993.

[75] S. S. Abeysekera, U. R. Abeyratne, and S. B. Goh, "Spectral information changes in obtaining heart rate variability from tachometer R-R interval signals," Crit. Rev. Biomed. Eng., vol. 28, no. 1-2, pp. 149–55, 2000.

[76] Spyridou KK, Hadjileontiadis LJ, "Analysis of fetal heart rate in healthy and pathological pregnancies using wavelet-based features", 29th Annual International Conference on the IEEE Engineering in Medicine and Biology Society, 2007. 22-26 Aug. 2007, pp. 1908-1911.

[77] N. R. Lomb, "Least-squares frequency analysis of unequally spaced data," Astrophysical Space Sci., vol. 39, pp. 447–462, 1976.

[78] J. D. Scargle, "Studies in astronomical time series analysis. II. Statistical aspects of spectral analysis of unevenly spaced data," Astrophysical J., vol. 263, pp. 835–853, 1982.

[79] W. H. Press, B. P. Flannery, S. A. Teukolsky, and W. T. Vetterling, "Numerical Recipes in C", 2nd ed. Cambridge, U.K.: Cambridge Univ. Press, 1992, pp. 615–619.

[80] G. D. Clifford, L. Tarassenko, "Quantifying errors in spectral estimates of HRV due to beat replacement and resampling," IEEE Trans. on Biomedical Engineering, vol. 52, no.4, april 2005.

[81] E. Ferrazzi, G. Pardi, P. Levi Setti, M. Rodolfi, S. Civardi, S. Cerutti, "Power spectral analysis of the heart rate of the human fetus at 26 and 36 weeks of gestation," Clin. Phys. Meas.,1989, 10 (suppl. B): 57-60 1989.

[82] G. Magenes, M.G. Signorini, M. Ferrario, F. Lunghi, "2CTG2: A new system for the antepartum analysis of fetal heart rate", 11th Mediterranean Conference on Medical and Biomedical Engineering and Computing MEDICON 2007.

[83] S. C. Chan, Z. Zhang, "Adaptive window selection and smoothing of lomb periodogram for time-frequency analysis of time series," The 47th International Midwest Symposium on Circuits and Systems 2004.

[84] N. Colley, D. G. Talberg, D. P. Southall, "Biophysical Profile in the Foetus from a Phonocardiographic Sensor", Eur. J. Obstet. Reprod. Biol. Biol., Vol. 23, pp. 261-266, 1986

[85] F. Kovacs, Cs. Horváth, M. Török, G. Hosszú. Long-term phonocardiographic foetal home monitoring for telemedicine systems. Proceedings of the 2005 IEEE. Engineering in Medicine and Biology 27th Annual Conference. Shanghai, China, September 1-4, 2005

[86] Moghavvemi, M., Tan, B.H. and Tan, S.Y. (2003) 'A non-invasive PC based measurement of foetal phonocardiography', Journal of Sensors and Actuators, Vol. A 107, pp.96–103

[87] A. Baskaran, N. Sivalingam, Foetal heart sound analysis: a preliminary evaluation, Med. J. Malaysia 51 (1) (1996) 64–67

[88] Talbert DG, Davies WL, Johnson F, Abraham NG, Colley N, Southall DP. Wide bandwidth fetal phonography using a sensor matched to the compliance of the mother's abdominal wall. IEEE Trans Biomed Eng 1986; 33:175-181

[89] Reed, T.R., Reed, N.E. and Peter, F. (2004) 'Heart sound analysis for symptom detection and computer aided diagnosis', Journal of Simulation Modeling Practices and Theory, Vol. 12, pp.129–146

[90] Nagal, J. (1986) 'New diagnostic and technical aspects of fetal phonocardiography', European Journal of Obstetrics and Gynecology and Reproductive Biology, Vol. 23, pp.295–303

[91] Jimenez, A.; Ortiz, M.R.; Pena, M.A.; Charleston, S.; Aljama, A.T.; Gonzalez, R., The use of wavelet packets to improve the detection of cardiac sounds from the fetal phonocardiogram, Computers in Cardiology 1999, 26-29 Sept. 1999 Page(s):463 – 466

[92] Zhang, X., Durand, L., Senhadji, L., Lee, H. and Coatrieux, J. (1998) 'Time-frequency scaling transformation of the phonocardiogram based of the matching pursuit method', IEEE Transactions on Biomedical Engineering, Vol. 45, No. 8, pp.972–979

[93] A.K. Mittra, Anupam Shukla, A.S. Zadgaonkar. System simulation and comparative analysis of foetal heart sound de-noising techniques for advanced phonocardiography. Int. J. Biomedical Engineering and Technology, Vol. 1, No. 1, 2007

[94] Kaiser, J.F. (1990), "On a simple algorithm to calculate the 'energy of a signal'," ICASSP-90. pp.381-384, Albuquerque, New Mexico.

[95] Atlas, L. and Fang, J. (1992), "Quadratic Detectors for General Nonlinear Analysis of Speech," IEEE Proc. ICASSP'92, San Francisco, CA, pp. II-9-II-12, March 23-26, 1992.

[96] M. Ruffo, M. Romano, M. Cesarelli, P. Bifulco: Extraction of heart rate from fetal phonocardiographic signals. Primo Congresso Nazionale di Bioingegneria – GNB-2008

[97] M. Cesarelli, M. Ruffo, M. Romano, P. Bifulco, F. Kovacs, S. Iaccarino: An Algorithm for fetal heart rate extraction from maternal abdomen sounds. 4th European Congress For Medical and Biomedical Engineering 2008, November 23-27, Antwerp – MBEC 2008

[98] M. Ruffo, M. Cesarelli, M. Romano, P. Bifulco, A. Fratini, G. Pasquariello, S. Iaccarino: Comparison of software developed for FHR extraction from PCG signals. Medical Physics and Biomedical Engineering World Congress 2009, September 7-12, Munich

[99] M. Cesarelli, M. Romano, M. Ruffo, P. Bifulco, M. Iaccarino, S. Iaccarino: Home care phonocardiography: an Italian experience. 9th International Conference on Information Technology and Applications in Biomedicine- ITAB 2009, November 5-7, Larnaca, Cyprus

[100] M. Ruffo, M. Cesarelli, M. Romano, P. Bifulco: Testing a FHR extraction algorithm by means of a simulating software of foetal phonocardiographic recordings. Secondo Congresso Nazionale di Bioingegneria – GNB-2010

[101] G. Donadono , M. Ruffo, M. Romano, P. Bifulco, M. Cesarelli, D. Gargiulo, A. Fratini: Recording of fetal heart sound using a PVDF piezoelectric film sensor. Secondo Congresso Nazionale di Bioingegneria – GNB-2010

[102] M. Ruffo, M. Cesarelli, M. Romano, P. Bifulco, A. Fratini; A simulating software of fetal phonocardiographic signals. The 10th IEEE International Conference on Information Technology and Applications in Biomedicine, ITAB 2010, Corfu, Greece, November 2-5, 2010

[103] M. Ruffo, M. Cesarelli, M. Romano, P. Bifulco, A. Fratini. An algorithm for FHR estimation from foetal phonocardiographic signals. Biomedical Signal Processing and Control, Vol. 5, Issue 2, April 2010, pp. 131-141

[104] A. P. Yoganathan, R. Gupta, F. E. Udwadia, J. W. Miller, W. H. Corcoran, R. Sarma, J. L. Johnson, and R. J. Bing, "Use of the fast Fourier transform for frequency analysis of the first heart sound in normal man," Med Biol Eng, vol. 14, pp. 69-73, 1976

[105] Kobayashi, K., Yasuda, T., and Suzuki, K., "Piezoelectric highpolymer film for foetal phonocardiograph and the monitor," Journal of the Acoustical Society of America, vol. 64, Supplement no. 1, Fall 1978

[106] Hikoro Matsui, Helena Gardiner. Current aspects of foetal cardiovascular function. Foetal and Maternal Medicine Review 2008; 19:1 61–84 Cambridge University Press

[107] Signal processing methodologies for an acoustic foetal heart rate monitor (1992) : final report for the period January 1, 1988 to September 30, 1991 / by Robert A. Pretlow III and John W. Stoughton; principal investigator ; NASA contractor report ; NASA CR-190828

[108] Hewlett-Packard GMBH, Operating and Service Manual for Model 8020A Cardiotacograph, Boblingen, West Germany, 1970

[109] Jenssen, H., "Foetal systolic time intervals after paracervical block during labor," Acta Obstet. Gynecol. Scand., vol. 59, pp. 115-121, 1980

[110] Talbert, D. G., Dewhurst, J., Southall, D. P., "New transducer for detecting foetal heart sounds: Use of compliance matching for maximum sound transfer," Lancet, February 25, 1984, pp. 426-427

[111] A. A. Luisada, F. Mendoza, M. M. Alimurung, The duration of normal heart sounds, British Heart Journal. 1949 January; 11(1): 41–47

[112] M. Merri, D.C. Farden, J.G. Mottley, E.L. Titlebaum. Sampling frequency of the electrocardiogram for spectral analysis of the heart rate variability. IEEE Transactions on Biomedical Engineering, January 1990, 37 (1): 99-106

[113] J.G. Proakis, D.G. Manolakis. Digital signal processing – Principles, algorithms, and applications. Third edition – Prentice Hall. 1996

[114] A. Bruce Carlson, Paul B. Crilly, Janet C. Rutledge. Communication systems. An introduction to signals and noise in electrical communication. McGraw-Hill Higher Education. Fourth edition. 2002

[115] James F. Kaiser. Some useful properties of teager's energy operators. ICASSP-93 Vol 3, pp.149-152, Acoustics, Speech, and Signal Processing, 1993. 1993 IEEE International Conference on, 1993

[116] A. Jimenez-Canas, C. Fernandez-Castellanos, V. Castro-Castillo, A. Ruiz-Toledo, A. Sotomayor-Ortega. Implementation of real time autocorrelation method employing the

DS87C550 microcontroller. Journal of Applied Research and Technology. Vol. 1. No. 1 April 2005

[117] C. Ahlstrom, T. Lanne, P. Ask, A. Johansson. A method for accurate localization of the first heart sound and possible applications. Physiol. Meas. 29 (2008): 417-428

[118] Bert-Uwe Köhler, Carsten Hennig, Reinhold Orglmeister. The Principles of Software QRS Detection. IEEE Engineering In Medicine And Biology January/February, 2002

[119] R Bailon, S Olmos, P Serrano, J Garcıa, P Laguna. Robust Measure of ST/HR Hysteresis in Stress Test ECG Recordings. Computers in Cardiology 2002; 29: 329–332

[120] Piotr Rozentryt, Jacek Leski, Jacek Sroczynski, Ernest Czogala. A new beat-by-beat spectrotemporal analysis of variability in ECG morphology. Med Sci Monit, 1999; 5(4): 777-785

[121] Markus M. Breunig, Hans-Peter Kriegel, Raymond T. Ng, Jörg Sander. LOF: Identifying density-based local outliers. Proc. ACM SIGMOD 2000 Int. Conf. On Management of Data, Dalles, TX, 2000

[122] Jianfeng Chen, Koksoon Phua, Ying Song, Louis Shue. Fetal heart signal monitoring with confidence factor. ICME pp.1937-1940, 2006. IEEE International Conference on Multimedia and Expo, 2006

[123] Xiaoyan Li, Ping Zhou, Alexander S. Aruin. Teager–Kaiser Energy Operation of Surface EMG improves muscle activity onset detection. Annals of Biomedical Engineering, Vol. 35, No. 9, September 2007 pp. 1532–1538

[124] L. Durand, "Digital signal processing of the phonocardiogram," IEEE Engineering in Medicine and Biology Society 9th Annual International Conference Proceedings, 1987, pp. 906-907

[125] M. Cesarelli, M. Romano, P. Bifulco, F. Fedele, M. Bracale, An algorithm for the recovery of foetal heart rate series from CTG data, Computers in Biology and Medicine, Volume 37, Issue 5, Pages 663-669

[126] L.J. Groome, D.M. Mooney, L.S. Bentz, K.P. Singh. Spectral analysis of heart rate variability during quiet sleep in normal human foetuses between 36 and 40 weeks of gestation. Early Human Development 1994, 38: 1-10 (1994)

[127] N.S. Padhye, Z. Duan, M.T. Verklan. Response of foetal heart rate to uterine contractions. Proceedings of the 26th annual international conference of the IEEE EMBS. San Francisco, CA, USA. September 1-5, 2004 (2004)

[128] E. Ferrara, B. Widrow, "Foetal electrocardiogram enhancement by time-sequenced, Adaptive filtering," IEEE Transactions on Biomedical Engineering, vol. BME-29, no. 6, June 1982, pp.458-460

[129] Kumar D, Carvalho P, Antunes M, Henriques J, Eugenio L, Schmidt R, Habetha J., Detection of S1 and S2 heart sounds by high frequency signatures, Conf Proc IEEE Eng Med Biol Soc. 2006;1:1410-6

[130] Brusco, M. and Nazeran, H. (2004) 'Digital phonocardiography, a PDA-based approach', Proceedings of the 26th Annual International Conference of the IEEE EMBS, San Francisco, California, Vol. 1, pp.2299–2302

[131] E. C. Karvounis, M. G. Tsipouras, D.I. Fotiadis, K. K. Naka, An automated methodology for fetal heart rate extraction from the abdominal electrocardiogram, IEEE Trans Inf. Technol. Biomed. 2007 Nov; 11(6): 628-38.

[132] E. M. Symond, D. Sahota, and A. Chang, Fetal Electrocardiography. London, U.K.: Imperial College Press, 2001.

[133] A. Jimenez, Mr Ortiz, Ma Pena, S Charleston, R Gonzalez, At Aljama, S Carrasco. Performance of a method to generate foetal cardiotachograms using foetal phonocardiography. Computers in Cardiology 2001; 28: 453-456

[134] R. Ortiz; R. Gonzàlez; M. A. Pe a; S. Carrasco; M. J. Gait n; C. Vargas; Differences in foetal heart rate variability from phonocardiography and abdominal electrocardiography, Journal of Medical Engineering & Technology, Volume 26, Issue 1 February 2002 , pages 39 – 45

[135] R.Kerner, Y.Yogev, A.Belkin, A.Ben-Haroush, B.Zeevi, M.Hod, "Maternal self-administered fetal heart rate monitoring and transmission from home in high-risk pregnancies," International Journal of Gynecology and Obstetrics 84, 2004, pp. 33–39

[136] A. Di Lieto, U. Giani, M. Campanile, M. De Falco, M. Scaramellino, R. Papa, "Prenatal telemedicine: clinical experience with conventional and computerised antepartum telecardiotocography," European Journal of Obstetrics & Gynecology and Reproductive Biology 103, 2002, pp. 114-118

[137] M. Ruffo, M. Cesarelli, C. Jin, G. Gargiulo, A. McEwan, C. Sullivan, P. Bifulco, M. Romano, R. W. Shephard, A. van Schaik: Non invasive foetal monitoring with a combined ECG - PCG system. "Biomedical Engineering, Trends, Researches and Technologies", To be published by INTECH, Jan. 2011

[138] Rosen KG, Kjellmer I (1975) Changes in the fetal heart rate and ECG during hypoxia. Acta Physiol Scand 93(1):59–66

[139] Greene KR, Dawes GS, Lilja H, Rosen KG (1982) Changes in the ST waveform of the fetal lamb electrocardiogram with hypoxemia. Am J Obstet Gynecol 144(8):950–958

[140] Braunwald E, Maroko PR (1976) ST-segment mapping. Realistic and unrealistic expectations. Circulation 54(4):529– 532

[141] Camps G., Martinez M., Soria E., Fetal ECG extraction using an FIR neural network, Computers in Cardiology 2001, pp.249-252, 2001.

[142] Kezi Selva vijila C., Kanagasabapathy P., Johnson S., Fetal ECG Extraction using Softcomputing Technique, Journal of Applied Sciences, Vol.6, No.2, 251-256, 2006.

[143] Camps-Valls G., Martínez-Sober M., Soria-Olivas E., Guerrero-Martínez J. Calpe-Maravilla J., Foetal ECG recovery using dynamic neural networks, Artificial Intelligence in Medicine, Vol. 31(3), pp 197-209, 2004.

[144] Roberts R.A., Mullis C.T., Digital signal processing, Adison-Wesley, Reading, Mass, 1987.

[145] Longini Richard L., Reichert Thomas A., Man Cho Yu Joseph, Crowley Jerry S., Near-Orthogonal Basis Functions: A Real Time Fetal ECG Technique, Biomedical Engineering, IEEE Transactions on, vol. BME-24, no.1, pp.39-43, Jan. 1977.

[146] Budin N., Abboud S., Real Time Multichannel Abdominal Fetal ECG Monitor Using Digital Signal CoProcessor, Computers in Biology and Medicine, Vol. 24 (6): 451-462, 1994.

[147] Mochimaru F., Fujimoto Y., Ishikawa Y., The Fetal Electrocardiogram by Independent Component Analysis and Wavelets, Japanese Journal of Physiology, Vol.54, 457-463, 2004.

[148] Mallat S., Hwang W.L., Singularity detection and processing with wavelets, Information Theory, IEEE Transactions on, vol.38, no.2, pp.617-643, Mar. 1992.

[149] Richter M., Schreiber T., Kaplan D.T., Fetal ECG extraction with nonlinear state-space projections, Biomedical Engineering, IEEE Transactions on, vol.45, no.1, pp.133-137, Jan 1998.

[150] Schreiber T., Richter M., Nonlinear projective filtering in a data stream, Wuppertal preprint WUB-98-8, 1998.

[151] Kardec Barros A., Cichocki A., Extraction of Specific Signals with Temporal Structure, Neural Computation, Vol. 13, Issue 9, September 2001.

[152] Zhi-Lin Zhang, Zhang Yi, Robust extraction of specific signals with temporal structure, Neurocomputing, Vol. 69, Issues 7-9, New Issues in Neurocomputing: 13th European Symposium on Artificial Neural Networks, Pages 888-893, March 2006.

[153] Assaleh K., Al-Nashash H., A novel technique for the extraction of fetal ECG using polynomial networks, Biomedical Engineering, IEEE Transactions on, vol.52, no.6, pp. 1148-1152, June 2005.

[154] Stone J. V., Independent component analysis: an introduction, TRENDS in Cognitive Sciences, Vol.6 No.2, pp. 59-64, February 2002.

[155] Hyvärinen A., Oja E., Independent component analysis: algorithms and applications, Neural Networks Volume 13, Issues 4-5, Pages 411-430, June 2000.

[156] Hyvarinen A., A family of fixed-point algorithms for independent component analysis, Acoustics, Speech and Signal Processing, 1997 ICASSP-97, IEEE International Conference on, vol.5, pp.3917-3920, vol.5, 21-24 Apr 1997.

[157] Yan Li, Powers D., Peach J., Comparison of Blind Source Separation Algorithms, Advances in Neural Networks and Applications, WSES, pp.18-21, 2000.

[158] Goddard B. A., A Clinical Foetal Electrocardiograph, Med. Biol. Engineering 4, 159–167, 1996.

[159] R Bailon, S Olmos, P Serrano, J Garcıa, P Laguna. Robust Measure of ST/HR Hysteresis in Stress Test ECG Recordings. Computers in Cardiology 2002; 29: 329–332

[160] Piotr Rozentryt, Jacek Leski, Jacek Sroczynski, Ernest Czogala. A new beat-by-beat spectrotemporal analysis of variability in ECG morphology. Med Sci Monit, 1999; 5(4): 777-785

[161] J.E.E. Fleming, S.P.W. Raymond, G.C.S. Smith and C.R. Whitfield, The measurement of fetal systolic time intervals: lessons from ultrasound. Eur. J. Obstet. Gynecol. Reprod. Biol., 23 (1986) 289-294

[162] DeVore GR, Donnerstein RL, Klcinman CS, Hobbins JC. Real-time-directed M-mode echocardiography: A new technique for accurate and rapid quantitation of the fetal preejection period and ventricular ejection time of the right and left ventricles. Am J Obstet Gynecol 1981; 141: 470-471.

[163] Giorlandino C, Gentili P, Vizzone A, Rizzo G, Arduini D. A new method for the measurement of pre-ejection period in the human fetus. Br J Obstet Gynecol 1986; 93: 307-309.

[164] Adam AH, Doig JR, Fleming JEE, Smith MC, Houston A, Adam K, Aitchison T. Fetal Heart Electrom&usnical Intervals. In 'Recent Advances in Ultrasonic Diagnosis' Vo12: Kurjak A, ed. 1979.

[165] Robinson HP, Adam AH, Fleming JEE, Houston A, Clark DM. Fetal electromechanical intervals in labour. Br J Obstet Gynecol 1978; 3: 172-177.

[166] Campbell S, Trickey N, Whittle MJ. Report of the Royal College of Obstetricians and Gynaecologists Working Party on routine ultrasound examination in pregnancy. R Co11 Obstet Gynecol 1984.

[167] M. David, M. Hirsch, S. Akeselrod, "Maturation of fetal cardiac autonomic control as expressed by fetal heart rate variability", Computers in Cardiology 2006, 33, 901–904

[168] R. Logier, J. De jonckheere, M. Jeanne, R. Matis, "Fetal distress diagnosis using heart rate variability analysis: design of a high frequency variability index", 30th Annual International IEEE EMBS Conference Vancouver, British Columbia, Canada, August 20-24, 2008

[169] Dirk Hoyer, Esther Heinicke, Susann Jaekel, Florian Tetschke, Dania Di Pietro Paolo, Jens Haueisen, Ekkehard Schleußner, Uwe Schneider, "Indices of fetal development derived from heart rate patterns", Early Human Development 2009, 85: 379–386.

[170] H. Cao, D. E. Lake, C. A. Chisholm, J. E. Ferguson, M. P. Grifin, J. R. Moorman, "Toward quantitative monitoring of human cardiotocography during labor", Proceedings of the 25th Annual International Conference of the IEEE EMBS, Cancun, Mexico, September 17-21, 2003

[171] S. Gudmudsson, P. Olofsson, "Acute changes of cerebral venous blood flow in growth-restricted human fetuses in response to uterine contractions", Ultrasound Obstet Gynecol 2004, 24, 516-521

[172] H. Li, S. Gudmundsson, P. Olofsson, "Acute increase of umbilical artery vascular flow resistance in compromised fetuses provoked by uterine contractions", Early Human Development 2003, 74, 47–56

[173] E. Salamalekis, N. Vitoratos, C. Loghis, N. Panayotopoulos, D. Kassanos, G. Creatsas, "Evaluation of fetal heart rate patterns during the second stage of labor through fetal oximetry", Gynecologic and Obstetric Investigation 1999, 48, 151-154

[174] E. Z. Zimmer, Y. Paz, J. A. Copel, Z. Weiner, "The effect of uterine contractions on intrapartum fetal heart rate analyzed by a computerized system", American Journal of Obstetrics and Ginecology 1998, 178 (3), 436-440

[175] O. H. Rognerud Jensen, G. Narverud, "Fetal heart rate decelerations and umbilical cord blood gas values", European Journal of Obstetrics & Gynecology and Reproductive Biology 1994, 53, 103-106

[176] N. S. Padhye, Z. Duan, M. T. Verklan, "Response of fetal heart rate to uterine contractions", Proceedings of the 26th annual international conference of the IEEE EMBS, San Francisco, CA, USA, September 1-5, 2004

[177] Y. Kodama, H. Sameshima, T. Ikeda, T. Ikenoue, "Intrapartum fetal heart rate patterns in infants ($\geq$34 weeks) with poor neurological outcome", Early Human Development 2009, 85, 235–238

[178] K. Goeschen, "Cardiotocografia pratica", Roma, V edizione CIC Edizioni Internazionali, 1998

[179] T. Rantonen, E. Ekholm, S. Siira, T. Metsala, R. Leino, U. Ekblad, I. Valimaki, "Periodic spectral components of fetal heart rate variability reflect the changes in cord arterial base deficit values: a preliminary report", Early Hum Dev 2001, 60 (3), 233-238

[180] J. Jezewski, J. Wrobel, K. Horoba. Comparison of Doppler ultrasound and direct electrocardiography acquisition techniques for quantification of fetal heart rate variability. IEEE Trans Biomed Eng. 2006 May;53(5):855-64

[181] H.P. Van Geijn, H.W. Jongsma, J. Haan, T.K.A.B. Eskes, Analysis of heart rate and beat-to-beat variability: interval difference index. American Journal of Obstetrics and Ginecology, 1° Ottobre 1980, 138 (3): 246-252

[182] Philip A. Warrick, Emily F. Hamilton, Doina Precup, Robert E. Kearney, "Identification of the dynamic relationship between intra-partum uterine pressure and fetal heart rate for normal and hypoxic foetuses", IEEE Transactions on Bio-Medical Engineering 2009, 56 (6), 1587-1597

[183] M. Romano, P. Bifulco, M. Cesarelli, M. Sansone, M. Bracale, "Fetal heart rate power spectrum response to uterine contraction", Medical & Biological Engineerin & Computing 2006, 44 (3), 188-201

[184] Ross G. , Devoe L. D., Rosen K. G., St-Segment Analysis Of The Fetal Electrocardiogram Improves Fetal Heart Rate Tracing Interpretation And Clinical Decision Making. J Matern Fetal Neonatal Med. 2004 Mar; 15 (3): 181-5